İSTANBUL TECHNICAL UNIVERSITY ★ INSTITUTE OF SCIENCE AND TECHNOLOGY

ESTIMATION OF SLIDING DISPLACEMENT OF GRAVITY TYPE QUAY WALLS UNDER NEAR FAULT GROUND MOTION

M.Sc. Thesis by
Alper AĞDAŞAN

Department : Coastal Sciences and Engineering

Programme : Coastal Sciences and Engineering

SEPTEMBER 2011

İSTANBUL TECHNICAL UNIVERSITY ★ INSTITUTE OF SCIENCE AND TECHNOLOGY

ESTIMATION OF SLIDING DISPLACEMENT OF GRAVITY TYPE QUAY WALLS UNDER NEAR FAULT GROUND MOTION

M.Sc. Thesis by
Alper AĞDAŞAN
(517081006)

Date of submission : **16 September 2011**
Date of defence examination: **23 September 2011**

Supervisor (Chairman) : **Assc.Prof.Dr. Şevket ÇOKGÖR (ITU)**
Co-supervisors : **Dr. U. Utku CELEP (BU)**
Members of the Examining Committee : **Prof. Dr. Sedat KABDAŞLI (ITU)**
Assc.Prof.Dr.Abdullah GEDIKLI (ITU)
Asst.Prof.Dr. V. Ş. Özgür KIRCA (ITU)

SEPTEMBER 2011

İSTANBUL TEKNİK ÜNİVERSİTESİ ★ FEN BİLİMLERİ ENSTİTÜSÜ

YAKIN FAY YER HAREKETİ ALTINDA AĞIRLIK TİPİ KIYI DUVARLARININ KAYMA DEPLASMANLARININ TAHMİNİ

YÜKSEK LİSANS TEZİ
Alper AĞDAŞAN
(517081006)

Tezin Enstitüye Verildiği Tarih : 16 Eylül 2011
Tezin Savunulduğu Tarih : 23 Eylül 2011

Tez Danışmanı : Doç. Dr. Şevket ÇOKGÖR (İTÜ)
Eş Danışman: Dr. U. Utku CELEP (BÜ)
Diğer Jüri Üyeleri : Prof. Dr. Sedat KABDAŞLI (İTÜ)
Doç. Dr. Abdullah GEDİKLİ (İTÜ)
Yard. Doç. Dr. V. Ş. Özgür KIRCA (İTÜ)

EYLÜL 2011

Canım aileme,

FOREWORD

I would like to express my deep appreciation and thanks for my advisor Assoc. Prof. Dr. Şevket Çokgör for his suggestion and his interest, and my co-supervisor Dr. U. Utku Celep for his valuable criticisim and suggestions, is also my colleague and chief, whose understanding, encouraging and personal guidance have provided a good basis for the present thesis and made a deep impression on me. He monitored my study and encouraged me to advance and continue with my thesis, enriched my knowledge with his exceptional insights into engineering.
I would like to express my gratitude Osman Müyesser for his valuable guidance and support, unlimited understanding and patience.
I am greatly indepted to my dear colleagues at OSM Engineering is my second family for their understanding.
Finally, I express my deepest love to my parents for their encouragement and understanding. I would like to thank them so much for their endless love and support.
This work is supported by ITU Institute of Science and Technology.

September 2011

Alper Ağdaşan

(Civil Engineer)

TABLE OF CONTENTS

Page

ABBREVIATIONS

APP	**:** Appendix
ASCE	**:** American Civil Society of Civil Engineering
DLH-DTY	**:** Technical Seismic Regulation on Construction of Coastal and Harbor Structures, Railways and Airports
PEER	**:** The Pacific Earthquake Engineering Research Center
PIANC	**:** Permanent International Association for Navigation Congresses, Working Group No.34 of the Maritime Navigation Commission International Navigation Association
RHA	**:** General Directorate for Construction of Railways, Harbors and Airports of Ministry of Transportation of Turkey
SEAOC	**:** Structural Engineers Association of California

LIST OF TABLES

Page

LIST OF FIGURES

Page

ESTIMATION OF SLIDING DISPLACEMENT OF GRAVITY QUAY WALLS UNDER NEAR FAULT GROUND MOTION

SUMMARY

Gravity type marine structures develop their resistance to soil pressure and miscellaneous loads primarily from their own weights, and grip on the foundations. Generally, this type of structures are called port related waterfront structures, quay walls or gravity type breakwaters. These structures are the most common type of construction for harbors because of their durability. The resistance based design method expresses the safety and stability of a waterfront retaining structure. The stability is subjected to static and/or dynamic earth and water forces in terms of the factor of safety against sliding along the base of the wall, the ability of the wall to resist the earth and water forces acting to overturn the wall. This method is called conventional design method. However, this design method does not give any information about the potential performance and damage of the structure. In contrast to resistance based design, deformation based design takes into account the workability, predicting deformation, assessment of the structure. And also, deformation based design considers the related damage for shakings above the limit equilibrium for the structure will be designed with operational and structural considerations including performance criteria and damage criteria. Sliding block methods of analysis calculates an estimated permanent displacement of a gravity type marine structure system due to a user specified design earthquake event. Sliding block methods of analysis is one of deformation based design methods described as simplified dynamic analysis.

The study covers the estimated minimum seaward displacement of a structure is computed by integrating the acceleration time history that exceeds the threshold limit for sliding over the duration until the structure ceases sliding. The structure is idealized as sliding rigid block based on Newmark's method. Threshold acceleration represents the yielding limit assuming with the permanent displacements founded beginning from this point. Threshold acceleration makes the coefficient of safety against sliding is 1.0. Time histories dependent near fault ground motions are used with its rupture directivity, component and soil condition properties within some acceptance bounds. This study is different from the previous studies about deformation based design related to estimating of permanent sliding displacements with its acceptance bounds.

A set of simple charts and formulas for seismic performance evaluation for gravity type quay walls have been proposed based on parametric study by taking account of acceptance and assumptions of near fault ground motion parameters and selected earthquake record.

YAKIN FAY YER HAREKETİ ALTINDA AĞIRLIK TİPİ KIYI DUVARLARININ KAYMA DEPLASMANLARININ TAHMİNİ

ÖZET

Deniz tabanı üzerine oturtulan rıhtım duvarı, dalgakıran gibi kıyı koruma yapıları ağırlık tipi deniz yapıları olarak tanımlanmaktadır. Bu yapılar toprak basıncı vb. çevresel yüklere karşı dayanımlarını öncelikli olarak kendi ağırlıkları ile karşılamaktadırlar. Dayanıklılıkları sebebiyle genellikle tipik kıyı koruma yapıları olarak inşa edilirler. Ağırlık tipi kıyı koruma yapılarının tasarımında yaygın olarak kullanılan kuvvet bazlı tasarım yönteminde; eş değer statik-dinamik toprak ve su kuvvetlerine karşı yapının kaymaya ve devrilmeye göre stabilite tahkiki güvenlik katsayılarıyla tanımlanır. Nitekim, bu tasarım yöntemi yapının olası performansı ve hasarı konusunda herhangi bir bilgi vermemektedir. Kuvvet bazlı tasarım yöntemiyle kıyaslandığında deformasyona dayalı tasarım; çeşitli hasar ve performans kriterleri gözönünde bulundurularak yapının deprem itkisi altındaki davranışını dikkate alıp, yapıya ait olası deformasyon ve hasar konusunda bilgi vermektedir. Literatürde basitleştirilmiş dinamik analiz yöntemi olarak tanımlanan kayan blok analizi, ağırlık tipi deniz yapılarının deprem etkisi altında yapacağı tahmin edilen kalıcı yatay yer değiştirmelerin hesaplanmasında kullanılan bir metottur.

Bu çalışmada Newmark Kayan Blok Analizi yöntemi idealleştirilerek; deprem etkisi altında herhangi bir ağırlık tipi rijit deniz yapısının denize doğru yapacağı tahmin edilen minimum yatay yer değiştirmesi, deprem ivme kaydı kullanılarak deprem süresi boyunca eşik ivmesi olarak tanımlanan eş değer deprem ivmesi katsayısının aşıldığı bölgelerin alanlarının iki defa integralinin alınmasıyla bulunmuştur.

Eşik ivme değeri, yapının kalıcı deformasyon yapmaya başlayacağı kabul edilen ve kaymaya karşı güvenlik katsayını 1.0 değeri yapan akma limitini tanımlar. Daha öncesinden deformasyona dayalı tasarım başlığı altında yapılan kayan blok analiz yöntemlerinden farklı olarak; yakın fay yer hareketine ait fay yırtılma yönü, fay bileşeni ve zemin koşulllarının tahmini yatay kayma deplasmanları üzerindeki etkisi incelenmiştir.

Yakın fay yer hareketi özelliklerine ait kabul ve sınırlamalardan yola çıkılarak; yakın fay yer hareketine ait çeşitli deprem kayıtları kullanılarak ağırlık tipi kıyı duvarlarının deformasyona göre değerlendirilmelerinde kullanılmak üzere parametrik olarak bir dizi grafikler oluşturulmuş, ilgili birtakım formül önermesi yapılmıştır.

1. INTRODUCTION

In view of the significance of ports in today's society, obviously the extended loss of function of major ports for any reason could have major regional and even world-wide economic impacts. During the service life of port structures, destruction caused by an earthquake might be a not often event. However, even if it occurs once, the intensity of the earthquake results could be so big that the effects of earthquakes can be an important, of national interest. And thus, earthquakes perform low probability high consequence threats to the port structures. The consequences can be most devastating if a port happens to be located in the seismic source area. This was actually the case for Kobe, Japan, earthquake of 1995. The Kocaeli, earthquake of August 17, 1999 which is the most recent example for Turkey (PIANC, 2001). The Tokachi-Oki, Japan earthquake of 2003 (Kawamata et al., 2003) and The West of Fukuoka Prefecture Earthquake, Japan earthquake of 2005 are the most recent examples that port structures have damaged (Honda et al., 2005). Gravity type marine structures develop their resistance primarily from their own weights, and grip on the foundations. All the forces on structure such as resultant earth pressure behind the wall, resultant pressure forces of marine facilities, surface loadings, earthquake thrust and so on are resisted by the walls own weight and the base friction between foundation material and wall.

1.1 Motivation of the Thesis

Since a key requirement to analyze seismic design is a quantitative specification of the design ground motion. It is important to characterize between the level of ground shaking that a structure or facility is to resist safely. And also a parameter generally called a seismic coefficient that is used as input to a simplified, pseudo-static analysis. The resistance based design method expresses the safety and stability of a waterfront retaining structure subjected to static and/or dynamic earth and water forces in terms of the factor of safety against sliding along the base of the wall.

In addition to this, the ability of the wall to resist the earth and water forces acting to overturn the wall. This design method is called conventional design method. But, this design method does not give any information about the potential performance and damage of the structure under any possible seismic condition. In contrast to resistance based design, deformation based design considers the utility of the structure after an earthquake, predicting deformation, assessment of the structure. Additionally, it takes into account the associated damage for shakings above the limit equilibrium for the structure will be designed with operational and structural considerations including performance criteria and damage criteria. The possible damage to the elements of the load-bearing system due to certain levels of seismic ground motion is estimated quantitatively. It is checked if the damage to each element is under the limit of acceptable damage. Estimation of sliding deformation under near fault ground motion is the primary focus of this study. The typical characteristic of this study is concentrating on near fault ground motion parameters for any gravity type marine structure, which is different from previous sliding block analyis studies. The previous sliding block analyis studies had not specially researched near fault ground motion.

1.2 Scope of the Thesis

In this study, estimated minimum seaward displacement of a structure is computed by integrating the acceleration time history that exceeds the threshold limit for sliding over the duration until the structure ceases sliding by idealizing the structure sliding rigid block based on Newmark's method (1965). This analysis method is described as Simplified Dynamic Analysis in PIANC (2001). Threshold acceleration represents the yielding limit assuming with the permanent displacements founded beginning from this point. It acts the coefficient of safety against sliding is 1.0. Time histories dependent near fault ground motions are used with its rupture directivity, component and soil condition properties within some acceptance bounds. The study is different from the previous studies about seismic deformation based design related to estimate minimum permanent sliding displacements.

In Chapter 2, typical examples of seismic damage to gravity type marine structures are summarized.

In Chapter 3, a number of studies are expressed which define several approaches to make an appropriate deformation based design for gravity type marine structures.

In Chapter 4, seismic design approaches of gravity type marine structures are explained with referring to several design guides and related design approaches.

In Chapter 5, the study is explained under the title of deformation based design approach. In this context, firstly Newmark's Sliding Block Analysis has been referred. In addition to this the study has been explained. The earthquake motions parameters of Near Fault Groud Motion are used with in the study. Finally, the performed analysises and results have been presented respectively.

In Chapter 6, recommendations and conclusions of the study have been mentioned.

In Appendices, earthquake records used in study, detail of regression analysis and a number of figures related to analysis results have been presented. In Appendix G, a case study is evaluated considering deformation based design and sliding block analysis methods. The results are compared with this study and previous similar studies.

2. DAMAGE TO GRAVITY TYPE MARINE STRUCTURES IN PAST EARTHQUAKES

Gravity type marine structures have sustained important to destructive damage in a number of earthquakes for many years. There are many failure types valid for gravity type marine structures, caused by earthquake such as seaward displacement, settlement, tilting, liquefaction, foundation collapse, deformation of soil.

For gravity quay walls on firm foundations, typical failure modes during earthquakes are seaward displacements and tilting as shown in (**Figure 2.1**). For a loose backfill or natural loose sandy foundation, the failure modes involve overall deformation of the foundation beneath the wall, resulting in large displacement away from the shoreline, tilting and settlements (**Figure 2.2**) (PIANC, 2001).

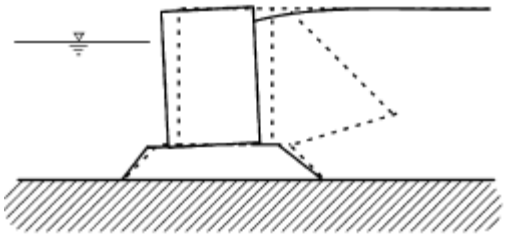

Figure 2.1 : Deformation/failure modes of gravity quay wall on firm foundation (PIANC, 2001)

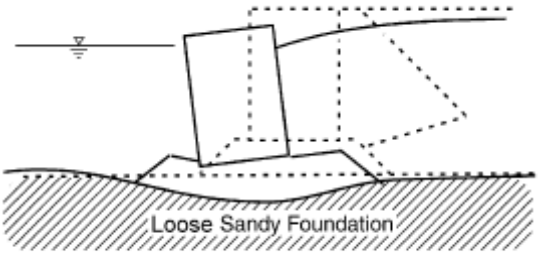

Figure 2.2 : Deformation/failure modes of gravity quay wall on loose sandy foundation (PIANC, 2001)

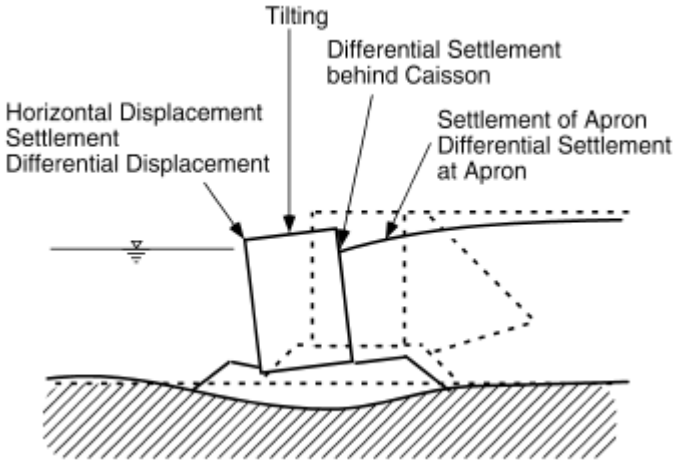

Figure 2.3 : Parameters for specifying damage criteria for gravity quay wall (PIANC, 2001)

Parameters that may be used for specifying damage criteria include displacements, settlements, tilting, and differential displacements along the face line of a wall, and the deformations at apron including settlement, differential settlement at and behind apron, and tilting (**Figure 2.3**).

As indicated in PIANC (2001), deformation and failure types should be summarized as follows:

- Most damage to port structures is often associated with significant deformation of a soft or liquefiable soil deposit.

- Most failures of port structures, from a practical perspective, result from excessive deformations, not catastrophic collapses.

- Most damage to port structures is the result of soil-structure interaction.

Typical examples of seismic damage to gravity type port structures are summarized in (**Table 2.1**).

Table 2.1: Typical examples of seismic damage to gravity type port structures

Earthquake	Year	Country	Port	Damage Type
Nihonkai-Chubu	1983	Japan	Akita Port	-Liquefaction
Great Hanshin	1995	Japan	Kobe	-Seaward Displacement -Settlement -Tilt -Liquefaction
Kocaeli	1999	Turkey	Haydarpaşa	-Minor damage
			Tuzla	-Movement of quay wall -Backfill settlement
			Derince	-Movement of quay wall -Backfill settlement
Tokachi-Oki	2003	Japan	Hiroo-cho, Hiroo-gun	-Movement of quay wall
			Toyokoro-cho, Nakagawa-gun	-Movement of quay wall -Liquefaction
			Kushiro-shi	-Movement of quay wall -Liquefaction
West of Fukuoka Prefecture Earthquake	2005	Japan	Suzaki	-Movement of quay wall -Liquefaction
			Chuo-Pier	-Movement of quay wall -Settlement behind wall

Some case histories are presented in (**Figure 2.4**) and (**Figure 2.5**) to clarify the typical damage to gravity quay walls referred to PIANC (2001). Structural and seismic conditions and seismic performance of case histories are summarized in (**Table 2.2**) and (**Table 2.3**) for each figure respectively.

Table 2.2: Structural and seismic summary of the case history of Kushiro Port, Japan (PIANC, 2001)

Structural and seismic conditions	Structure and location: East Quay, Kita Wharf, East Port District Height: + 2.5 m Water depth: – 8.5 m Design seismic coefficient: k_h = 0.15 Construction (completed): 1950 Earthquake: January 15, 1993 Kushiro-Oki earthquake Magnitude: M_J = 7.8 (JMA) Peak ground surface acceleration (a_{max}): 0.47 g Peak ground surface velocity (v_{max}): 0.63 m/s a_{max}/v_{max} evaluated based on strong motion earthquake records.
Seismic performance	Horizontal displacement: 1.9 m Vertical displacement: 0.2 to 0.5 m
Cross section:	Caisson quay wall

The damage had been caused because of liquefaction of backfill as declared in PIANC (2001). Seaward horizontal displacement of caisson constructed on firm foundation had been measured 1.9m. The damage also leads to vertical displacement.

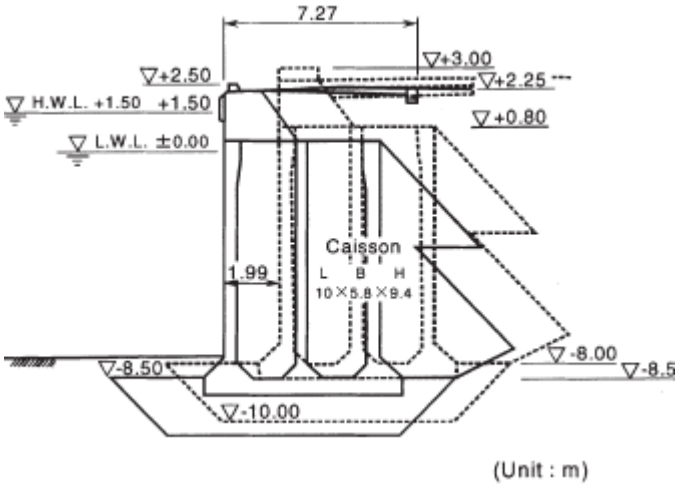

Figure 2.4 : Deformation/failure modes of gravity quay walls. Cross section of a caisson quay wall at Kushiro Port (PIANC, 2001)

Table 2.3: Structural and seismic summary of the case history of Kobe Port, Japan (PIANC, 2001)

Structural and seismic conditions	Structure and location: Breakwater No. 7 Height: + 5.0 m Water depth: – 15.0 m Construction (completed): 1970–1972 Earthquake: January 17, 1995 Hyogoken-Nambu earthquake Magnitude: M_J = 7.2 (JMA) Peak ground surface acceleration (a_{max}): 0.53 g Peak ground surface velocity (v_{max}): 1.06 m/s a_{max} / v_{max} evaluated based on strong motion earthquake records.
Seismic performance	Horizontal displacement: 0.6 m Vertical displacement: 1.4 to 2.6 m
Cross section:	Vertical composite type

Typical failure mode of the case history of Kobe port is settlement associated with significant foundation deformation beneath the caisson/rubble foundation as referred PIANC (2001).

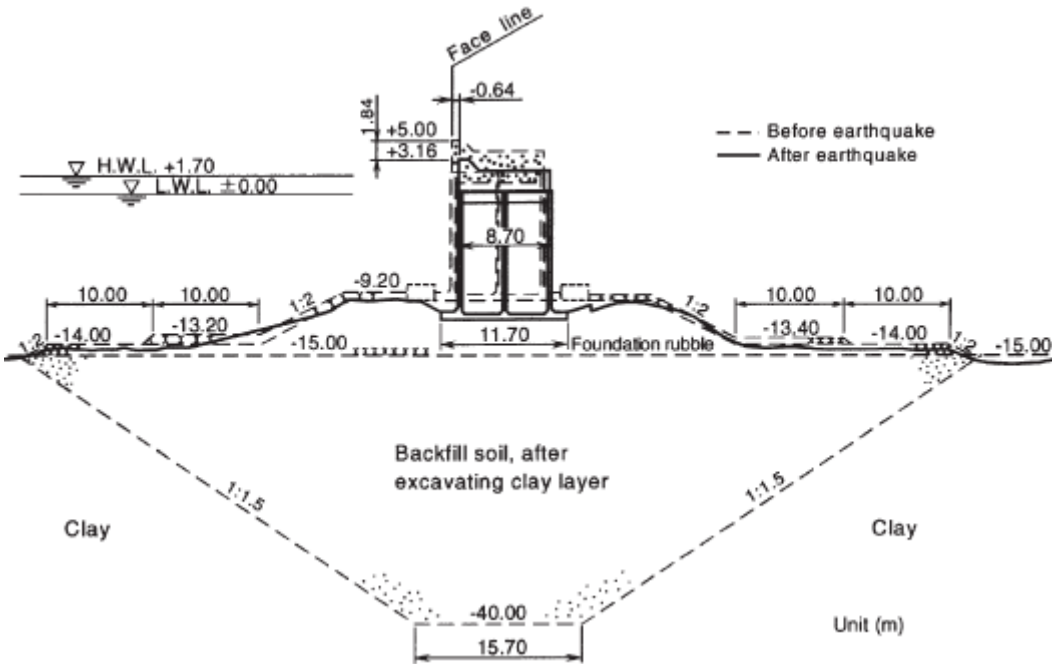

Figure 2.5 : Deformation/failure modes of gravity quay walls. Cross section of a caisson quay wall at Kobe Port (PIANC, 2001)

3. LITERATURE REVIEW

Deformation based design has been developed to overcome force balance conventional seismic design. In deformation based design, two earthquake levels define the design earthquake motions. Displacement specifies the required performance of the structure, and varying levels of the earthquake motions defines stress levels. Based on the analogy of a rigid block sliding, Newmark (1965) developed a technique to estimate limited induced slope movements in earthquakes. His approach has been used extensively and described by numerous authors. He proposed a formula by integrating the several earthquake acceleration record two times to compute the maximum displacement of a slope for a given yield acceleration (Equation 3.1). Yield (threshold) acceleration makes the coefficient of safety against sliding is 1.0. Yield acceleration is obtained from pseudo-static analysis methods. Generally, the other authors also used pseudo static analysis procedure to calculate yield acceleration values. In the sliding block analysis, structural and geotechnical conditions are represented by a threshold acceleration for sliding (PIANC, 2001).

$$d_{\max} = \frac{v^2_{\max}}{2a_y}\frac{a_{\max}}{a_y} \qquad \textbf{(3.1)}$$

d_{max} is the maximum permanent displacement (cm), v_{max} is the peak ground velocity (cm/s), a_{max} is the peak ground acceleration (cm/s^2), and a_y is the yield acceleration (cm/s^2).

Numerical studies based on the sliding block method of analysis have led to the development of simplified relationships between ground motion intensity and seismically-induced deformations (PIANC, 2001). Chang et al. (1977) indicated using numerical integration techniques to compute the net displacement of a soil slope by using a measured or predicted seismic acceleration history. They proposed a chart which contains slide displacements related to the ratio of threshold acceleration and peak ground acceleration (**Figure 3. 1**). They used a large database of nearly 200 earthquake records, conservative envelopes for evaluating sliding displacements. The

results were obtanied from a peak acceleration and velocity of 0.5g and 76 cm/s, respectively (PIANC, 2001).

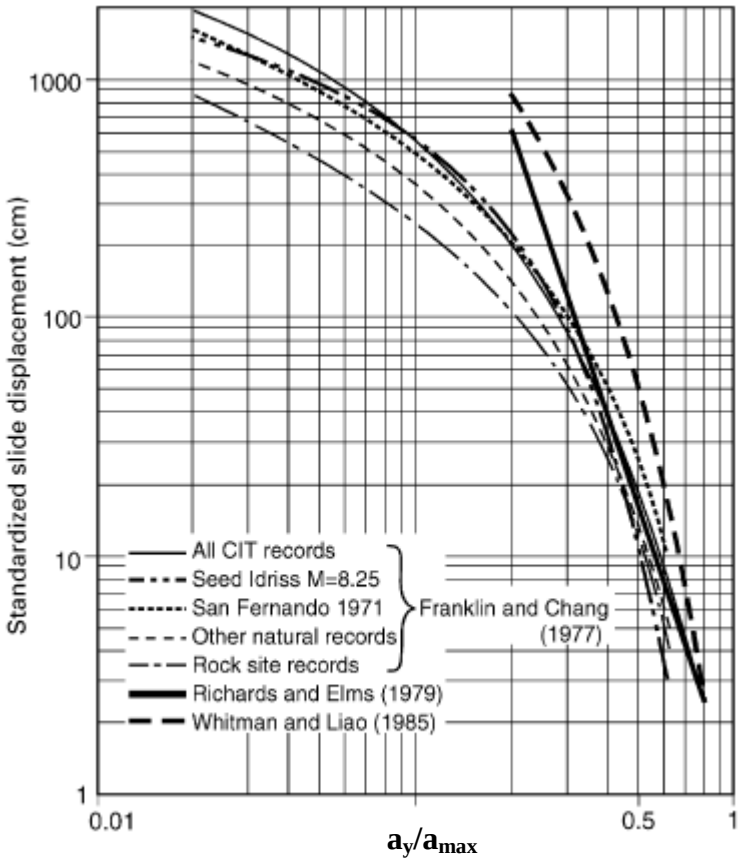

Figure 3. 1 : Proposed simplified results for evaluating sliding displacement of Chang et al. (1977) refer to PIANC (2001)

The Richards and Elms (1979) procedure was developed using a sliding block analogy to calculate the magnitude of wall displacements in sliding during earthquake shaking (Equation 3.2). The formula is valid for $a_y/a_{max} \geq 0.3$. They define yield acceleration as the level of acceleration that is just large enough to cause the wall on its base (Kramer, 1996).

$$d_{\max} = 0.087 \frac{v^2_{\max} a^3_{\max}}{a^4_y} \qquad \textbf{(3.2)}$$

d_{max} is the maximum permanent lateral displacement (cm), v_{max} is the peak ground velocity (cm/s), a_y is the yield acceleration (cm/s^2), and a_{max} is the peak ground acceleration (cm/s^2). The 0.087 is a dimensionless coefficient. Equation 3.2 provides displacement estimations that are close to the predicted maximum displacements (Equation 3.1) of Newmark (1965).

Nadim and Whitman (1984) developed a method to evaluate permanent rotation and sliding movements of gravity retaining walls with dry, cohesionless backfill. Whitman and Liao (1985) improved their procedure by using statistical methods to address the several sources of uncertainty in the displacement controlled procedure by using the results of sliding block analyses of 14 ground motions by Wong (1982). They proposed a formula in which the permanent displacements were lognormally distributed with mean value (Equation 3.3). The formula is valid for $a_y/a_{max} \geq 0.4$.

$$d_{\max} = \left(\frac{37 v^2_{\max}}{a_{\max}} \right) \exp\left(-\frac{9.4 a_y}{a_{\max}} \right) \qquad \textbf{(3.3)}$$

d_{max} is the mean maximum permanent lateral displacement (cm), v_{max} is the peak ground velocity (cm/s), a_y is the yield acceleration (cm/s^2), and a_{max} is the peak ground acceleration (cm/s^2). *37* and *-9.4* values in the formula are dimensionless coefficients. The matching of Chang et al. (1977) proposition, The Richards and Elms (1979) procedure and Nadim and Whitman (1984) method can be seen on (**Figure 3. 1**). The number and properties of earthquake records and also determining of yield acceleration may make difference between these formulas. Newmark (1965), Chang et al. (1977), Richards and Elms (1979), Nadim and Whitman (1984) had not considered vertical acceleration on their formulas.

As it is mentioned in next sections, this study is essentially an idealization of sliding block analysis with its specific assumptions. The comparison of the results of this study with the aforementioned previous sliding block analyis methods are matched. Same peak ground accelerations (a_{max}) and same peak ground velocities (v_{max}) are used to compute the maximum sliding displacements considering near fault ground motion properties for each constant yield (threshold) acceleration (a_y) values (0.10g, 0.15g, 0.20g, 0.25g, 0.30g, 0.35g, 0.40g, 0.45g, and 0.50g). All the calculated sliding displacements feature same fault normal component, forward directivity, and soil conditions. Newmark (1965), Richards and Elms (1979), Whitman and Liao (1985) have been compared with the proposal formulated equations (Equation 5.7, Equation 5.8, and Equation 5.9) of this study. Any ratio of a_y/a_{max} has not taken into consideration. Proposed simplified results for evaluating maximum sliding displacement of Thesis Study (2011) for constant yield acceleration $a_y=0.10g$ presented in the following figure (**Figure 3. 2**).

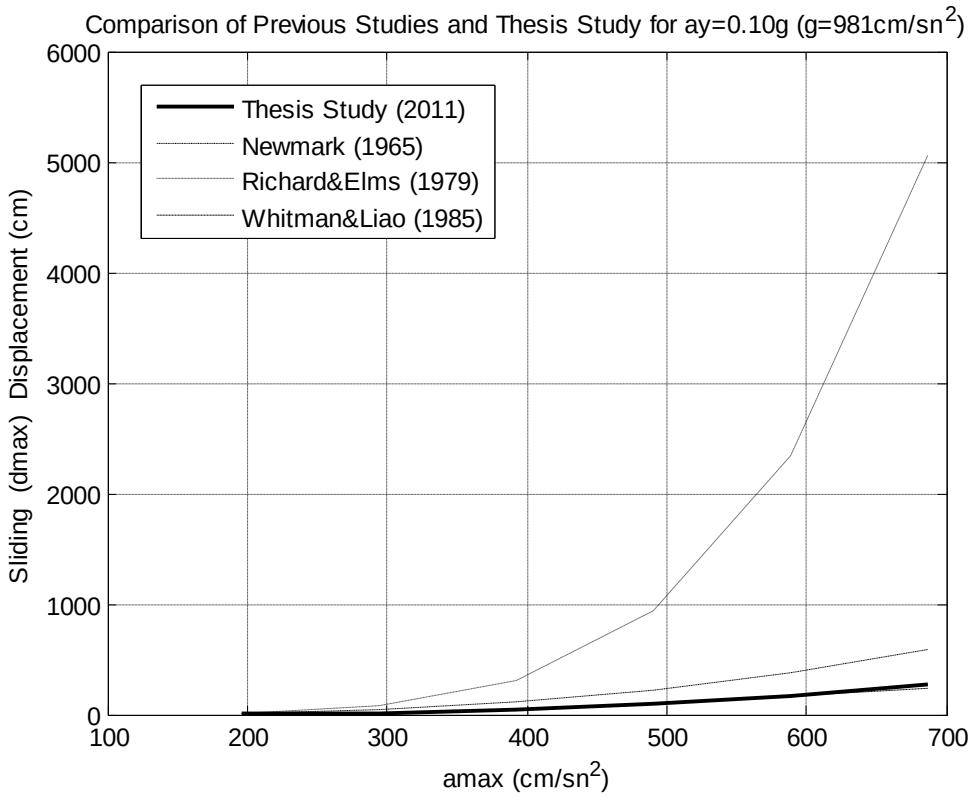

Figure 3. 2 : Proposed simplified results for evaluating sliding displacement of Thesis Study (2011) for constant yield acceleration $a_y=0.10g$

As it can be seen (**Figure 3. 2**), the curve considered proposed equations with respect to the results of this study shows similar distribution with Richard&Elms (1979) especially with Whitman&Liao (1985). Here, Whitman&Liao (1985) and the curve of the study seem like matched up with one another . They have close analogy. On the other hand, the curve of the study and Richard&Elms (1979) appears like interrelated and show parallel distribution. Newmark (1965) does not have any clear similarity with the curve of the study relatively to the others. And also, it has no any distinct similarity with Whitman&Liao (1985) and Richard&Elms (1979). Newmark (1965) did not use any earhtquake record to develop his approach and method. His approach is just a displacement estimation technique based mathematical integration. It is thought that this is the main reason of the marked difference between with the other studies. Highly variable nature of ground motion characteristics effect computed displacement and make displacement variable. The typical characteristic of this study is the consideration of Near Fault Ground Motion characteristics. On the other hand, the small differecences between the curve of this study and Richard&Elms (1979) and Whitman&Liao (1985) may be caused because of the

number and characteristics of earthquake records used for statistical analysis. And also, the ratio of a_y/a_{max} may be an other reason of the differences between the each method based computed displacements. The similar analogy between this study and other studies can be seen on other figures. The other comparison figures considered the rest of constant yield acceleration values (0.15g, 0.20g, 0.25g, 0.30g, 0.35g, 0.40g, 0.45g, and 0.50g) are presented in App. E.

Iai and Ichii (1998) declared their study on the seismic deformation based design for port structures. In the seismic design it is needed to define the required performance of a structure in terms of stress levels and allowable displacements by considering the seismic performance criteria. ASCE (1998) published a seismic guideline name called "Seismic Guidelines for Ports". This guideline intends to provide a first step in the eventual development of a nationally recognized manual of recommended seismic risk reduction practice for seaports and inland waterway ports throughout the United States. ASCE (1998) contains a summary of the state of knowledge and practice for evaluating seismic risks to port systems and components. And also, for reducing these risks through sound engineering design, analysis, and strengthening measures as well as emergency response and recovery planning have been recommended. "Seismic Design Guidelines for Port Structures" published by PIANC (2001) which covers the basic limitations in conventional design, and establish the background for a new design approach. The guideline specially aimed to be deformation based, permitting a certain degree of damage depending on the specific functions and response characteristics of a port structure and probability of earthquake occurrence in the region. Ichii (2002, 2004) proposed an approach by using a simulation to achieve the fragility curve for each damage level to estimate displacement of quay wall. A new seismic design code DLH-DTY enforced in Turkey (2008) for transportation structures officially administered by RHA that most important aspect of the code rests on its main approach incorporating "performance-based design". The code refers deformation based seismic design approach as well as strength based conventional method and covers the classification of port structures, definition of deformation-based performance levels, multi-level earthquake actions and performance objectives.

4. SEISMIC DESIGN APPROACHES OF GRAVITY TYPE MARINE STRUCTURES

There are many developed design methods for gravity type marine structures during earthquakes by using different approaches. A whole seismic design procedure shall consist of the following elements:

-Decision of seismic performance requirements

-Assignment and specification of loads

-Estimation and evaluation of the economics of the design and the reliability of the structure.

Seismic analyses for gravity type marine structures focuses on the dynamic behavior of the foundation and backfill soils, as well as the overall stability of the walls. Potential failure modes include; sliding, overturning, bearing capacity failure, and deep seated instability.

4.1 Design Methods

4.1.1 Resistance Based Design

The most commonly used seismic design methods for gravity structures are based on standard pseudo static limit equilibrium methods of analysis. Pseudo static methods of analysis is based on ensuring stability of the system and adequacy of structural elements resistance. The analysis must be in accordance with the linear elastic analysis performed under the influence of reduced equivalent forces, wherein a static horizontal seismic coefficient is applied as an additional body force. Horizontal seismic coefficient is defined for Level 1 (L1) and Level 2 (L2) seperately as per DLH-DTY (2008) in Equation 4.1 and Equation 4.2 respectively.

$$k_h = \frac{2}{3}\left(\frac{a_{\max}}{g}\right) \qquad \textbf{(4.1)}$$

k_h is the dimensionless horizontal seismic coefficient, a_{max} (cm/s^2) is the maximum horizontal pseudo static acceleration and g (cm/s^2) is the gravitational acceleration.

$$k_h = \left(\frac{a_{\max}}{g} \right) \qquad a_{\max} \le 0.20g$$
$$k_h = \frac{1}{3}\left(\frac{a_{\max}}{g} \right)^{1/3} \qquad a_{\max} > 0.20g \qquad \textbf{(4.2)}$$

k_h is the dimensionless horizontal seismic coefficient, a_{max} (cm/s^2) is the maximum horizontal pseudo static acceleration and g (cm/s^2) is the gravitational acceleration. For simplicity, it is often assumed in design practice that vertical seismic coefficient $k_v = 0$.

Horizontal seismic coefficient is a dimensionless coefficient applied to the mass of the structure. If force balance design is based on a more frequent seismic event, then it is difficult to estimate the seismic performance of the structure when subjected to ground motions that are greater than those used in design (PIANC, 2001). In this design approach the stability inspection of the system is defined with factor of safeties against for both sliding and overturning.

$$F_{sk} = \frac{\mu W}{P} \qquad \textbf{(4.3)}$$

F_{sk} is the factor of safety against sliding, W and P are resultant vertical and horizontal loads and μ is the bottom friction coefficient.

$$F_{sd} = \frac{eW}{M_d} \qquad \textbf{(4.4)}$$

F_{sd} is the factor of safety against overturning, e is the horizontal distance between the resultant vertical load and the seaward side of the quay wall toe, W is resultant vertical load, M_d is the sum of horizontal load moments in relation to the wall base, in other words it is the total overturning moment. Factor of safety against sliding F_{sk} and factor of safety against overturning F_{sd} for gravity type marine structures refer to DLH-DTY (2008) are summarised in the following table (**Table 4.1**).

Table 4.1: Acceptable level of factor of safeties against sliding and overturning (DLH-DTY, 2008)

Stability Inspection	MD (Minimum Damage) Level 1 (L1)	CD (Controlled Damage) Level 2 (L2)
Sliding	1.2	1.0
Overturning	1.3	1.1

4.1.2 Deformation Based Design

4.1.2.1 Design Approach

Even if the stability of the structure is satisfied against sliding with acceptable factor of safety values, this does not mean that the structure will have zero sliding under earthquake effects. The gravity structure may slide and may displace toward sea under any factor of safety. Uwabe (1983) proposed an emprical method for estimating the approximately damage related factor of safety during an earthquake (**Table 4.2**).

Table 4.2: Empirical equations for a gravity quay wall Uwabe (1983) (PIANC, 2001)

Deformation	Empirical equations**	Correlation coefficient	Standard deviation
Max. horizontal displacement (cm)	$d = -74.2 + 98.2(1/F_s)$	0.34	130
Settlement of gravity wall (cm)	$s = -16.5 + 32.9(1/F_s)$	0.50	30
Normalized displacement* (%)	$r = -7.0 + 10.9(1/F_s)$	0.38	13

* Maximum horizontal displacement normalized with a wall height *H*.
** F_s: Factor of safety against earthquake = k_y/k_h
k_y: Yield (threshold) seismic coefficient from pseudo static analysis
k_h: Equivalent seismic coefficient based on design level ground motions

Considering a factor of safety against earthquake for induced deformation during an earthquake calculated as presented above estimated maximum horizontal displacement can be predicted. Here, yield (threshold) seismic coefficient is determined from pseudo static analysis. It corresponds the yield acceleration, that yield acceleration $a_y=k_yg$. As can be seen from Uwabe (1983), the gravity structure can be damaged due to sliding and displacement for a considered factor of safety against earthquake.

Conventional resistance based design does not give information on the performance of a structure even though when the limit of the force balance is achieved or

exceeded. The damage to elements of the load-bearing system due to certain levels of seismic ground motions is estimated quantitatively. It is checked if the damage to each element is under the limit of acceptable damage. Limits of acceptable damage are defined to comply with performance level objectives foreseen for the structure on various earthquake levels. Due to the fact that the seismic damage to be calculated on the element level generally occurs beyond linear elastic borders in response to nonlinear deformation or displacement in line with deformation during severe earthquakes. Performance-based design is an emerging methodology, which was born from the lessons learned from earthquakes in the 1990s (SEAOC, 1995; Iai and Ichii, 1998; Steedman, 1998). Deformation based design recognizes that a port structure's performance is measured by the amount of damage it sustains due to seismic effects. This damage must be limited so that its economic, operational, life-safety, and environmental impacts are acceptable to the owner and, in the case of a port, to port stakeholders as well (ASCE, 1998). However, the structure is designed to resist a decided in advance level of seismic loading specified due to seismic acceleration in resistance based design approach. This design approach does not provide information on the degree of damage, the loss of serviceability. In contrast to resistance based design, deformation based design takes into account the serviceability, predicting deformation, assessment of the structure and the related damage for shakings above the limit equilibrium for the structure will be designed. Earthquake levels to be taken into account in deformation based design as design reference motions defined Level 1 (L1) and Level 2 (L2) in both PIANC (2001) and ASCE (1998). DLH-DTY (2008) defined Level 3 (L3) in addition to both PIANC (2001) and ASCE (1998). The Earthquake Level 1 (L1) represents seismic ground motions that are likely to occur relatively often but of not very high intensity during the service time of structures. The Earthquake Level 1 (L1) has the exceedance probability of 50% in 50 years, which corresponds to a return period of 72 years. The Earthquake Level 2 (L2) represents seismic ground motions that are not very likely to occur, rare but of very high intensity during the service time of structures. The Earthquake Level 2 (L2) has the exceedance probability of 10% in 50 years, which corresponds to a return period of 475 years. The Earthquake Level 3 (L3) represents the most severe seismic ground motions that structures. The rare (L3) level earthquakes have the probability of exceedance of 2% in 50 years, which corresponds to a return period of 2475 years. Based on operational and structural

considerations the damage caused by a specific earthquake is classified according to DLH-DTY (2008) in four levels as shown in (**Table 4.3**).

Table 4.3: Acceptable level of damage in performance-based design (DLH-DTY, 2008)

Level of damage	Structural	Operational
MD: Minimum Damage	Minor or no damage	Little or no loss of workability
CD: Controlled Damage	Controlled damage	Short term loss of workability
ED: Extensive Damage	Extensive damage in near collapse	Long term or complete loss of workability
SC: State of Collapse	Complete loss of structure	Complete loss of workability

As referred to DLH-DTY (2008) the required performance of a structure may be specified by the appropriate performance grade Special, Normal, Simple, or Unimportant defined in (**Table 4.4**). In deformation based design, a structure is designed to satisfy these performance grades.

Table 4.4: Performance grades (DLH-DTY, 2008)

Performance grade	Design earthquake		
	Level 1 (L1)	Level 2 (L2)	Level 3 (L3)
Special	-	MD	CD
Normal	MD	CD	(ED)
Simple	CD	(ED)	-
Unimportant	(ED)	(SC)	-

Special grade structures are those with a possible for huge loss of human life and property. These grade type structures are needed to be undamaged for improvement purposes, installations handling hazardous materials. Normal grade structures have less serious effects than Special grade structures, or if damaged, are difficult to restores. These grade type structures needs difficult and time consuming repair and retrofit after an earthquake. Simple structures are ordinary structures, and Unimportant grade structures are small, easily restorable structures.

4.1.2.2 Damage Criteria for Gravity Type Marine Structures

(**Figure 2.3**) shows the potential failure modes for giving description to the damage criteria for gravity quay wall. A wall with a relatively small width to height ratio, typically less than about 0.75, will exhibit a predominant tilting failure mode rather than horizontal displacements (PIANC, 2001). (**Table 4.5**) shows the proposed and acceptable displacement/deformation criteria for (MD) and (CD) performance levels gravity quay walls (DLH-DTY, 2008).

Table 4.5: Proposed damage criteria for gravity quay walls (DLH-DTY, 2008)

Displacement/Deformation Limits	Performance Level	
	MD	CD
Ratio of residual horizontal displacement to wall height (%)	<1.5	1.5-5
Residual tilting towards the sea (degrees)	<3	3-5
Differential settlement on apron (cm)	3-10	-
Differential settlement between apron and non-apron areas (cm)	30-70	-

5. ESTIMATION OF SLIDING DISPLACEMENT GRAVITY WALLS

5.1 Methodology

As mentioned in PIANC (2001) several numerical studies based on the sliding block method of analysis. These analyis methods have guided to the development of simplified relationships between ground motion intensity and seismically induced deformations. Considering Newmark's sliding block analysis (1965), this study incorporates lateral movements explicitly in the stability analysis of an any rigid gravity structure, founded on a rigid soil for near fault ground motion properties. Assuming when the factor of safety against sliding is around 1.0, the potential failure mass of the soil behind the structure is no longer in equilibrium that the active wedge mobilizes the structure with the dynamic thrust. As a consequence, the structure will be accelerated by the unbalanced forces. Newmark (1965) used this analogy to develop a method for prediction of the permanent displacement of a slope subjected to any ground motion. This procedure of analysis represents an alternative to the conventional equilibrium method of analysis which expresses the stability of a rigid wall in terms of a selected factor of safety against sliding along its base. The proposal of this study is, in effect, a procedure for choosing a horizontal seismic coefficient or ground velocity based upon explicit choice of an allowable residual displacement. This study considers the damage criteria of performance design approach for especially near fault ground motion with their component, directivity and soil conditions. No safety factor is applied assuming the factor of safety against sliding is around 1.0. The level of factor of safety is incorporated into the step used to calculate the horizontal seismic coefficient. It is called yield (threshold) acceleration will cause the structure to move relative to the sliding plane.

Since earthquake based accelerations vary during an earthquake, the pseudo static factor of safety will vary throughout an earthquake. Factor of safety does not give any information about deformations associated with displacement. Because of the serviceability of a structure after an earthquake is controlled by deformations, analyses shall predict the seaward displacements to provide a more useful approach

for seismic design of gravity type marine structures. Newmark (1965) sliding block approach concludes that permanent displacement begins during earthquake based inertial forces acting on a potential sliding mass exceed the yield resistance of the slip surface. Rigid soil and block behavior, and one direction occurred displacement, and ignored vertical accelerations are the main assumptions of Newmark's proposal. Newmark (1965) considered the behavior of a slope under such conditions. When the factor of safety is less than 1.0, the potential failure mass is not in equilibrium. Factor of safety, 1.0, is obtained with iterations. Consequently, it will be accelerated by the unbalanced force. The situation is analogous to that of a block resting on an inclined plane (**Figure 5.1**). Newmark used this analogy to develop a method for prediction of the permanent displacement of a slope related to any ground motion.

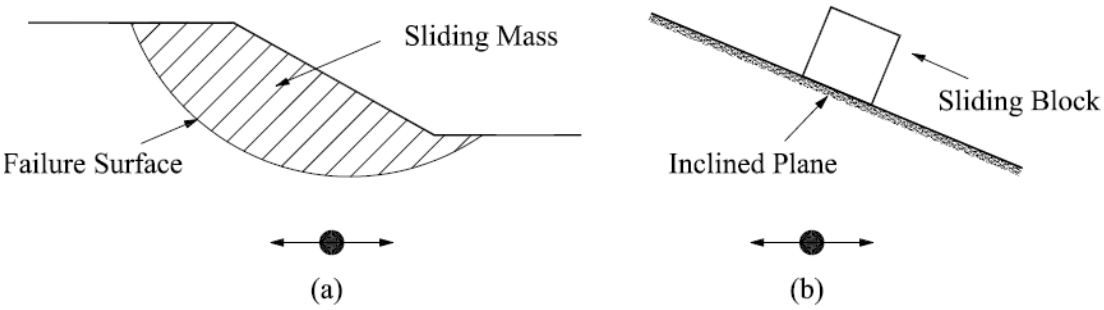

Figure 5.1: Analogy between (a) potential landside and (b) block resting on inclined (Kramer, 1996)

It is considered that the block is in stable, static equilibrium on the inclined plane of (**Figure 5.1**). Stability of the block in the direction parallel to the plane demands that the achievable static resisting force, R_S, exceed the static acting force, D_S under static conditions (**Figure 5.2**). It is assumed that the block's resistance to sliding is completely frictional (c=0). ϕ is the angle of friction between the block and plane.

$$FS = \frac{Achievable\ resisting\ force}{Static\ acting\ force} = \frac{R_S}{D_S} = \frac{W\cos\beta\tan\phi}{W\sin\beta} = \frac{\tan\phi}{\tan\beta} \qquad \textbf{(5.1)}$$

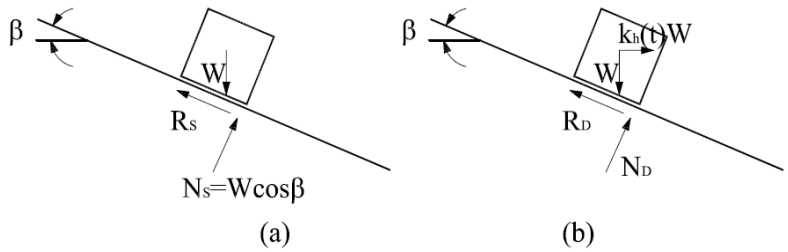

Figure 5.2: Forces acting on a block resting on an inclined plane: (a) static conditions; (b) dynamic conditions (Kramer, 1996)

For simplicity, the effects of vertical accelerations are neglected. The effect of inertial forces transmitted to the block by horizontal vibration of the inclined plane is defined with the acceleration $a_h(t)=k_h(t)g$. Here, k_h is a dimensionless coefficient. Horizontal acceleration of the block causes a horizontal inertial force, k_hW, at a particular instant of time (**Figure 5.2**). When the inertial force acts in the downslope direction, resolving forces perpendicular to the inclined plane gives

$$FS_d(t)=\frac{Achievable\ resisting\ force}{Pseudo\ static\ acting\ force}=\frac{R_d(t)}{D_d(t)}=\frac{\cos\beta-k_h(t)\sin\beta\ \tan\phi}{\sin\beta+k_h(t)\cos\beta} \qquad \textbf{(5.2)}$$

It is seen that, the dynamic factor of safety decreases as k_h increases. This coefficient, called the yield coefficient (threshold), k_y, corresponds the yield acceleration, $a_y=k_yg$. The yield acceleration is the minimum pseudo static acceleration required to result in instability of the block.

While a block on an inclined plane is subjected to pulse of acceleration that exceeds the yield acceleration, the block will move relative to the plane. To illustrate the procedure by which the resulting permanent displacements to be calculated, by considering the case in which an inclined plane is subjected to a single rectangular acceleration pulse of amplitude A and duration Δt.

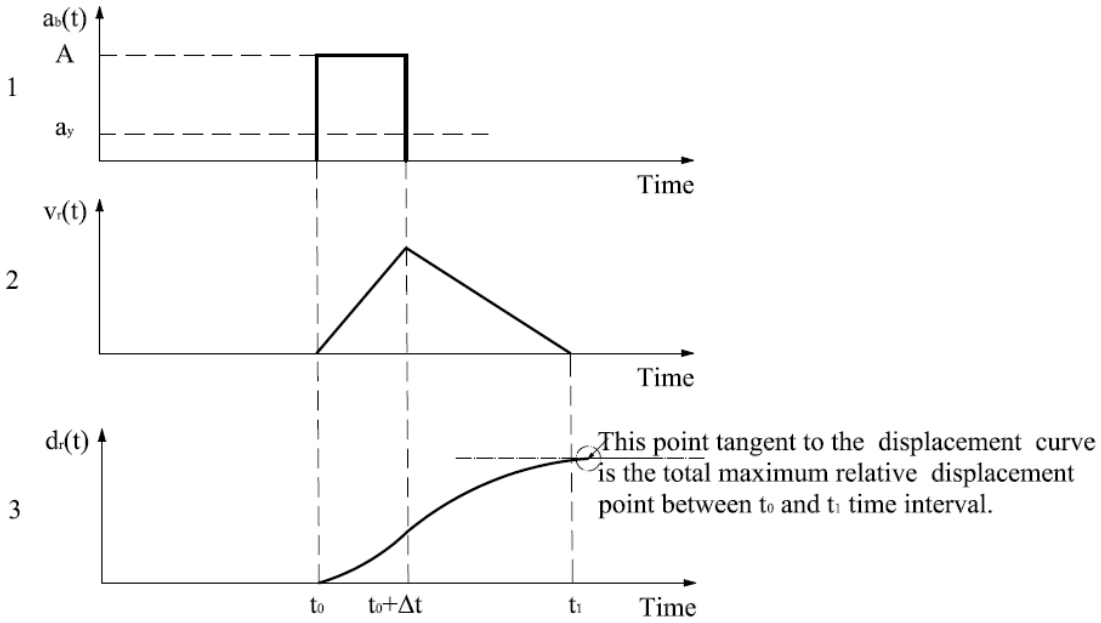

Figure 5. 3: Variation of relative velocity and relative displacement between sliding block and plane (Kramer, 1996)

If the yield acceleration, a_y, is less than A, the acceleration of the block relative to the plane during the period from t_0 to $t_0+\Delta t$ is

$$a_{rel}(t) = a_b(t) - a_y = A - a_y \qquad t_0 \le t \le t_0 + \Delta t \tag{5.3}$$

$a_b(t)$ is the acceleration of the inclined plane. The resulting permanent displacements can be calculated by considering his assumption by integrating the relative acceleration twice.

$$v_{rel}(t) = \int_{t_0}^{t} a_{rel}(t)dt = \left[A - a_y \right](t - t_0) \qquad t_0 \le t \le t_0 + \Delta t \tag{5.4}$$

$v_{rel}(t)$ is the relative velocity.

$$d_{rel}(t) = \int_{t_0}^{t} v_{rel}(t)dt = \frac{1}{2}\left[A - a_y \right](t - t_0)^2 \qquad t_0 \le t \le t_0 + \Delta t \tag{5.5}$$

$d_{rel}(t)$ is the total relative displacement.

As seen from (**Figure 5. 3**) at $t=t+\Delta t$, the relavite velocity reaches maximum value. The sliding block is decelerated by friction force acting on its base following the base acceleration decreases to zero (at $t=t_0+\Delta t$). The block undergoes negative acceleration, or deceleration, during the interval $t_0+\Delta t \le t \le t_1$. The relative velocity decreases which eventually reaches zero in this interval. The block continues to slide on the plane with its own inertia. After time t_1 the block and inclined plane slide together. During the total period of time between $t=t_0$ and $t=t_1$ the relative movement of the block is as shown in (**Figure 5. 3).** Between t_0 and $t_0+\Delta t$ the relative velocity increases linearly and the relative displacement quadratically. At $t_0+\Delta t$, the relative velocity has reached its maximum value, after which it decreases linearly. The relative displacement continues to increase (but at a decreasing rate) until $t=t_1$. The resultant relative displacement depends certainly on both the amount by which and the length of time that the yield acceleration is exceeded. This proposes that the relative displacement caused by a single pulse of strong ground motion should be related with both the amplitude and the frequency content of that pulse. On the other hand, an earthquake motion can exceed the yield acceleration a number of times and related to this produce a number of increments of displacement in fact. Thus the total

displacement will be influenced by strong ground motion duration with amplitude and frequency content.

5.2 Selection of Near Fault Ground Motion Records

Near fault earthquake is the motion that close to the epicenter and seismic source, and the far field earthquake motion is beyond the near fault and far to the seismic source. As referred to Somerville (1997) strong ground motions at locations near the earthquake source are strongly influenced by the geometry of the fault and the rupture directivity relative to the site. The near fault rupture directivity pulse is a narrow band pulse. The frequency of the pulse decreases with magnitude. It has high period, high amplitude and high velocity characteristic. Near fault ground motions are different from ordinary ground motions in that they often contain strong coherent dynamic long period pulses and permanent ground displacements (Somerville, 2003).

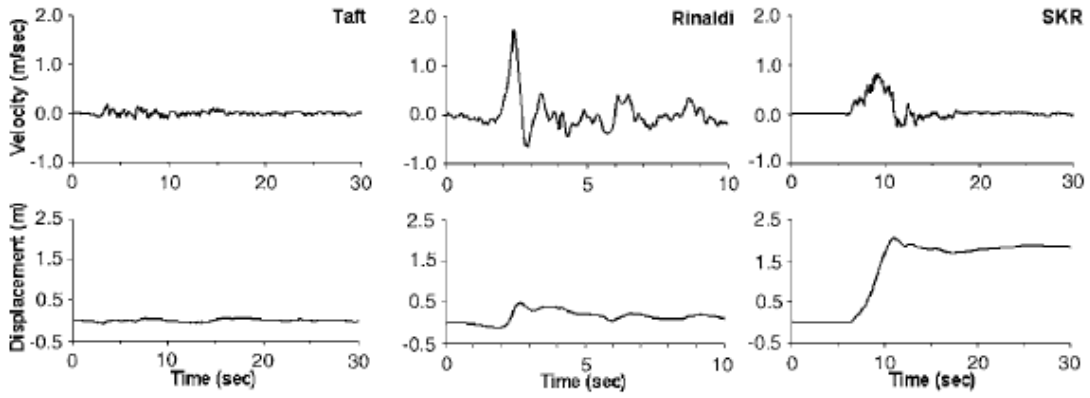

Figure 5. 4: Typical velocity and displacement time histories of (a) far-fault, (b) near-fault (forward-directivity), and (c) near-fault (fling-step) ground motions (Kalkan et al., 2006)

The velocity and displacement time histories of typical near-fault ground motions having forward-directivity (Rinaldi record of 1994 Northridge earthquake) and fling-step (Sakarya—SKR record of 1999 Kocaeli earthquake) effects are compared to that of ordinary far-fault motion (Taft record of 1952 Kern County earthquake) in (**Figure 5. 6**). High-velocity pulses are quite distinctive for Rinaldi and SKR records; such pulses do not exist in a typical far-fault ground motion like Taft (Kalkan et al., 2006). The radiation pattern, faulting process, of the shear dislocation of the fault causes the pulse to be mostly adapted perpendicular to the fault. This causes the fault-normal component of the motion to be more severe than the fault-parallel

component. Depending on the rupture directivity the forward directivity occurs when the rupture propagates toward the site and the direction of the slip on the fault is justified with the site. However, the backward directivity occurs when the rupture propagates in the rear of the site (Chen, 2003). As seen in (**Figure 5. 5**), forward directivity has high amplitude and high velocity. On the other hand, backward directivity has low velocity and low amplitude.

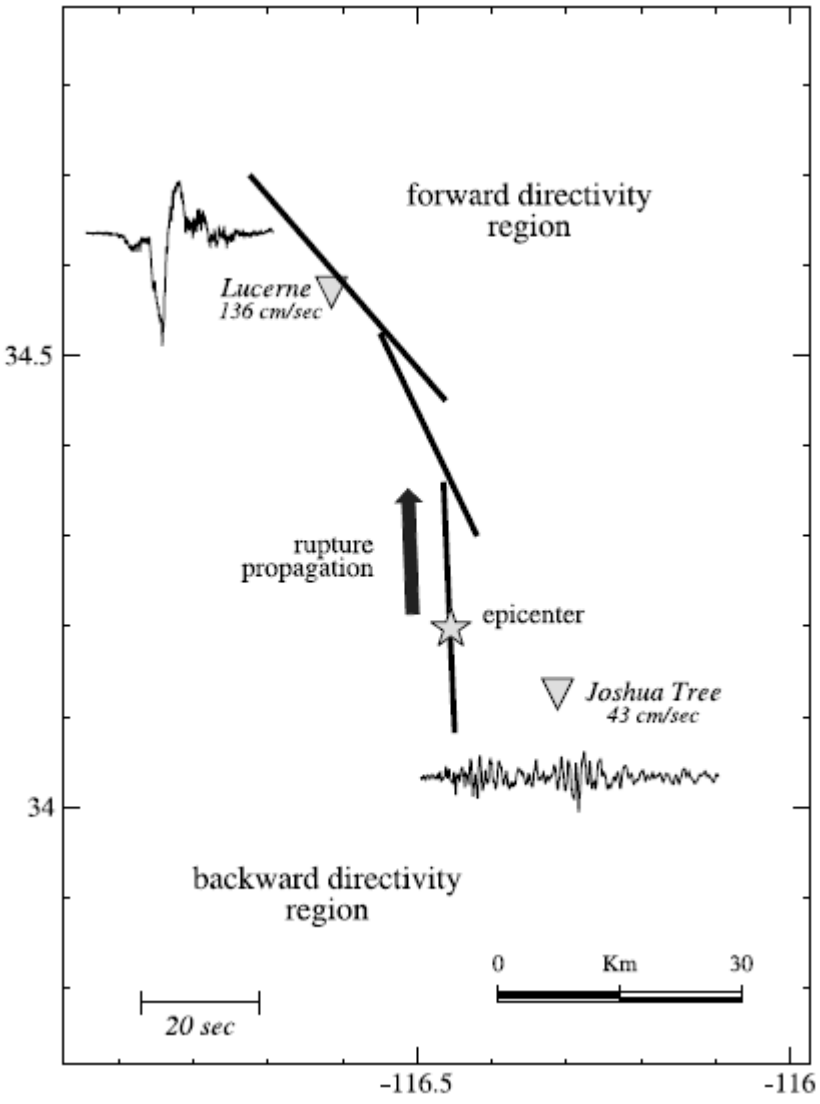

Figure 5. 5: Map of the Landers region showing the location of the rupture of the 1992 Landers earthquake with the magnitude of 7.3 (which occurred on three fault segments), the epicenter, and the recording stations at Lucerne and Joshua Tree. The fault normal velocity time histories at Lucerne and Joshua Tree exhibit forward and backward rupture directivity effects, respectively (Somerville, 1997).

Several earthquake records are selected and accessed via PEER Strong Motion Database.Time histories of those records are used with the assumption and

consideration of the description of the rupture directivity. *F* represents forward directivity. *B* represents backward directivity. Closest distance of the recorded station to the epicenter is selected as *R*<10km for near fault. Ground type that *S* represents soil, and *R* represents rock. Fault components *FN* represents fault normal, and *FP* represents fault parallel. Peak ground velocity is selected as v_{max}≥80cm/sec. The magnitude of the earthquake is selected as M_w≥6.5. The moment magnitude (denoted as M_w) is used by seismologists to measure the size of earthquakes in terms of the energy released (Hanks, 1979). All of the records are presented in (**Table A. 1**) in App. A. There are 58 earthquake records have been used in this study.

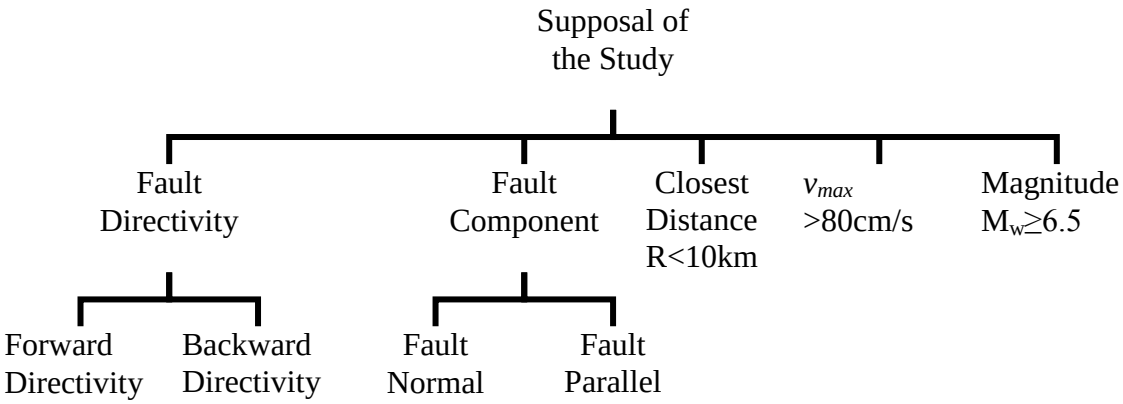

With the rigid soil and block behavior assumption peak ground accelerations (a_{max}) of the earthquakes are scaled individually to 0.2g, 0.3g, 0.4g, 0.5g, 0.6g, and 0.7g to simplify and to see if and which input effects the displacement respectively (*g=gravitational acceleration*). And so, the peak ground velocities (v_{max}) are scaled. The displacement does not occur when the horizontal yield (threshold) acceleration ($a_y=k_yg$) that makes the factor of safety against sliding is around 1.0 is bigger than 0.50g. Because of this, a_y values are limited 0.10g, 0.15g, 0.20g, 0.25g, 0.30g, 0.35g, 0.40g, 0.45g, and 0.50g. An unscaled and scaled earthquake record are shown in (**Figure 5. 6**), and (**Figure 5. 7**) which are used in this study respectively.

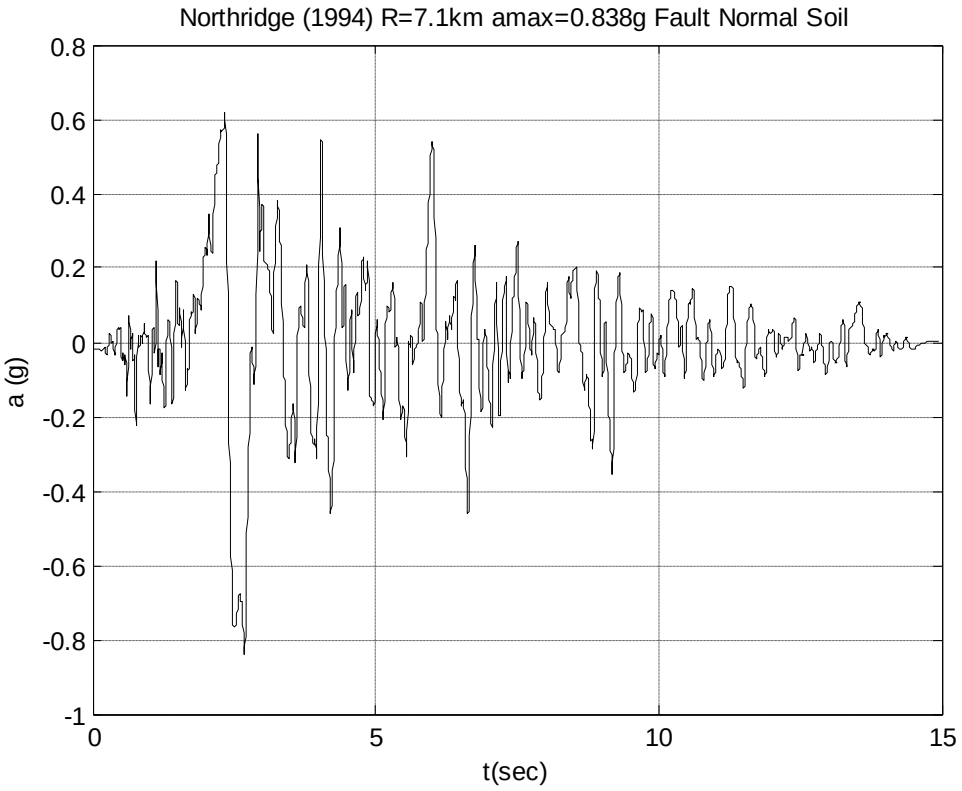

Figure 5. 6: A sample earthquake record belonging Northridge, 1994 earthquake

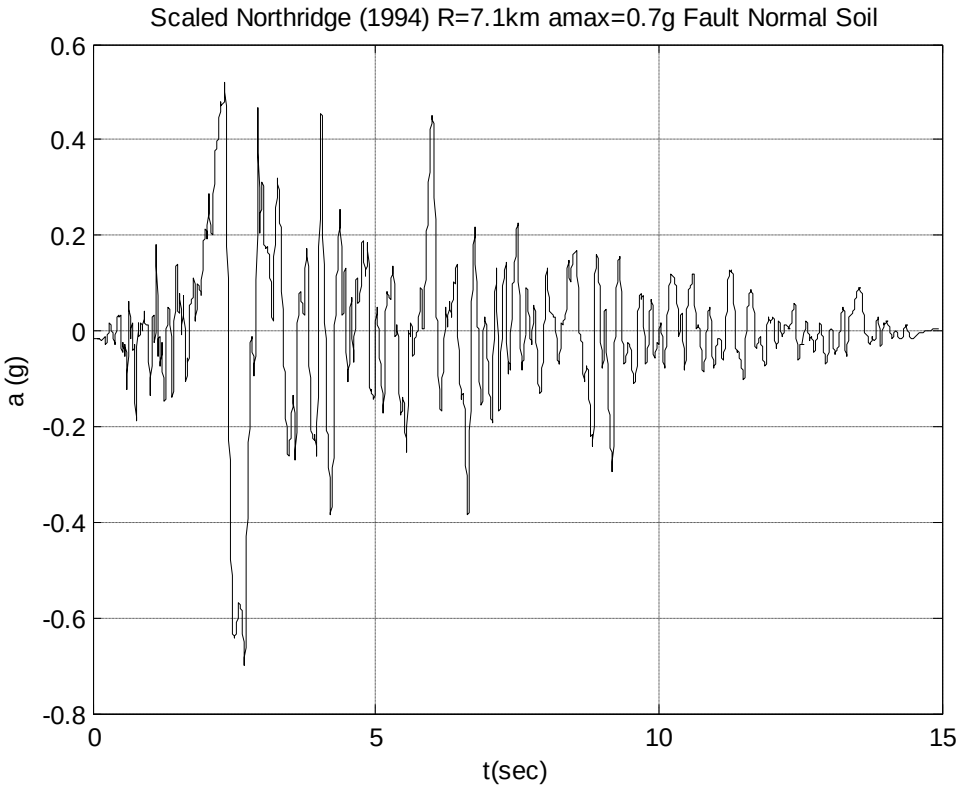

Figure 5. 7: A sample scaled earthquake record belonging Northridge, 1994 earthquake

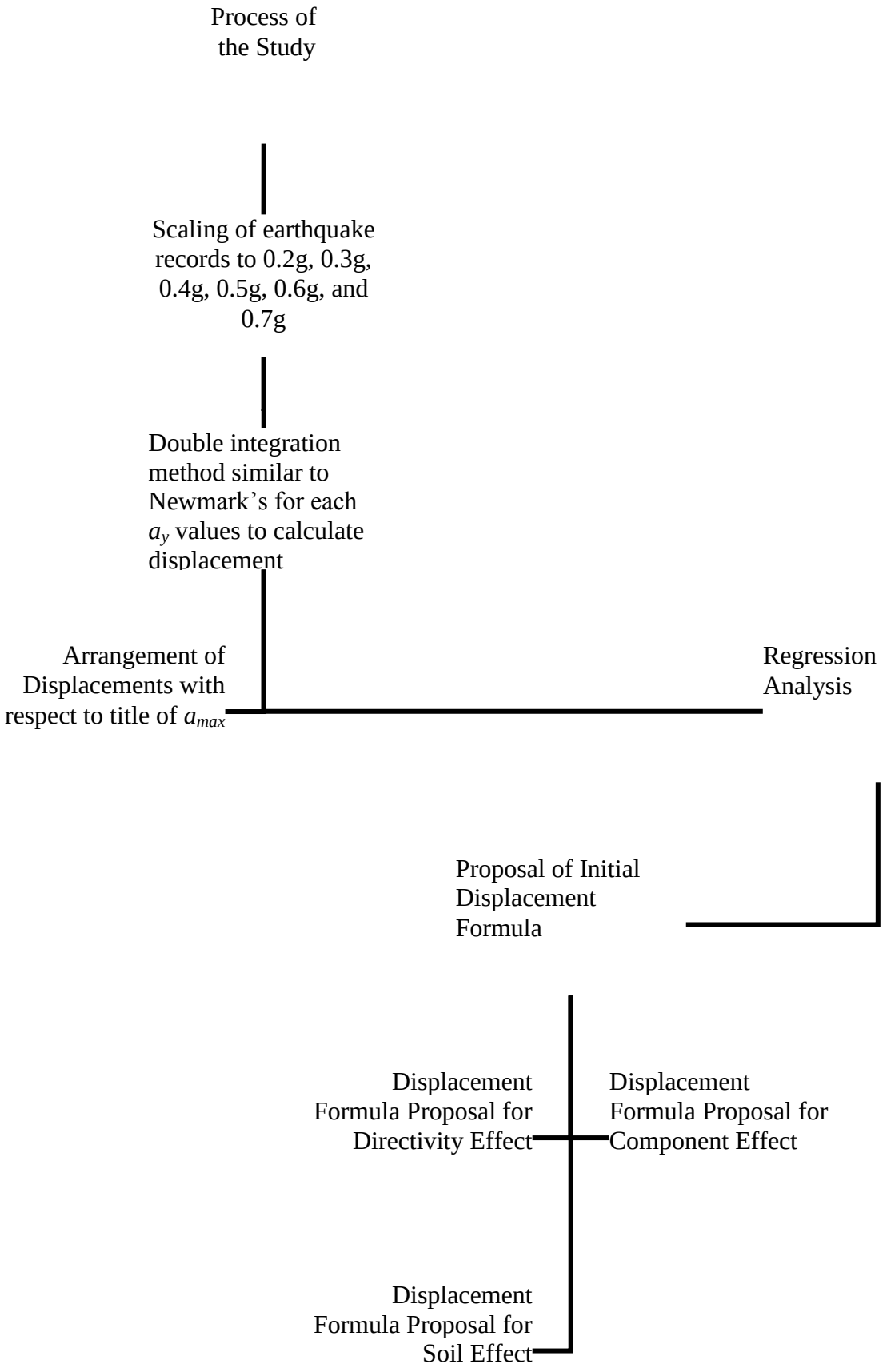
Process of the Study
Scaling of earthquake records to 0.2g, 0.3g, 0.4g, 0.5g, 0.6g, and 0.7g
Double integration method similar to Newmark's for each a_y values to calculate displacement
Arrangement of Displacements with respect to title of a_{max}
Regression Analysis
Proposal of Initial Displacement Formula
Displacement Formula Proposal for Directivity Effect
Displacement Formula Proposal for Component Effect
Displacement Formula Proposal for Soil Effect

5.3 Analysis of Generic Gravity Walls

Within the scope of the study, based on simplified dynamic analysis methods, Newmark (1965) and other sliding block studies, the analysis of generic gravity walls is considered independent from any wall dimension, foundation or backfill properties. The analysis begins with the first step that scaling of peak ground accelerations *(a_{max})* of selected time histories of each earthquake to 0.2g, 0.3g, 0.4g, 0.5g, 0.6g, and 0.7g.

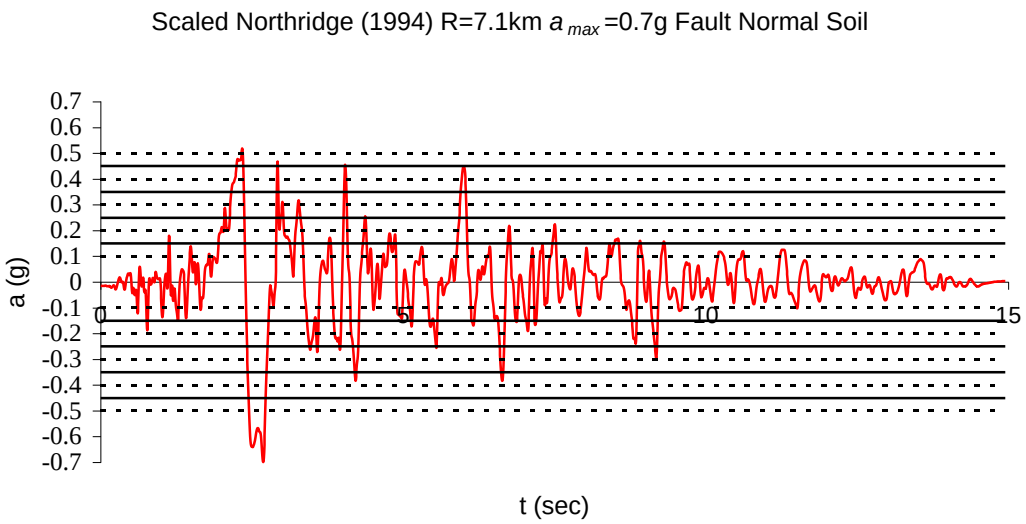

Figure 5. 8: An illustrative sample scaled earthquake record and yield acceleration values on same chart

And then the scaled earthquake records are used individually to calculate the resultant maximum displacement during the length of time that the each yield acceleration (a_y) 0.10g, 0.15g, 0.20g, 0.25g, 0.30g, 0.35g, 0.40g, 0.45g, and 0.50g values are exceeded (**Figure 5. 8**), by double integration method similar to Newmark's (1965) sliding block analysis. In (**Figure 5. 8**) each dashed and normal horizontal lines represent a_y values and the other red line represents the earthquake record. Considering (**Figure 5. 8**), a_y=0.10g yield acceleration is used to explain and illustrate the next steps of the study. (**Figure 5. 9**) shows all the relative accelerations trimmed above the assumed yield acceleration (a_y=0.10g) during the sample scaled earthquake Northridge (1994). Black line represents the absolute values of negative accelerations during the earthquake. Blue line represents positive accelerations during the earthquake. Negative and positive acceleration represent the (–) and (+) direction of earthquake. In this earthquake record, the absolute values of

negative accelerations are a bit greater that positive accelerations. Acceleration values may incrase or decrease during earthquake. All the positive and negative accelerations vary during earthquake. Acceleration values may go to zero at any time during earthquake.

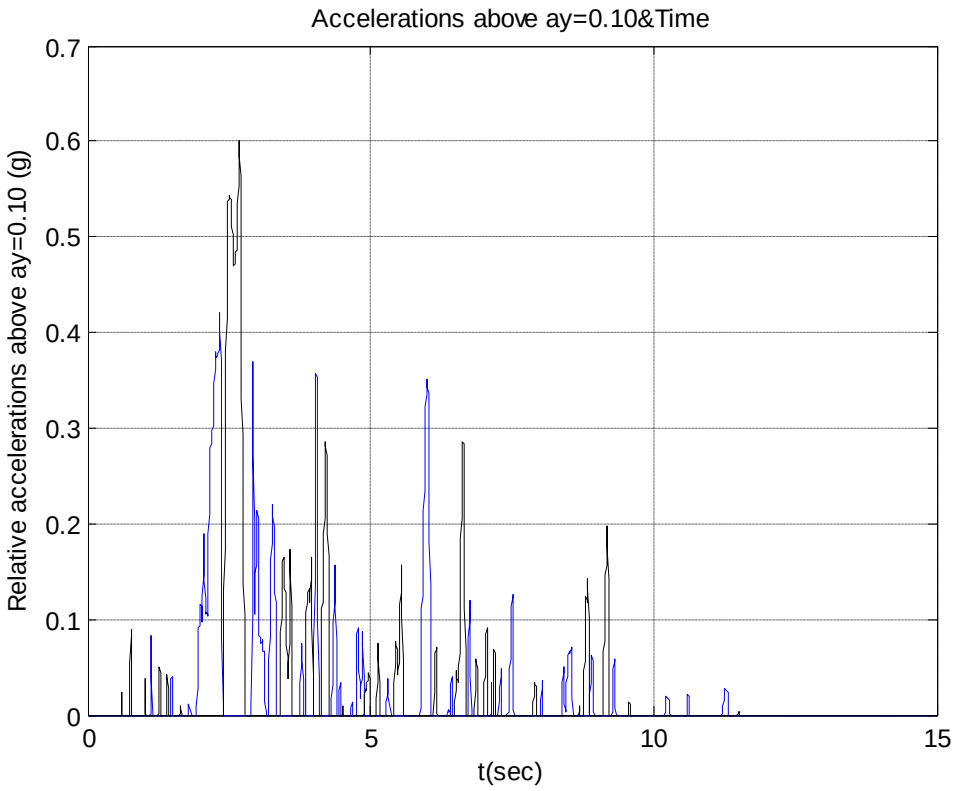

Figure 5. 9: An illustrative sample of accelerations above assumed a_y=0.10g

(**Figure 5. 10**) shows the calculated velocities obtained from the 1st integration of accelerations above the assumed yield acceleration (a_y=0.10g) during the earthquake. The velocity may not be zero when the the relative acceleration undergoes to zero. The relative velocity decreases which eventually reaches zero in this interval. The velocity is the sum of the area below any relative accelerations between any two time interval.

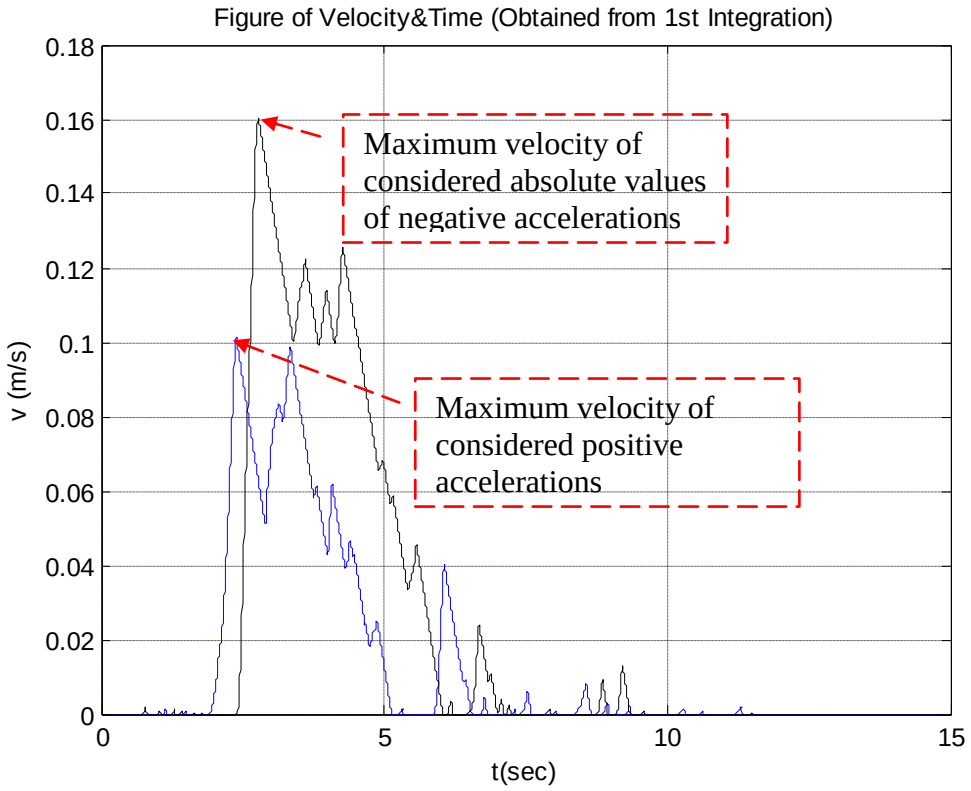

Figure 5. 10: An illustrative sample of velocities obtained by the 1st integration of accelerations above assumed a_y=0.10g

(**Figure 5. 11**) shows the calculated displacement values obtained from the 2nd integration of accelerations above the assumed yield acceleration (a_y=0.10g) during the earthquake. In other words, the calculated displacement values are equal the sum of the area below any calculated relative velocities between any two time interval. As mentioned before, the resultant relative displacement depends certainly on both the amount by which and the length of time that the yield acceleration is exceeded. In this sample earthquake record, maximum displacement values obtained from negative accelerations are greater than obtained from positive accelerations.

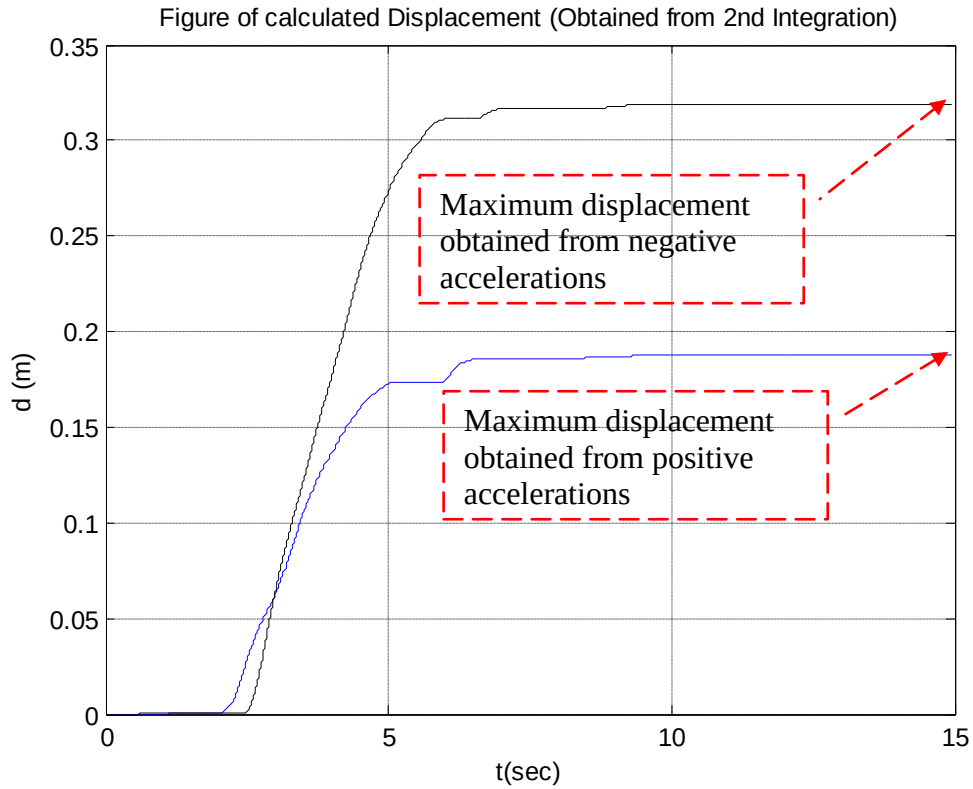

Figure 5. 11: An illustrative sample of calculated displacements obtained by the 2nd integration of accelerations above assumed $a_y=0.10g$

In this study, the maximum is considered whichever calculated displacement of negative or positive acceleration is greater. The calculated displacements are the maximum absolute average displacement values belong to each yield acceleration values of each earthquake record. Afterwards, these displacements are arranged properly as under the same all yield acceleration values. Each yield acceleration value has different displacements related to different each scaled a_{max} values. And also, scaled v_{max} values due to scaled a_{max} are arranged for each yield acceleration. a_{max} represents peak ground acceleration and v_{max} represents peak ground velocity. Finally, by considering the assumptions and the analysis process, these results are used for regression analysis with a simplified classification under the title of each near fault ground motion properties. Several formulas are proposed considering near fault ground motion properties by considering regression analysis results. MATLAB Software Programme (2004) has been used to calculate displacement values. Several analyses have been performed after scaling the a_{max}'s of selected earthquakes by considering all the assumptions and the process for this study. The selected earthquakes are simply classified in itselves under the title of component, directivity

and soil type with different combinations. And then a regression analysis has been made to measure combination against combination else thinking that the combinations are intercorrelated. As a result of these regressions several formulas are proposed to associate with the combination in simple terms. DataFit Software Programme has been used for regression analysis.

5.3.1 Near Fault-Soil-Forward Directivity-Fault Normal

The initial combination contains soil, fault normal and forward directivity properties, which's displacement is defined d_{max0} coupled with a_y values (0.10g, 0.15g, 0.20g, 0.25g, 0.30g, 0.35g, 0.40g, 0.45g, and 0.50g), a_{max} (each scaled 0.2g, 0.3g, 0.4g, 0.5g, 0.6g, and 0.7g) and v_{max}. The resultant maximum displacement values (d_{max0}) are calculated and obtained with respect to the stages aforementioned. Displacement values are valid for the earthquake records which contain soil, fault normal and forward directivity properties. Displacement values (d_{max0}) are the average maximum resultant displacement values with respect to each scaled a_{max} and a_y. Displacement shows an exponential distribution, that displacement increases with the increasing of v_{max} and a_{max}. v_{max} values are not obtained from any special calculation. v_{max} (cm/s) is a component of earthquake record, obtained from earthquake records. Each v_{max} describes the average velocity values of each scaled a_{max} values of earthquake records. (**Figure 5. 12**) shows the variation of displacement depending on a_{max} and a_y values. (**Figure 5. 13**) shows the same variation of displacement depending on v_{max} and a_y values. It is seen clearly from the both two figures, when a_y increases the resultant maximum displacement (d_{max0}) decreases for any constant a_{max} and v_{max} values. The reason is that, as mentioned in previous sections the trimmed area above for any a_y decreases with the increasing of its value. Calculated resultant maximum displacement values are related with those trimmed areas. Displacement increases with the increasing of trimmed area at any time interval. Considering near fielt fault ground motion properties, it has high velocity pulses and so high displacement characteristic. The calculated resultant maximum displacement values increase with the increasing of v_{max}, which are obtained from earthquake records and a_{max} for any constant a_y value. These prediction and determination is illustrated for selected constant $a_{max}=0.4g$ on both (**Figure 5. 12**) and (**Figure 5. 13**) for clarity.

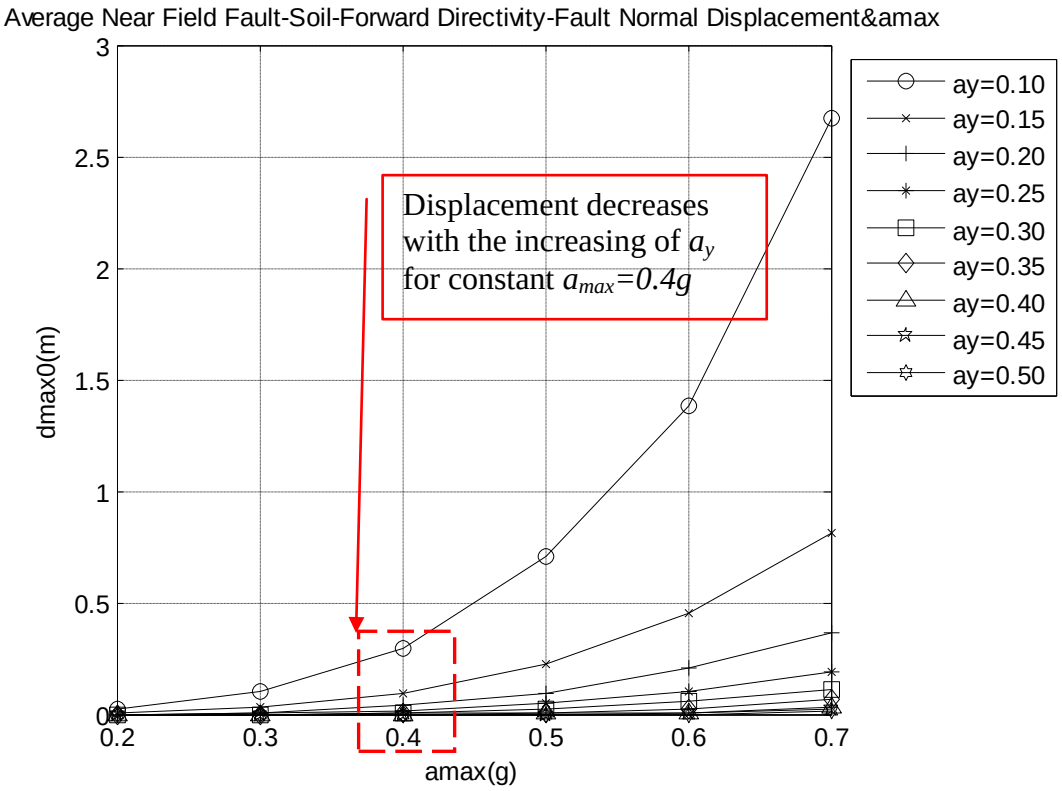

Figure 5. 12 : Variation of displacement depending on a_{max} and a_y

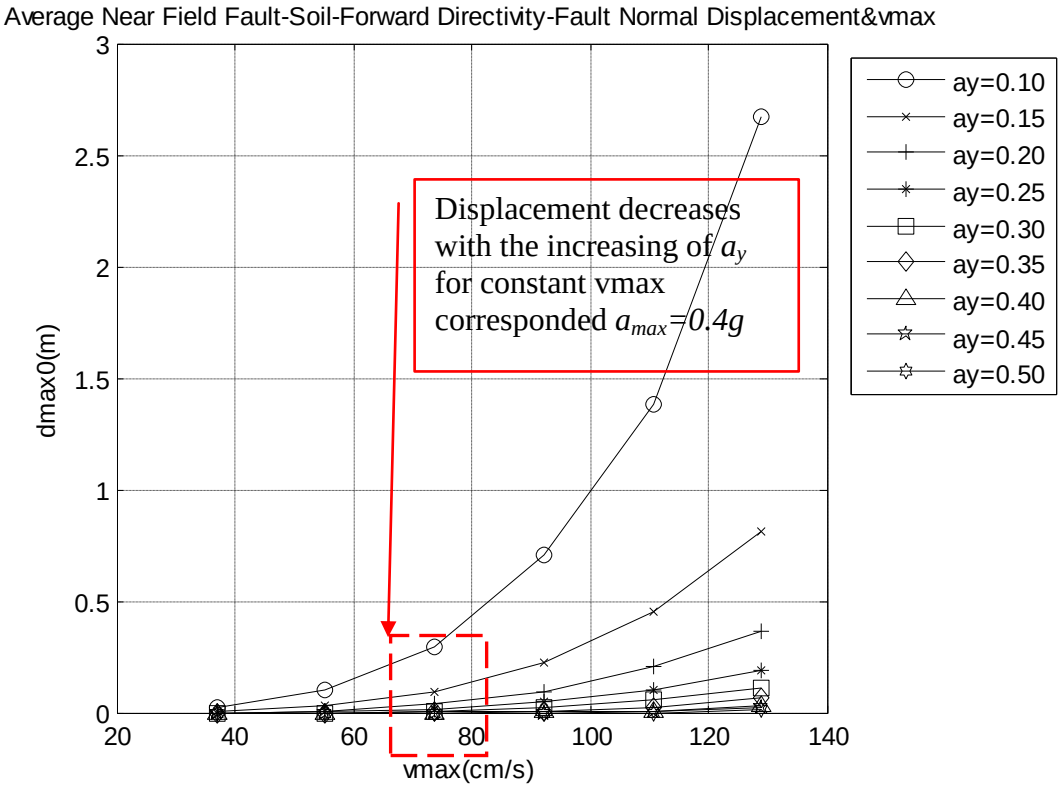

Figure 5. 13 : Variation of displacement depending on v_{max} and a_y

Since a proper formula curve could not fitted for all a_y values, d_{max0} is formulated seperately for specific a_y values. d_{max0-1}, d_{max0-2}, and d_{max0-3} cover fault normal and forward directivity properties, are d_{max0} derivative. The formulations are obtained from regression analysis. First of all, the dimensions of the components belong to each formulas converted to the same denominations. The components of the formulas are centimetre denominated. The inputs and outputs of the formulas are complied with dimension. And then, DataFit Software Programme is used for regression. The average resultant maximum displacement values d_{max0} (contains d_{max0-1} , $d_{max0-2,}$ and d_{max0-3}), a_{max} (0.10g, 0.15g, 0.20g, 0.25g, 0.30g, 0.35g, 0.40g, 0.45g, and 0.50g) values and v_{max} values obtained from earthquake records are used for regression with the same demoniations (cm). v_{max} values are the scaled average peak ground velocities dependent each scaled a_{max} with respect to earthquake records. These input values are inserted to the programme with an assumed offering formula considering the exponential distribution of displacement values (Equation 5.6). Same formula offer is used for d_{max0-1}, d_{max0-2}, and d_{max0-3}.

$$d_{\max 0} = a v_{\max}{}^{b} a_{\max}{}^{c} a_y{}^{d} \qquad \textbf{(5.6)}$$

d_{max0} is the maximum permanent displacement (cm), v_{max} is the peak ground velocity (cm/s), a_{max} is the peak ground acceleration (cm/sn^2), a_y (cm/sn^2) is the yield acceleration (cm/sn^2), a, b, c and d are uncertain coefficients. The programme presented many formulas considering input values and input formula offer. A formula (Equation 5.7) is selected from these presented formula offer, which has the minimum R (R-square) value. (See App. F for Regression Analysis for clarity)

$$d_{\max 0} = \frac{a v_{\max}{}^{2}}{a_{\max}} \exp\left(\frac{b a_y}{a_{\max}} \right) \qquad \textbf{(5.7)}$$

a and b are dimensionless coefficient differ for d_{max0-1}, d_{max0-2}, and d_{max0-3}.

(**Figure 5. 14**), (**Figure 5. 15**), and (**Figure 5. 16**) show the formulated displacement d_{max0-1} and regression distribution of fitness between the displacement formula and d_{max0-1} respectively. d_{max0-1} is the displacement calculated considering 0.10g, 0.15g, and 0.20g a_y values. It is valid and specific for 0.10g, 0.15g, and 0.20g a_y values. The formula is presented in Equation 5.8

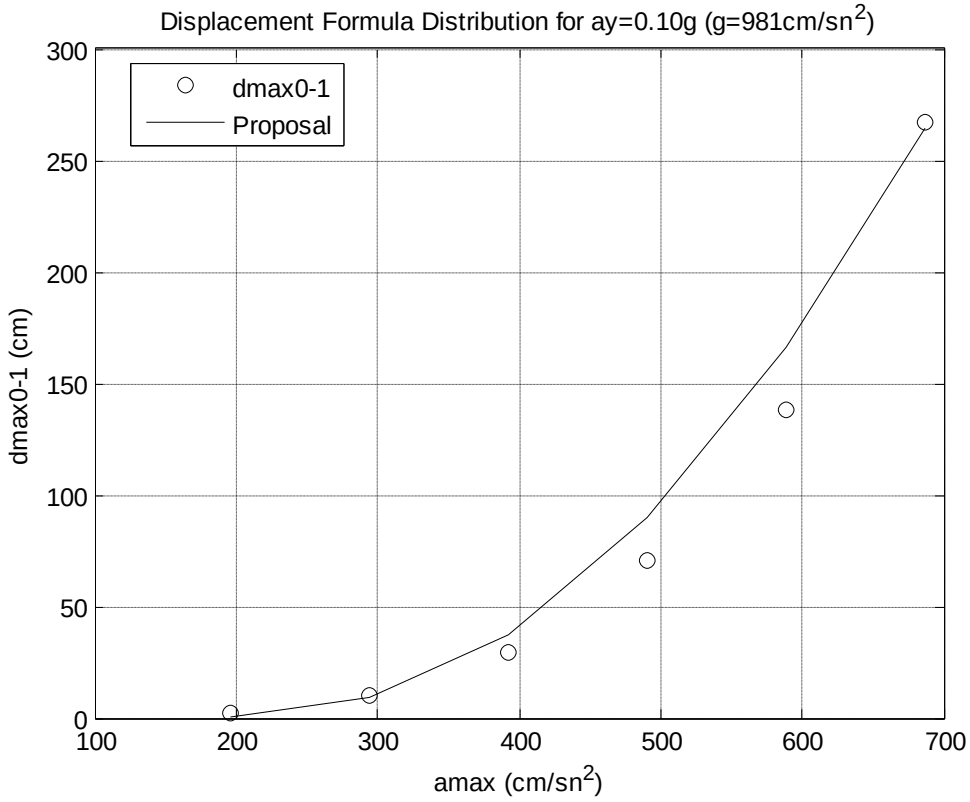

Figure 5. 14 : Relation between the calculated displacement distribution and proposed displacement formula for a_y=0.10g

$$d_{\max 0-1} = \frac{70 v_{\max}{}^2}{a_{\max}} \exp\left(\frac{-13 a_y}{a_{\max}} \right) \qquad \textbf{(5.8)}$$

d_{max0-1} is the maximum permanent displacement (cm), v_{max} is the peak ground velocity (cm/s), a_{max} is the peak ground acceleration (cm/sn^2), a_y is the yield acceleration (cm/sn^2). Values *70* and *-13* are dimensionless coefficients obtained from regression analysis complied with Equation 5.7. It can be said that, previously calculated d_{max0-1} values are complied with formulated displacement considering (**Figure 5. 14**), (**Figure 5. 15**), and (**Figure 5. 16**) and Equation 5.8.

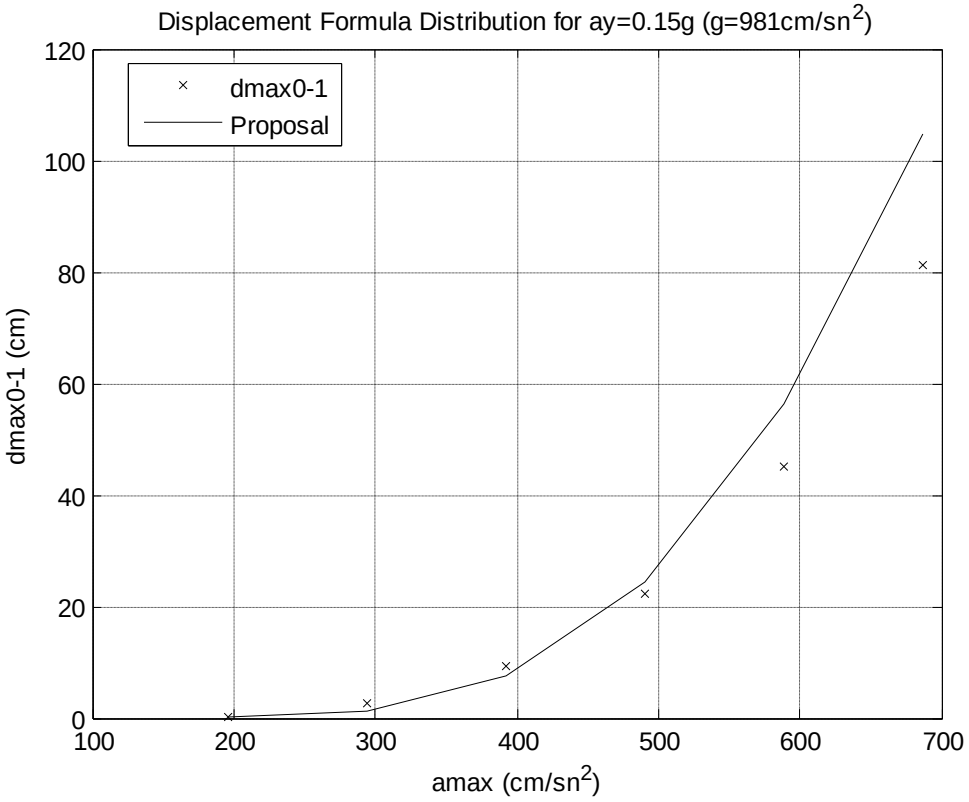

Figure 5. 15 : Relation between the calculated displacement distribution and proposed displacement formula for a_y=0.15g

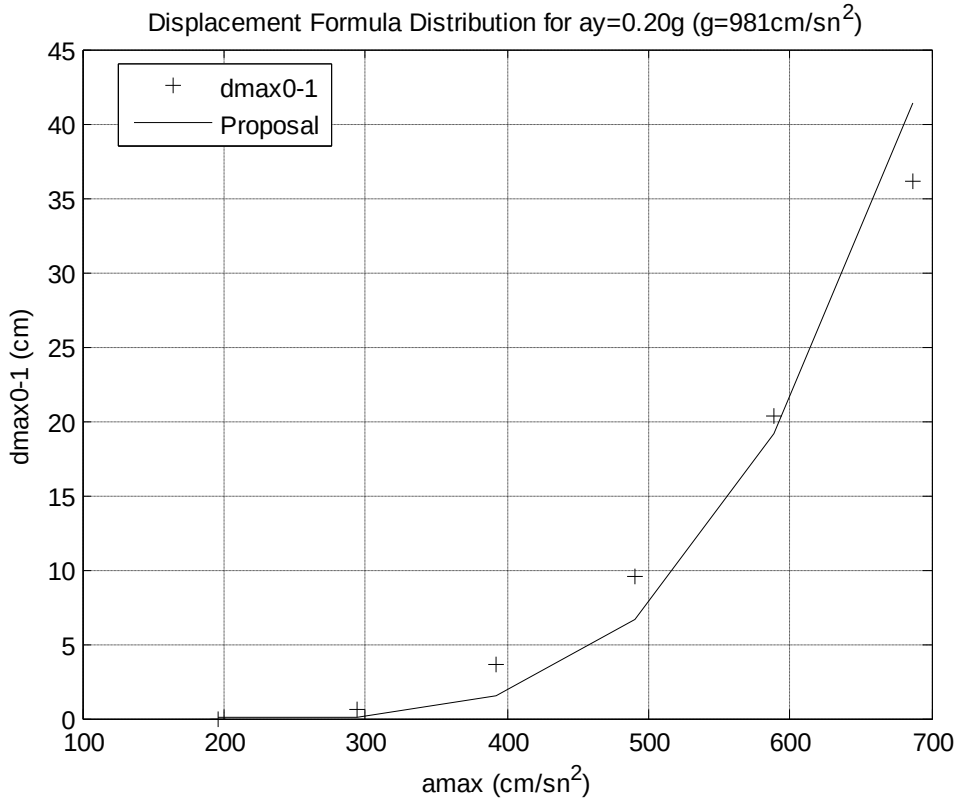

Figure 5. 16 : Relation between the calculated displacement distribution and proposed displacement formula for a_y=0.20g

(**Figure 5. 17**), (**Figure 5. 18**), and (**Figure 5. 19**) show the formulated displacement $d_{max0\text{-}2}$ and regression distribution of fitness between the displacement formula and $d_{max0\text{-}2}$ respectively. $d_{max0\text{-}2}$ is the displacement calculated considering 0.25g, 0.30g, and 0.35g a_y values. It is valid and specific for 0.25g, 0.30g, and 0.35g a_y values. The formula is presented in Equation 5.9.

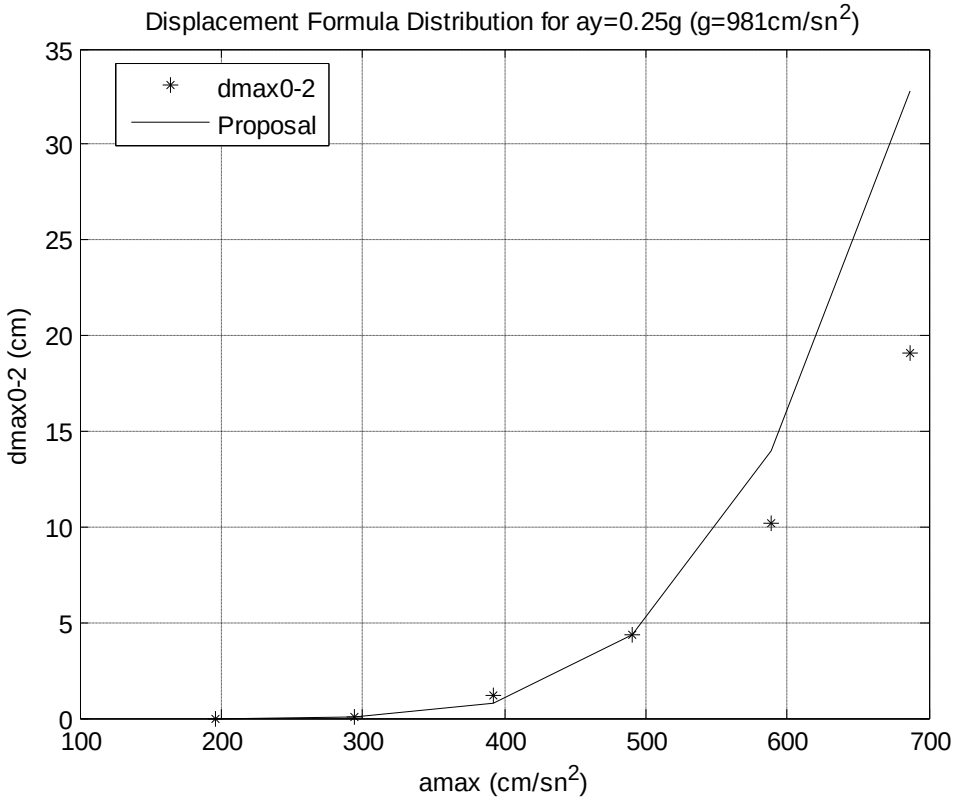

Figure 5. 17 : Relation between the calculated displacement distribution and proposed displacement formula for a_y=0.25g

$$d_{\max 0-2} = \frac{90 v_{\max}{}^2}{a_{\max}} \exp\left(\frac{-11.75 a_y}{a_{\max}}\right) \qquad \textbf{(5.9)}$$

$d_{max0\text{-}2}$ is the maximum permanent displacement (cm), v_{max} is the peak base velocity (cm/s), a_{max} is the peak ground acceleration (cm/sn^2), and a_y is the yield acceleration (cm/sn^2). Values *90* and *-11.75* are dimensionless coefficients obtained from regression analysis complied with Equation 5.7. It can be said that, previously calculated $d_{max0\text{-}2}$ values are complied with formulated displacement considering (**Figure 5. 17**), (**Figure 5. 18**), and (**Figure 5. 19**) and Equation 5.9.

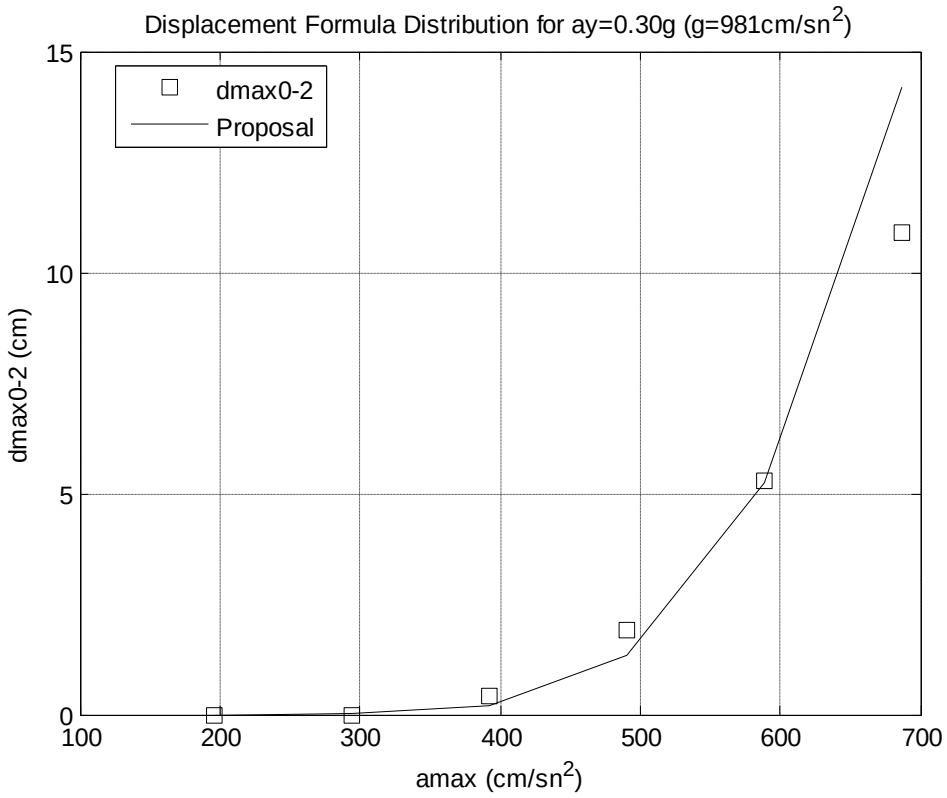

Figure 5. 18 : Relation between the calculated displacement distribution and proposed displacement formula for a_y=0.30g

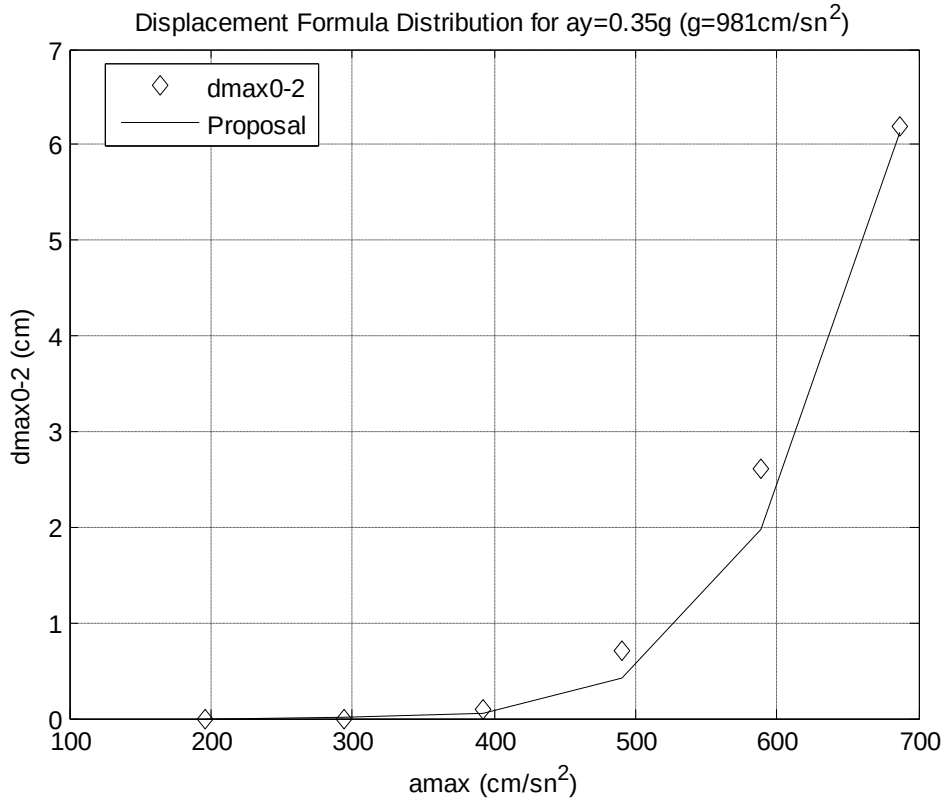

Figure 5. 19 : Relation between the calculated displacement distribution and proposed displacement formula for a_y=0.35g

(**Figure 5. 20**), (**Figure 5. 21**), and (**Figure 5. 22**) show the formulated displacement $d_{max0\text{-}3}$ and regression distribution of fitness between the displacement formula and $d_{max0\text{-}3}$ respectively. $d_{max0\text{-}3}$ is the displacement calculated considering 0.40g, 0.45g, and 0.50g a_y values. It is valid and specific for 0.40g, 0.45g, and 0.50g a_y values. The formula is presented in Equation 5.10.

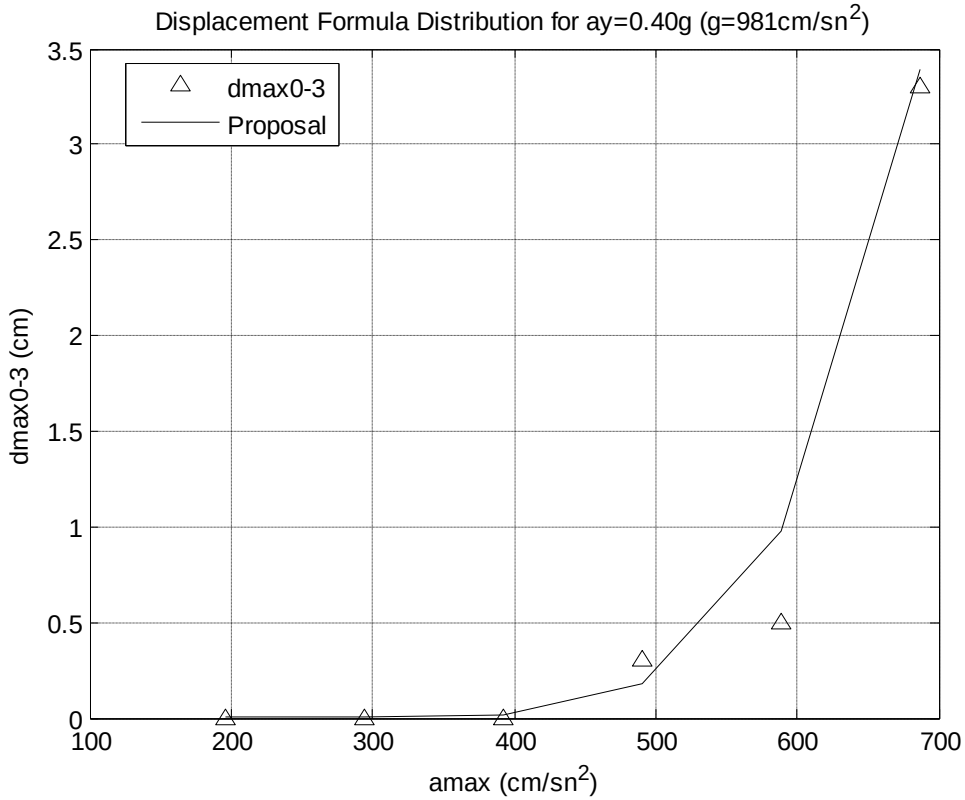

Figure 5. 20 : Relation between the calculated displacement distribution and proposed displacement formula for a_y=0.40g

$$d_{\max 0-3} = \frac{100 v_{\max}{}^2}{a_{\max}} \exp\left(\frac{-11.50 a_y}{a_{\max}}\right) \qquad \textbf{(5.10)}$$

$d_{max0\text{-}3}$ is the maximum permanent displacement (cm), v_{max} is the peak base velocity (cm/s), a_{max} is the peak ground acceleration (cm/sn^2), and a_y is the yield acceleration (cm/sn^2). Values *100* and *-11.75* are dimensionless coefficients obtained from regression analysis complied with Equation 5.7. It can be said that, previously calculated $d_{max0\text{-}3}$ values are complied with formulated displacement considering (**Figure 5. 20**), (**Figure 5. 21**), and (**Figure 5. 22**) and Equation 5.10. These figures show also the comparison and fitting between the calculated displacement before and the obtained displacement values considering formulas. As seen from the figures and

formulas for each specific constant a_y values, the exponential distributed displacement increases in parallel with the increment of a_{max} and v_{max} values. Proposed displacement formulas expressed in Equation (5.8), Equation (5.9), and Equation (5.10) looks like Whitman&Liao (1985) formula given in Equation (3.3). The differences between their formulas and the proposal formula of this study are the coeffiecents of v_{max} and a_y values. They had used 14 earthquake records, but in this study 58 earthquake records with respect to near fault ground motion. This may be one of the differences between two studies.

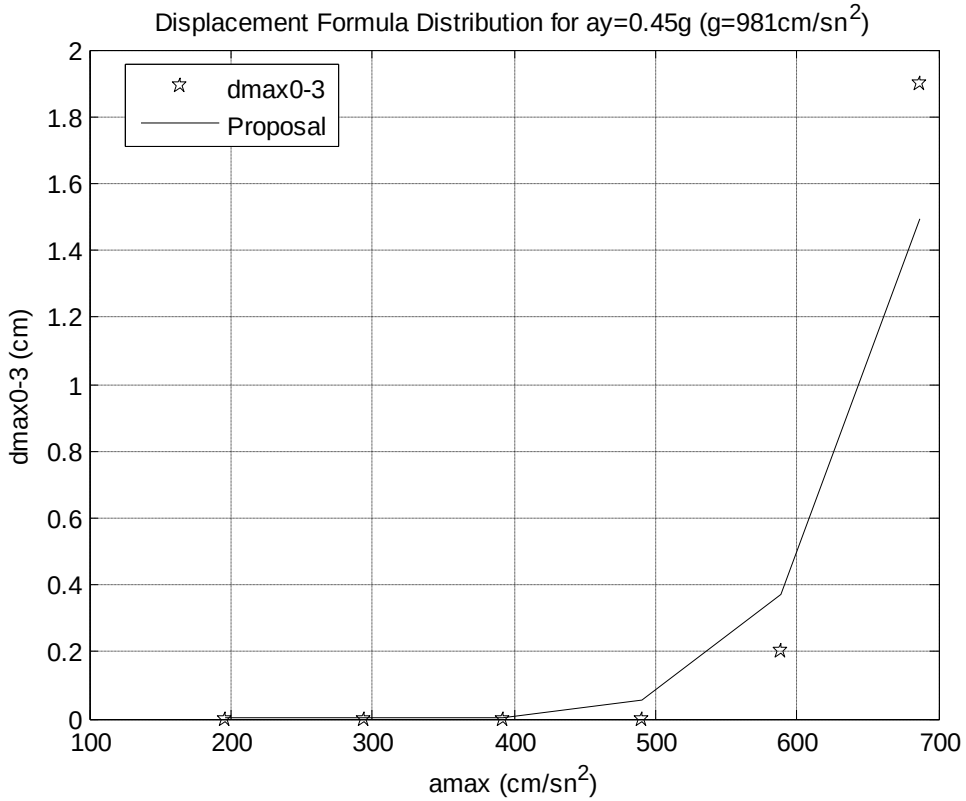

Figure 5. 21 : Relation between the calculated displacement distribution and proposed displacement formula for a_y=0.45g

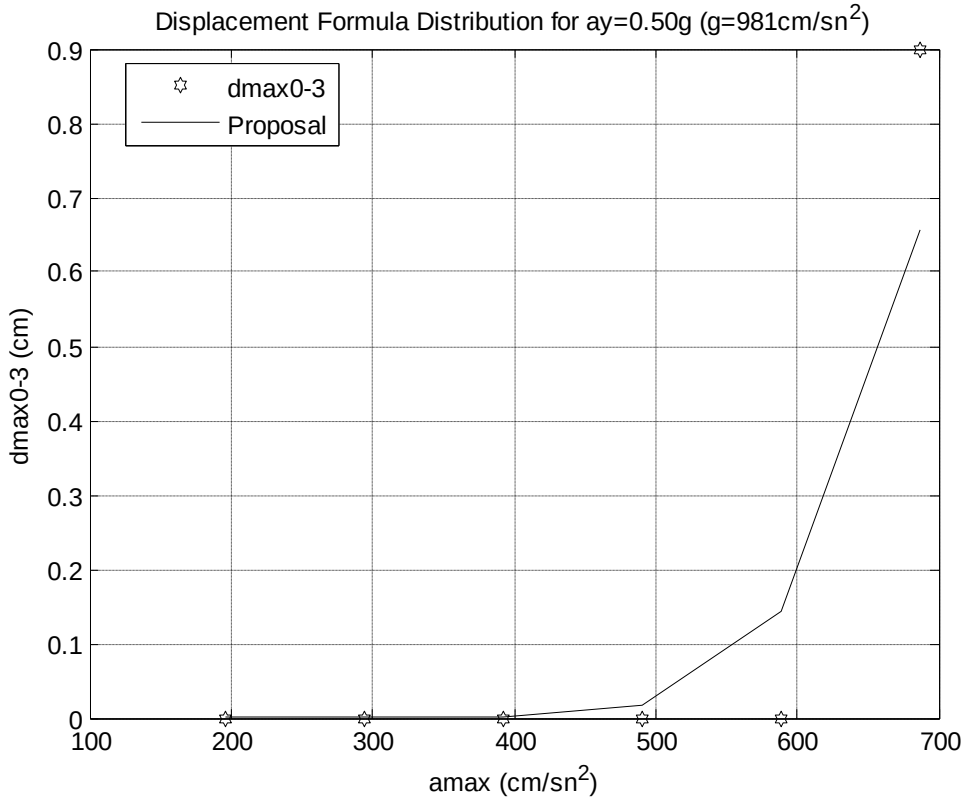

Figure 5. 22 : Relation between the calculated displacement distribution and proposed displacement formula for a_y=0.50g

5.3.2 Near Fault Correlation Between Properties of Ground Motion

A general formula is proposed considering Near Fault Ground Motion properties such as directivity, component and soil properties to correlate each other. The general formula contains some coefficients related to ground motion properties. It is assumed that the displacements related to ground motion properties apart from d_{max0} can be forecasted with these dimensionless coefficients. As it is mentioned that soil, fault normal, and forward directivity properties has been considered with defined d_{max0}.

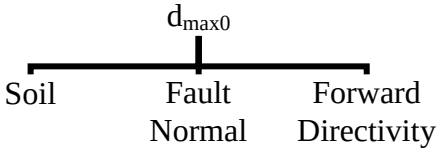

Three coefficients have been defined in this study. The first of these represents Directivity (C_D), the second represents Component (C_C) and the third represents Soil (C_S) property. For instance, anyone wants to predict the displacement of an other condition that covers such as backward directivity, soil and fault normal properties.

Based on d_{max0} using the coefficient of Directivity, the displacement related to backward directivity, soil and fault normal property can be guessed. Directivity is the only difference and variable between two displacements. The other two Component (C_C) and Soil (C_S) coefficients are neutral element (are equal to 1) in the circumstances. The general formula is described with the Equation 5.11.

$$d_{\max} = \frac{d_{\max 0}}{C_D C_C C_S} \qquad \textbf{(5.11)}$$

d_{max} is the maximum expected permanent displacement, d_{max0} is the initial calculated displacement values with respect to soil, fault normal, and forward directivity properties, C_D is the directivity coefficient that represents the ratio of Forward Directivity Displacement/Backward Directivity Displacement under all the properties are same, C_C is the component coefficient that represents the ratio of Fault Normal Displacement/Fault Parallel Displacement under all the properties are same, and C_S is the soil property coefficient that represents the ratio of Soil Displacement/Rock Displacement under all the properties are same. As can be seen in the next sections of this study, v_{max} is the main factor when obtaining the each coefficient value.

5.3.2.1 Directivity Effect

Sample number of earthquake records are less considering Backward Directivity property. Directivity coefficient (C_D) is only valid for under the soil property is Soil and the component property is Fault Normal conditions are assumed same for Forward Directivity and Backward Directivity. Directivity coefficient (C_D) represents directivity effect. That is to say, it is a relation between Forward and Backward Directivity under the assumed same conditions. It is formulated with the Equation 5.12 after regression. (See App. F for Regression Analysis for clarity)

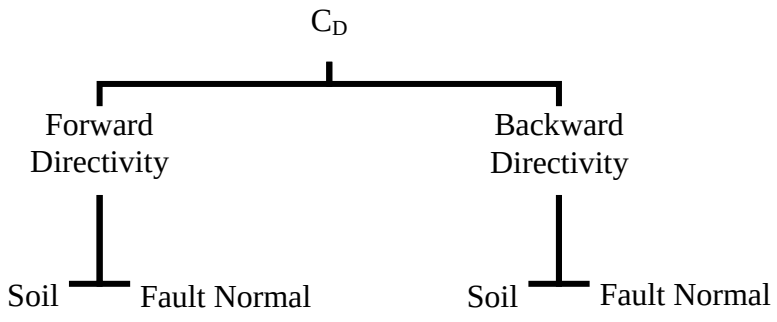

$$C_D = \left(133.3 - 82.9 \frac{v_{\max FD}}{v_{\max BD}} \right)$$

$$C_D = \left(\frac{d_{\max 0}}{d_{\max BD}} \right) \quad \textit{With respect to } C_C \textit{ and } C_S \textit{ are equal to } 1.0 \qquad \textbf{(5.12)}$$

C_D is the directivity coefficient that that represents the ratio of Forward Directivity Displacement to Backward Directivity Displacement considering C_C and C_S values are equal to 1.0, v_{maxFD} is the peak ground velocity of Forward Directivity (cm/s), v_{maxBD} is the peak ground velocity of Backward Directivity (cm/s), d_{max0} is the calculated (aforementioned) Forward Directivity Displacement, and d_{maxBD} is will be calculated Backward Directivity Displacement under the same Soil and Fault Normal condition. Values *133.3* and *-82.9* are dimensionless coefficients obtained from regression analysis complied with Equation 5.12. v_{maxFD} and v_{maxBD} are the scaled average peak ground velocities dependent each scaled a_{max} with respect to earthquake records. v_{maxFD} represents the velocity of Forward Directivity considered soil and fault normal component properties. v_{maxBD} represents the velocity of Backward Directivity considered soil and fault normal properties.

If anyone wants to estimate the Backward Directivity Displacement, who has v_{maxFD} and v_{maxBD} or the ratio of v_{maxFD} /v_{maxBD} and the calculated Forward Directivity Displacement (d_{max0}) under the same soil and component property, can use the Equation 5.12. In this study, since v_{maxFD} /v_{maxBD} ratio is 1.59, the proposed constant C_D value is 1.489. And this means, d_{max0} is equal to 1.489 times d_{maxBD} considering C_C and C_S values are equal to 1.0 ($d_{\max 0} = 1.489 \times d_{\max BD}$). As is seen, d_{max0} is larger than d_{maxBD}. The only variable in this formula is the ratios of v_{maxFD} /v_{maxBD}. The peak ground velocity of Forward Directivity (v_{maxFD}) is higher than the peak ground velocity of Backward Directivity (v_{maxBD}) considering Near Fault Ground Motion characteristics. Considering both these characteristics and C_D, it can be concluded that, the calculated displacement of Forward Directivity is larger than the obtained displacement of Backward Directivity under the same conditions (soil and fault normal component property). On the other hand, considering C_C and C_S values are equal to 1.0, obtained displacement values of Backward Directivity with respect to the coefficient C_D are compared with each calculated displacement values have the same characteristics of Backward Directivity, soil, and fault normal component. (**Figure B. 1**), (**Figure B. 2**), (**Figure B. 3**), (**Figure B. 4**), (**Figure B. 5**), (**Figure B.**

6), (**Figure B. 7**), (**Figure B. 8**), and (**Figure B. 9**) show the comparison of the obtained displacement distribution with respect to C_D (considering C_C and C_S values are equal to 1.0) and calculated displacement values contains backward directivity, soil and fault normal characteristics for a_y values 0.10g, 0.15g, 0.20g, 0.25g, 0.30g, 0.35g, 0.40g, 0.45g, and 0.50g respectively in App. B. There is a fitting between two displacement values. Especially, there is a clear fitting between the calculated displacement values considered a_y values 0.10g, 0.15g, 0.20g, 0.25g and obtained displacements with respect to *CD*. This fittings can be seen from these figures. The displacement increases in parallel with the increment of a_{max} for each specific constant a_y values considering backward directivity.

5.3.2.2 Component Effect

Component coefficient (C_C) is valid for under the soil property is Soil and Forward Directivity properties. These properties are assumed same for both two Fault Normal and Fault Parallel component. Component coefficient (C_C) symbolizes component effect. In other words, it is a relation between Fault and Parallel Component under same conditions. C_C is formulated is formulated with the Equation 5.13 considering the previous assumption. (See App. F for Regression Analysis for clarity)

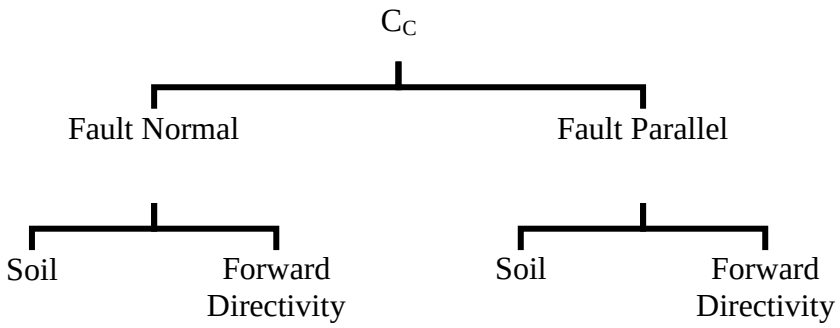

$$C_C = \left(7.2 \frac{v_{\max FN}}{v_{\max FP}} - 8.7 \right)$$

$$C_C = \left(\frac{d_{\max 0}}{d_{\max FP}} \right) \quad \textit{With respect to } C_D \textit{ and } C_S \textit{ are equal to } 1.0 \qquad \textbf{(5.13)}$$

C_C is the component coefficient that represents the ratio of Fault Normal Displacement to Fault Parallel Displacement considering C_D and C_S values are equal to 1.0, v_{maxFN} is the peak ground velocity of Fault Normal (cm/s), v_{maxFP} is the peak ground velocity of Fault Parallel (cm/s), d_{max0} is the calculated (aforementioned)

Fault Normal Displacement considering Forward Directivity and Soil properties, and d_{maxFP} is will be obtained Fault Parallel Displacement under the same Soil and Forward Directivity condition. Values *7.2* and *-8.7* are dimensionless coefficients obtained from regression analysis complied with Equation 5.13. v_{maxFN} and v_{maxFP} are the scaled average peak ground velocities dependent each scaled a_{max} with respect to earthquake records. v_{maxFN} represents the velocity of Fault Normal Component considered Soil and Forward Directivity properties. v_{maxFP} represents the velocity of Fault Parallel Component considered Soil and Forward Directivity properties. Using v_{maxFN} and v_{maxFP} or the ratio of v_{maxFN} /v_{maxFP} and the calculated Fault Normal Displacement (d_{max0}) under the same soil and forward directivity properties, Fault Parallel Displacement (d_{maxFP}) can be obtained with respect to the Equation 5.13. In this study, since v_{maxFN} /v_{maxFP} ratio is 1.37, the proposed constant C_C value is 1.164. In other words this means, d_{max0} is equal to 1.164 times d_{maxFP} considering C_D and C_S values are equal to 1.0 ($d_{\max 0} = 1.164 \times d_{\max FP}$). It can be said that, d_{max0} is larger than d_{maxFP}. The only variable in this formula is the ratios of v_{maxFN} /v_{maxFP}. The peak ground velocity of Fault Normal (v_{maxFN}) is more specificially higher than the peak ground velocity of Fault Parallel (v_{maxFP}) Near Fault Ground Motion characteristics. From this point of view, it can be concluded that Fault Normal Displacement is larger than Fault Parallel Displacement under the same conditions considering both these characteristics and C_C. Beside this, considering C_D and C_S values are equal to 1.0, obtained displacement values of Fault Parallel with respect to the coefficient C_C are compared with each calculated displacement values have the same characteristics of Fault Normal, soil and forward directivity properties. (**Figure C. 1**), (**Figure C. 2**), (**Figure C. 3**), (**Figure C. 4**), (**Figure C. 5**), (**Figure C. 6**), (**Figure C. 7**), (**Figure C. 8**), and (**Figure C. 9**) show the comparison of the obtained displacement distribution with respect to the component coefficient C_C (considering C_D and C_S values are equal to 1.0) and calculated displacement values covers Fault Normal, forward directivity and soil characteristics for a_y values 0.10g, 0.15g, 0.20g, 0.25g, 0.30g, 0.35g, 0.40g, 0.45g, and 0.50g respectively in App. C. It is seen that there is a fitting between two displacement values. There is an apparent fitting between the calculated displacement values exceptionally considered a_y values 0.10g, 0.15g, 0.20g, 0.25g and obtained displacements with respect to C_C. This adaptation can be seen from these figures. The displacement increases in parallel with the increment of a_{max} for each specific constant a_y values considering Fault Parallel Component.

5.3.2.3 Soil Effect

Soil coefficient (C_S) is valid for under the component property is Fault Normal the directivity is Forward Directivity. These properties are assumed same for both two Soil and Rock soil properties. Soil coeffient (C_C) comprises soil effect under these same conditions. In other words, it is a relation between Soil and Rock properties under the same circumstances. C_S is formulated with the Equation 5.14 considering the previous assumption. (See App. F for Regression Analysis for clarity)

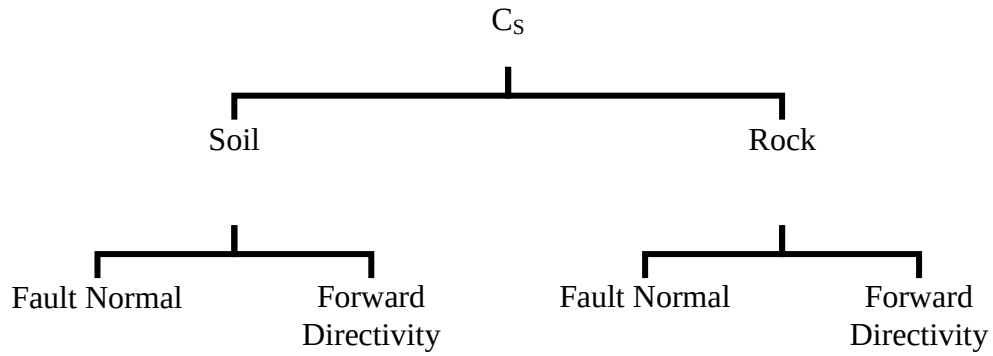

$$C_S = \left(63.1 \frac{v_{\max S}}{v_{\max R}} - 91.7 \right)$$

$$C_S = \left(\frac{d_{\max 0}}{d_{\max R}} \right) \quad \textit{With respect to } C_D \textit{ and } C_C \textit{ are equal to } 1.0 \qquad \textbf{(5.14)}$$

C_S is the component coefficient that represents the ratio of Soil Displacement to Rock Displacement, considering C_D and C_C values are equal to 1.0, v_{maxS} is the peak ground velocity of Soil (cm/s), v_{maxR} is the peak ground velocity of Rock (cm/s), d_{max0} is the calculated (aforementioned) Soil displacement considering Forward Directivity and Fault Normal component properties, and d_{maxR} is will be obtained Rock Displacement under the same Fault Normal component and Forward Directivity condition. Values *63.1* and *-81.7* are dimensionless coefficients obtained from regression analysis complied with Equation 5.14. v_{maxS} and v_{maxR} are the scaled average peak ground velocities dependent each scaled a_{max} with respect to earthquake records. v_{maxS} represents the velocity of Soil considered Fault Normal Component and Forward Directivity properties. v_{maxR} represents the velocity of Rock considered Fault Normal and Forward Directivity properties. Using v_{maxS} and v_{maxR} or the ratio of v_{maxS} /v_{maxR} and the calculated Fault Normal Displacement (d_{max0}) under the same fault normal component and forward directivity properties, Rock Displacement

(d_{maxR}) can be obtained with respect to the Equation 5.14. In this study, since v_{maxS} /v_{maxR} ratio is 1.48, the proposed constant C_S value is 1.688. In other words this means, d_{max0} is equal to 1.688 times d_{maxR} considering C_D and C_C values are equal to 1.0 ($d_{\max 0} = 1.688 \times d_{\max R}$). It can be said that, d_{max0} is larger than d_{maxR}. The only variable in this formula is the ratios of v_{maxS} /v_{maxR}. The peak ground velocity of Soil (v_{maxS}) is more specificially higher than the peak ground velocity of Rock (v_{maxR}) Near Fault Ground Motion characteristics. From this point of view, it can be concluded that Soil Displacemetn is larger than Rock Displacement under the same conditions considering both these characteristics and C_S. Beside this, considering C_D and C_C values are equal to 1.0, obtained displacement values of Rock with respect to the coefficient C_S are compared with each calculated displacement values have the same characteristics of Soil, fault normal, and forward directivity properties. (**Figure D. 1**), (**Figure D. 2**), (**Figure D. 3**), (**Figure D. 4**), (**Figure D. 5**), (**Figure D. 6**), (**Figure D. 7**), (**Figure D. 8**), and (**Figure D. 9**) show the comparison of the obtained displacement distribution with respect to the soil coefficient C_S (considering C_D and C_C values are equal to 1.0) and calculated displacement values covers Soil, forward directivity and fault normal characteristics for a_y values 0.10g, 0.15g, 0.20g, 0.25g, 0.30g, 0.35g, 0.40g, 0.45g, and 0.50g respectively in App. D. It is seen that there is a fitting between two displacement values. There is an obvious fitting between the calculated displacement values exceptionally considered a_y values 0.10g, 0.15g, 0.20g, 0.25g and obtained displacements with respect to C_S. This adjustmen can be seen from these figures. The displacement increases in parallel with the increment of a_{max} for each specific constant a_y values considering Rock.

.

6. CONCLUSION

In our day, as engineering forms for the seismic design, there are many different types of design techniques have been developed for gravity type marine structures. Some of design techniques are mentioned in Literature Review, Section 3 of the this study. Sliding block methods of analysis calculates a permanent deformation of a gravity type marine structure system due to a user-specified design earthquake event, is described as Simplified Dynamic Analysis in PIANC (2001). Earthquake shaking of the soil is represented by time histories of acceleration. Based on Newmark's (1965) sliding block analysis, the proposal and approach of the study incorporate lateral movements explicitly in the stability analysis of a rigid gravity structure, on a rigid soil. Assuming when the factor of safety against sliding is around 1.0, the potential failure mass of the soil behind the structure is no longer in equilibrium that the active wedge mobilizes the structure with the dynamic thrust. In other words the structure will be accelerated by the unbalanced force.

This study approach is, in effect, a procedure for using an obtained yield acceleration, ground acceleration or ground velocity based upon explicit choice of an allowable residual displacement by considering the damage criteria of performance design approach for especially near fault ground motion. No safety factor is needed assuming the factor of safety against sliding is around 1.0. The level of factor of safety is incorporated into the step used to calculate the threshold acceleration. It is called yield acceleration will cause the structure to move relative to the sliding plane. The resultant maximum sliding displacement during the length of time is obtained from two times integration of the areas that the yield acceleration is exceeded by ground accelerations. This is founded for each earthquake by considering the assumptions. Then these results are used for regression analysis. The results of regression analysis are presented in App.F. Several charts for seismic performance evaluation for gravity type marine structures have been proposed based on parametric study by taking account of acceptance and assumptions of near fault ground motion parameters and selected earthquake records. Considering the

difference and relation between the computed sliding displacements in case earthquake records and formulated displacement by the chart, a procedure to generate fitting curves based on formulas for each directivity, component, and soil property condition has been proposed. The estimated maximum displacement distribution looks like Whitman&Liao (1985). As it is commented earlier, the difference between their formula and this study is resulting from the number of earthquake records that are used in both studies, and this study is near fault ground motion oriented. The comparisons of this study with the previous similar sliding block analysis methods are presented in App.E. All in all, since the area above a_y decreases with increase of a_y, for any a_{max} and v_{max} values, when a_y increases the resultant displacement decreases. On the other hand for any constant a_y value the displacement increases with the increment of a_{max} or v_{max}. As stated in PIANC (2001), the computed displacement from sliding block analysis is sensitive to a number of key parameters, including those for evaluating threshold acceleration and the nature of the earthquake motion. To sum up, the marked difference between directivity, component, and soil property; it can be concluded that Forward Directivity Displacement is larger than Backward Directivity Displacement under the same conditions. Fault Normal Displacement is larger than Fault Parallel Displacement under the same conditions. Soil Displacement is larger than Rock Displacement under the same conditions. Beside this, since Forward Directivity contains in itself higher velocity values than Backward Directivity in title of directivity. Fault Normal contains in itself higher velocity values than Fault Parallel. Soil contains higher velocity values than Rock. For any scaled constant a_{max} values it is noticeable that the displacement increases with the increment of v_{max} values observing the displacement results. The variation of v_{max} plays a role on the difference of displacement for any condition.

The study is valid for any gravity type marine structure and is independently of the dimension of the wall. Considering the results of this study, formulations and charts of this study can be used by engineers for preliminary design with respect to near fault ground motion characteristics. If anyone wants to calculate and estimate the maximum horizontal residual sliding displacement of a gravity type marine structure for seismic condition, who has either of peak ground acceleration, peak ground velocity and soil conditions for near fault ground motion can use this the formulas,

and charts belonging to this proposed procedure. On the other hand, threshold acceleration represents the yielding limit assuming with the permanent displacements founded beginning from this point. It makes the coefficient of safety against sliding is 1.0. It is obtained by iteration. It can be used to estimate the minimum horizontal permanent displacement of a gravity wall under seismic conditions. Although the variety of the earthquake records are limited, more detailed variation of curves and formulas can be calibrated if more detailed parametric study were carried out.

As a conclusion, this procedure of analysis represents an improved alternative to the world wide known method of analysises that performance of a rigid gravity wall in terms of earthquake records. As stated in PIANC (2001), actual seismic performance of gravity quay walls during earthquakes often does not meet the assumptions inherent in sliding block analysis. Where the movement of the wall is associated with significant deformation in the foundation soils, the displacements computed by the sliding block approach were substantially smaller than the displacements observed in the field (Iai, 1998a; Yang, 1999). This study and the previous similar sliding block analysis methods are just an approach and estimation procedure of sliding displacement. As a matter of fact that, soil and structure interaction become part of an earthquake response. All together environmental conditions, soil and structure interaction play a significant role during an earthquake. Sliding block analysis methods do not consider any soil or any environmental condition. It is assumed sliding rigid block wall in this type analysis methods. Therefore, it is thought that the computed maximum displacement values may not be real in the fact. Because of this, the estimated computed maximum sliding displacement values may be assumed the minimum displacement values. Seismic evaluation of the case study summarised in (**Table 2.2**) justifies this thought in one way considering resistance based design and deformation based design properties. As can be seen in App.G, there is quite difference between the measured displacement and each sliding displacement prediction procedure methods. It can be concluded that, sliding block analyis methods are just an approximation procedure and methods of sliding displacement values under earthquake conditions. The obtained and calculated approximately sliding displacement values may not reflect and predict the real damage that may occur after an earthquake. Earthquake based damage and deformations can be just estimated. That is to say, nobody knows exactly what will occur during an

earthquake and the real resultant displacements after an earthquake. In the future, estimation of sliding displacement methods can be developed considering soil and structure interaction. Thus, this proposed method has a huge potential for future development.

REFERENCES

Asce, (1998): Seismic Guidelines for Ports, Technical Council on Lifeline Earthquake Engineering (TCLEE) Monograph No. 12., Oakland, CA, 377 pp.

Chen, W. F., and Scawthorn, C., Ed., (2003): Earthquake Engineering Handbook, CRC Press, pp. 1512.

Franklin, A. G., Chang, F. K., (1977): Permanent displacements of earth embankments by Newmark sliding block analysis, Report 5, Miscellaneous Paper S-71- 17, U.S. Army Corps of Engineers.

Hanks, Thomas C., (1979): Moment magnitude scale. Journal of Geophysical Research 84 (B5): 2348–50.

Honda, T., and Kiyota, T., (2005): Damages of structures around ports due to west off Fukuoka Prefecture Earthquake, Koseki Lab., Tokyo.

Iai, S., and Ichii, K., (1998): Performanced Based Design for Port Structures, U.S. Department of Commerce, Editors: Raufaste N, J.

Ichii, K., (2004): Fragility curves for gravity type quay walls based on effective stress analyses, 13th world conference on earthquake engineering, Vancouver, B. C., Canada. Paper No.3040.

Kalkan E., and Kunnath S.K., (2006): Effects of Fling-Step and Forward Directivity on the Seismic Response of Buildings, Earthquake Spectra, Vol. **22**, No. 2, pp. 367-390.

Kawamata, Y., and Ashford, S., (2003): Preliminary information on the 2003 Tokachi-Oki Earthquake, San Diego, CA.

Kramer, S. L., (1996): Geotechnical Earthquake Engineering, Editor; Hall W.J. 653 pages, ISBN 0-13-374943-6.

Nadim, F., and Whitman R. V., (1984): Coupled sliding and tilting of gravity retaining walls during earthquakes. In Proceedings of the Eighth World Conference on Earthquake Engineering, San Francisco III: 477-484.

Newmark, N., (1965): Effects of earthquakes on dams and embankments, Geotechnique, Vol. **15**, No.2, pp. 139-160.

Pianc, (2001): Seismic Design Guidelines for Port Structures, Working Group n.34 of the Maritime Navigation Commission, International Navigation Association, Balkema, Lisse, 474 pp.

RHA of Ministry of Transportation, Turkey (2008): Technical Seismic Regulation on Construction of Coastal and Harbor Structures, Railways and Airports.

Richards, R., Elms, D., (1979): Seismic behavior of gravity retaining walls, Journal of Geotechnical Engineering Division, ASCE, Vol. **105**, No. GT4, pp. 449-464.

Seaoc, (1995): Deformation Based Seismic Engineering of Buildings, Structural Engineers Association of California, Sacramento, California.

Somerville, P. G., N. F. Smith, R. W. Graves, and N. A. Abrahamson (1997): Modification of empirical strong ground motion attenuation relations to include the amplitude and duration effects of rupture directivity, Seism. Res. Lett. 68, No. 1, 199–222.

Somerville, P. G., (2003): Magnitude scaling of the near fault rupture directivity pulse, Phys. Earth Planet. Interiors 137, No. 1, 12.

Steedman, R.S., (1998): Seismic design of retaining walls, Geotechnical Engineering, Proc. Institution of Civil Engineers, Vol. **131**, pp. 12–22.

Sumer, B. M., Kaya, A., and Hansen, N.-E. O., (2002): Impact of liquefaction on coastal structures in the 1999 Kocaeli, Turkey Earthquake, Proc., 12th Int. Offshore and Polar Engineering Conf., KitaKyushu, Japan, Vol. **II**, 504–511.

Url-1 <*http*://peer.berkeley.edu/smcat/>, accessed at 02.10.2010.

Uwabe, T., (1983): Estimation of earthquake damage deformation and cost of quay walls based on earthquake damage records, Technical Note of Port and Harbour Research Institute, No. 473, 197 p.

Whitman, R. V., and Liao S., (1985): Seismic design of retaining walls, US Army Corps of Engineers, Waterways Experiment Station, Miscellaneous Paper GL-85-1.

Wong, C. P., (1982): Seismic analysis and an improved design procedure for gravity retaining walls, S.M. Thesis, Department of Civil Engineering, Massachusetts Institute of Technology, Cambridge, Massachusetts.

Yang, D.S., (1999): Deformation Based Seismic Design Models for Waterfront Structures, Ph.D. dissertation, Department of Civil, Construction and Environmental Engineering, Oregon State University, Corvallis, 260 p.

APPENDICES

APPENDIX A : Near Fault Ground Motion Earthquake Records, Adapted from Url-1

APPENDIX B : The Displacement Formula Distribution of Directivity Effect for a_y values, Fault Normal&Soil Condition

APPENDIX C : The Displacement Formula Distribution of Component Effect for a_y values, Soil&Forward Directivity Condition

APPENDIX D : The Displacement Formula Distribution of Soil Effect for a_y values, Fault Normal&Forward Directivity Condition

APPENDIX E : Matching of Previous Sliding Block Analysis Methods with the Thesis Study (Continue of Literature Section)

APPENDIX F : Regression Analyis

APPENDIX G: Evaluation of Case History of Kushiro Port (Japan) Considering Seismic Design Of Gravity Type Quay Walls

APPENDIX A

Table A. 1: Earthquake records

EARTHQUAKE	EARTHQUAKE DATE	STATION	RECORD & COMPONENT	CLOSEST DISTANCE (km)	SITE CODE	a_{max} (g)	v_{max} (cm/s)	d_{max} (cm)	DIRECTIVITY	MAGNITUDE (M_w)	CLOSEST STATUS	dt (s)	Component
Imperial Valley	15.10.1979	955 El Centro Array #4	IMPVALL/H-E04230	4.2	SL	0.36	76.6	59.02	F	6.5	NF	0.005	FN
Imperial Valley	15.10.1979	955 El Centro Array #4	IMPVALL/H-E04140	4.2	SL	0.485	37.4	20.23	F	6.5	NF	0.005	FP
Imperial Valley	15.10.1979	952 El Centro Array #5	IMPVALL/H-E05230	1.0	SL	0.379	90.5	63.03	F	6.5	NF	0.005	FN
Imperial Valley	15.10.1979	952 El Centro Array #5	IMPVALL/H-E05140	1.0	SL	0.519	46.9	35.35	F	6.5	NF	0.005	FP
Imperial Valley	15.10.1979	942 El Centro Array #6	IMPVALL/H-E06230	1.0	SL	0.439	109.8	65.89	F	6.5	NF	0.005	FN
Imperial Valley	15.10.1979	942 El Centro Array #6	IMPVALL/H-E06140	1.0	SL	0.41	64.9	27.69	F	6.5	NF	0.005	FP
Imperial Valley	15.10.1979	5028 El Centro Array #7	IMPVALL/H-E07230	0.6	SL	0.463	109.3	44.74	F	6.5	NF	0.005	FN
Imperial Valley	15.10.1979	5028 El Centro Array #7	IMPVALL/H-E07140	0.6	SL	0.338	47.6	24.68	F	6.5	NF	0.005	FP
Erzincan, Turkey	13.03.1992	95 Erzincan	ERZIKAN/ERZ-NS	2.0	SL	0.515	83.9	27.35	F	6.9	NF	0.005	FN
Erzincan, Turkey	13.03.1992	95 Erzincan	ERZIKAN/ERZ-EW	2.0	SL	0.496	64.3	22.78	F	6.9	NF	0.005	FP
Northridge	17.01.1994	24279 Newhall - Fire Sta	NORTHR/NWH360	7.1	SL	0.59	97.2	38.05	F	6.7	NF	0.02	FN
Northridge	17.01.1994	24279 Newhall - Fire Sta	NORTHR/NWH090	7.1	SL	0.583	75.5	17.57	F	6.7	NF	0.02	FP
Northridge	17.01.1994	77 Rinaldi Receiving Sta	NORTHR/RRS228	7.1	SL	0.838	166.1	28.78	F	6.7	NF	0.005	FN
Northridge	17.01.1994	77 Rinaldi Receiving Sta	NORTHR/RRS318	7.1	SL	0.472	73	19.76	F	6.7	NF	0.005	FP
Northridge	17.01.1994	74 Sylmar - Converter Sta	NORTHR/SCS052	6.2	SL	0.612	117.4	53.47	F	6.7	NF	0.005	FN
Northridge	17.01.1994	74 Sylmar - Converter Sta	NORTHR/SCS142	6.2	SL	0.897	102.8	46.99	F	6.7	NF	0.005	FP
Northridge	17.01.1994	74 Sylmar - Converter Sta East	NORTHR/SCE018	6.1	SL	0.828	117.5	34.22	F	6.7	NF	0.005	FN
Northridge	17.01.1994	74 Sylmar - Converter Sta East	NORTHR/SCE288	6.1	SL	0.493	74.6	28.69	F	6.7	NF	0.005	FP
Northridge	17.01.1994	24514 Sylmar - Olive View Med FF	NORTHR/SYL360	6.4	SL	0.843	129.6	32.68	F	6.7	NF	0.02	FN
Northridge	17.01.1994	24514 Sylmar - Olive View Med FF	NORTHR/SYL090	6.4	SL	0.604	78.2	16.05	F	6.7	NF	0.02	FP
Kobe	16.01.1995	0 KJMA	KOBE/KJM000	0.6	SL	0.821	81.3	17.68	F	6.9	NF	0.02	FN
Kobe	16.01.1995	0 KJMA	KOBE/KJM090	0.6	SL	0.599	74.3	19.95	F	6.9	NF	0.02	FP
Kobe	16.01.1995	0 Takarazuka	KOBE/TAZ090	1.2	SL	0.694	85.3	16.75	F	6.9	NF	0.01	FN
Kobe	16.01.1995	0 Takarazuka	KOBE/TAZ000	1.2	SL	0.693	68.3	26.65	F	6.9	NF	0.01	FP
Kobe	16.01.1995	0 Takatori	KOBE/TAK000	0.3	SL	0.611	127.1	35.77	F	6.9	NF	0.01	FN
Kobe	16.01.1995	0 Takatori	KOBE/TAK090	0.3	SL	0.616	120.7	32.72	F	6.9	NF	0.01	FP
Kocaeli, Turkey	17.08.1999	Yarimca	KOCAELI/YPT060	2.6	SL	0.268	65.7	57.01	F	7.4	NF	0.005	FN
Kocaeli, Turkey	17.08.1999	Yarimca	KOCAELI/YPT330	2.6	SL	0.349	62.1	50.97	F	7.4	NF	0.005	FP
Chi-Chi, Taiwan	20.09.1999	TCU075	CHICHI/TCU075-W	1.5	SL	0.333	88.3	86.45	F	7.6	NF	0.005	FN
Chi-Chi, Taiwan	20.09.1999	TCU075	CHICHI/TCU075-N	1.5	SL	0.264	38.2	33.23	F	7.6	NF	0.005	FP
Chi-Chi, Taiwan	20.09.1999	TCU076	CHICHI/TCU076-N	2.0	SL	0.416	64.2	35.37	F	7.6	NF	0.005	FN
Chi-Chi, Taiwan	20.09.1999	TCU076	CHICHI/TCU076-W	2.0	SL	0.303	62.6	31.47	F	7.6	NF	0.005	FP
Chi-Chi, Taiwan	20.09.1999	TCU129	CHICHI/TCU129-W	1.2	SL	1.01	60	50.15	F	7.6	NF	0.005	FN
Chi-Chi, Taiwan	20.09.1999	TCU129	CHICHI/TCU129-N	1.2	SL	0.634	36.1	28.87	F	7.6	NF	0.005	FP
Kocaeli, Turkey	17.08.1999	Sakarya	KOCAELI/SKR090	3.1	SL	0.376	79.5	70.52	F	7.4	NF	0.01	FN

Table A. 1: Earthquake records (continued)

EARTHQUAKE	EARTHQUAKE DATE	STATION	RECORD & COMPONENT	CLOSEST DISTANCE (km)	SITE CODE	a_{max} (g)	v_{max} (cm/s)	d_{max} (cm)	DIRECTIVITY	MAGNITUDE (M_w)	CLOSEST STATUS	dt (s)	Component
Landers	28.06.1992	24 Lucerne	LANDERS/LCN275	1.1	R	0.721	97.6	70.31	F	7.3	NF	0.005	FN
Landers	28.06.1992	24 Lucerne	LANDERS/LCN000	1.1	R	0.785	31.9	16.42	F	7.3	NF	0.005	FP
San Fernando	09.02.1971	279 Pacoima Dam	SFERN/PCD164	2.8	R	1.226	112.5	35.5	F	6.6	NF	0.01	FN
San Fernando	09.02.1971	279 Pacoima Dam	SFERN/PCD254	2.8	R	1.16	54.3	11.73	F	6.6	NF	0.01	FP
Morgan Hill	24.04.1984	57217 Coyote Lake Dam (SW Abut)	MORGAN/CYC285	0.1	R	1.298	80.8	9.63	F	6.2	NF	0.005	FN
Morgan Hill	24.04.1984	57217 Coyote Lake Dam (SW Abut)	MORGAN/CYC285	0.1	R	0.711	51.6	12	F	6.2	NF	0.005	FP
Northridge	17.01.1994	00000 LA Dam	NORTHR/LDM064	2.6	R	0.511	63.7	21.18	F	6.7	NF	0.005	FN
Northridge	17.01.1994	00000 LA Dam	NORTHR/LDM334	2.6	R	0.349	50.8	15.11	F	6.7	NF	0.005	FP
Northridge	17.01.1994	24207 Pacoima Dam (upper left)	NORTHR/PUL194	8.0	R	1.285	103.9	23.8	F	6.7	NF	0.02	FN
Northridge	17.01.1994	24207 Pacoima Dam (upper left)	NORTHR/PUL104	8.0	R	1.585	55.7	6.06	F	6.7	NF	0.02	FP
Kocaeli, Turkey	17.08.1999	Gebze	KOCAELI/GBZ000	17.0	R	0.244	50.3	42.74	F	7.4	NF	0.005	FN
Kocaeli, Turkey	17.08.1999	Gebze	KOCAELI/GBZ270	17.0	R	0.137	29.7	27.54	F	7.4	NF	0.005	FP
Loma Prieta	18.10.1989	16 LGPC	LOMAP/LGP000	6.1	R	0.563	94.8	41.18	F	6.9	NF	0.005	FN
Loma Prieta	18.10.1989	16 LGPC	LOMAP/LGP090	6.1	R	0.605	51	11.5	F	6.9	NF	0.005	FP
Imperial Valley	19.05.1940	117 El Centro Array #9	IMPVALL/I-ELC270	8.3	SL	0.215	30.2	23.91	B	7.0	NF	0.01	FN
Imperial Valley	15.10.1979	6616 Aeropuerto Mexicali	IMPVALL/H-AEP045	8.5	SL	0.327	42.8	10.1	B	6.5	NF	0.01	FN
Imperial Valley	15.10.1979	6618 Agrarias	IMPVALL/H-AGR273	0.8	SL	0.221	42.4	11.7	B	6.5	NF	0.01	FN
Imperial Valley	15.10.1979	5054 Bonds Corner	IMPVALL/H-BCR230	2.5	SL	0.775	45.9	14.89	B	6.5	NF	0.005	FN
Imperial Valley	15.10.1979	6619 SAHOP Casa Flores	IMPVALL/H-SHP270	11.1	SL	0.506	30.9	5.64	B	6.5	NF	0.01	FN
Imperial Valley	15.10.1979	6622 Compuertas	IMPVALL/H-CMP285	32.6	SL	0.147	9.5	2.49	B	6.5	NF	0.01	FN
Morgan Hill	24.04.1984	57191 Halls Valley	MORGAN/HVR240	3.4	SL	0.312	39.4	7.66	B	6.2	NF	0.005	FN
Landers	28.06.1992	22170 Joshua Tree	LANDERS/JOS090	11.6	SL	0.284	43.2	14.51	B	7.3	NF	0.02	FN

APPENDIX B

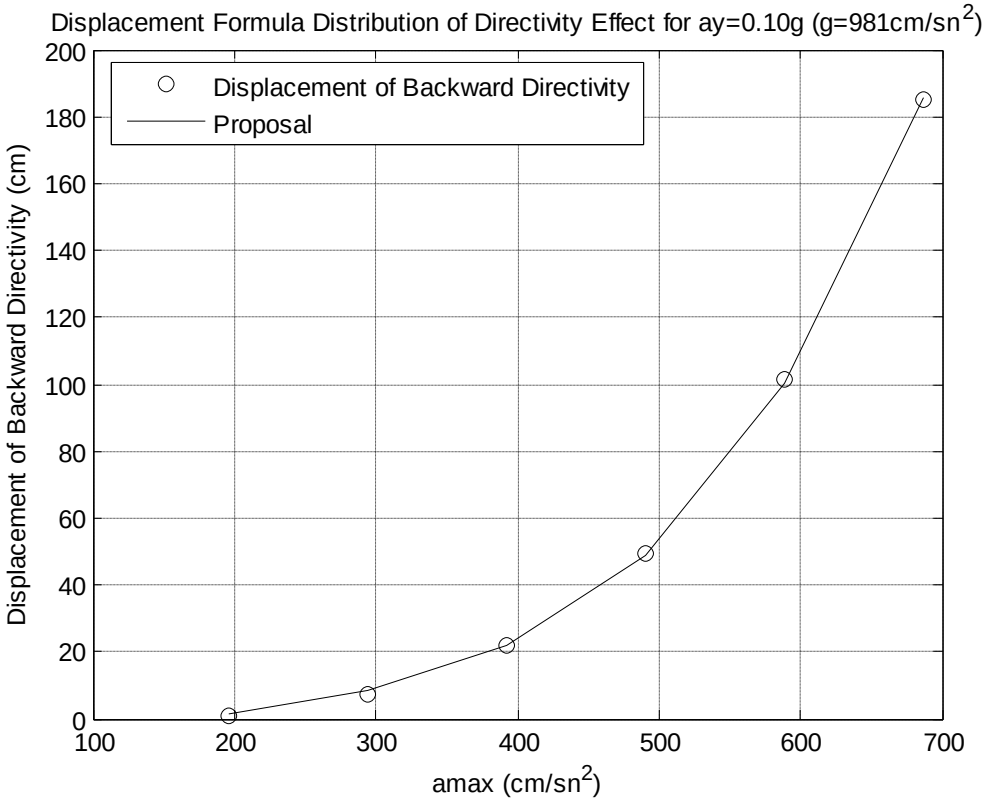

Figure B. 1 : Proposed displacement formula of backward displacement for a_y=0.10g, under same soil and fault normal component condition

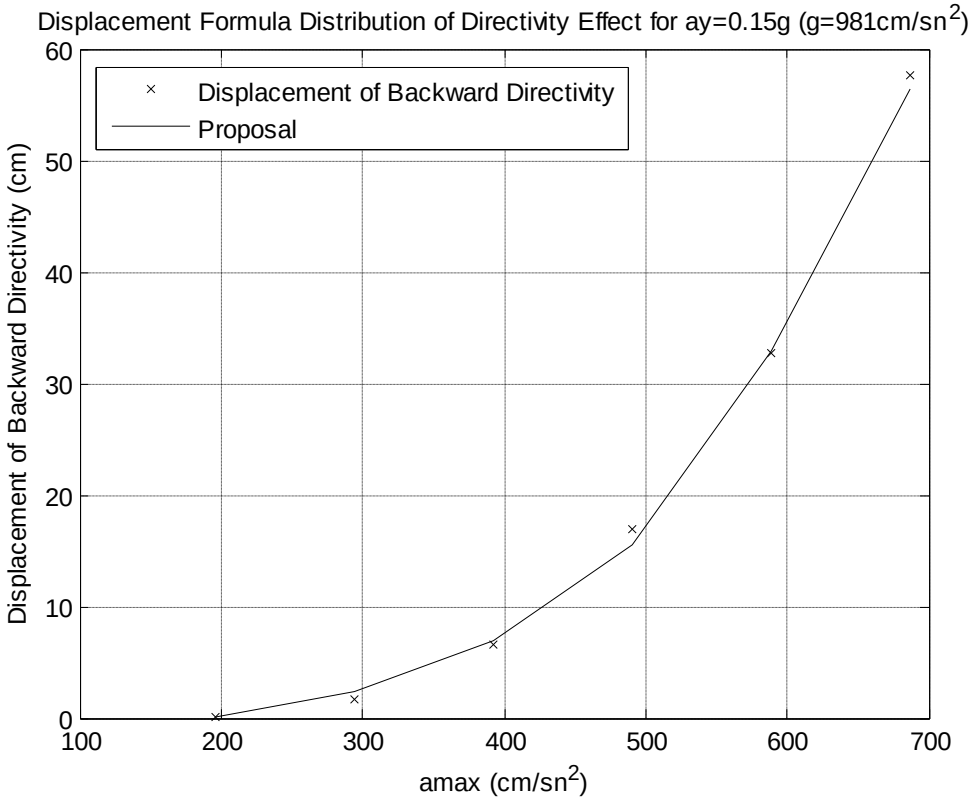

Figure B. 2 : Proposed displacement formula of backward displacement for a_y=0.15g, under same soil and fault normal component condition

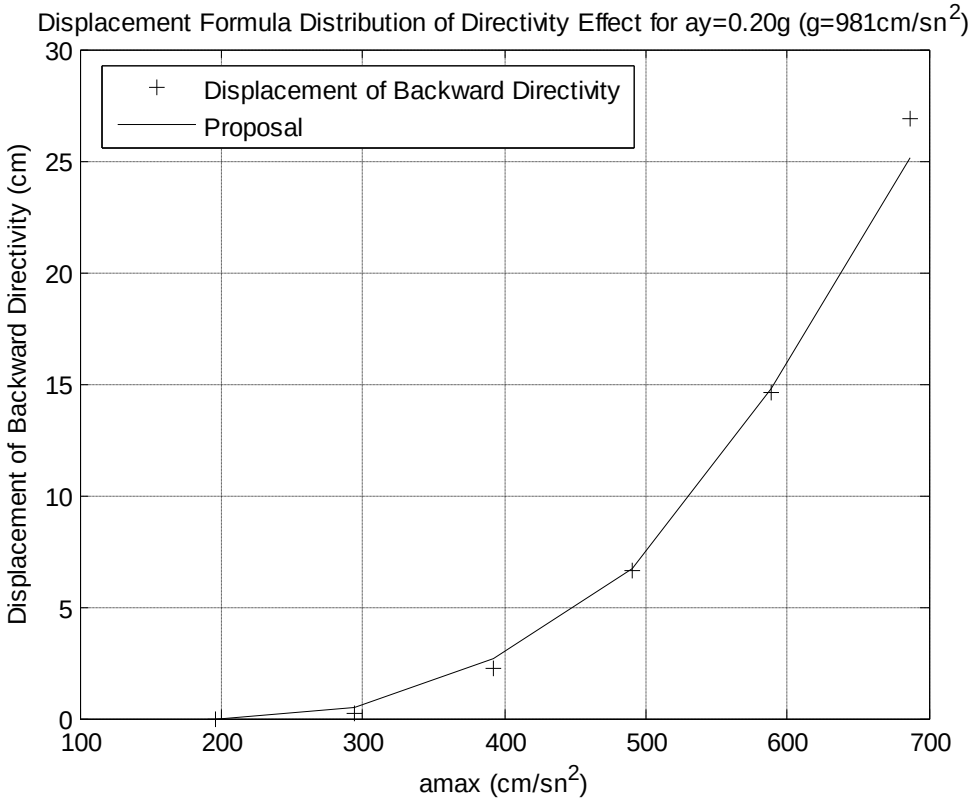

Figure B. 3 : Proposed displacement formula of backward displacement for a_y=0.20g, under same soil and fault normal component condition

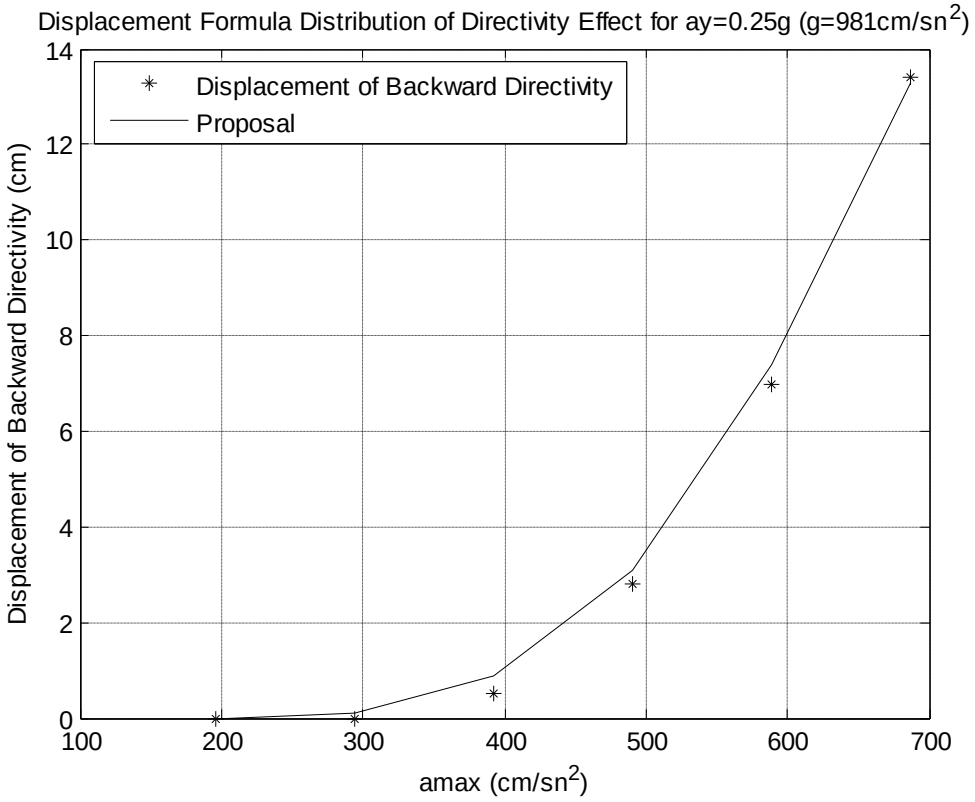

Figure B. 4 : Proposed displacement formula of backward displacement for a_y=0.25g, under same soil and fault normal component condition

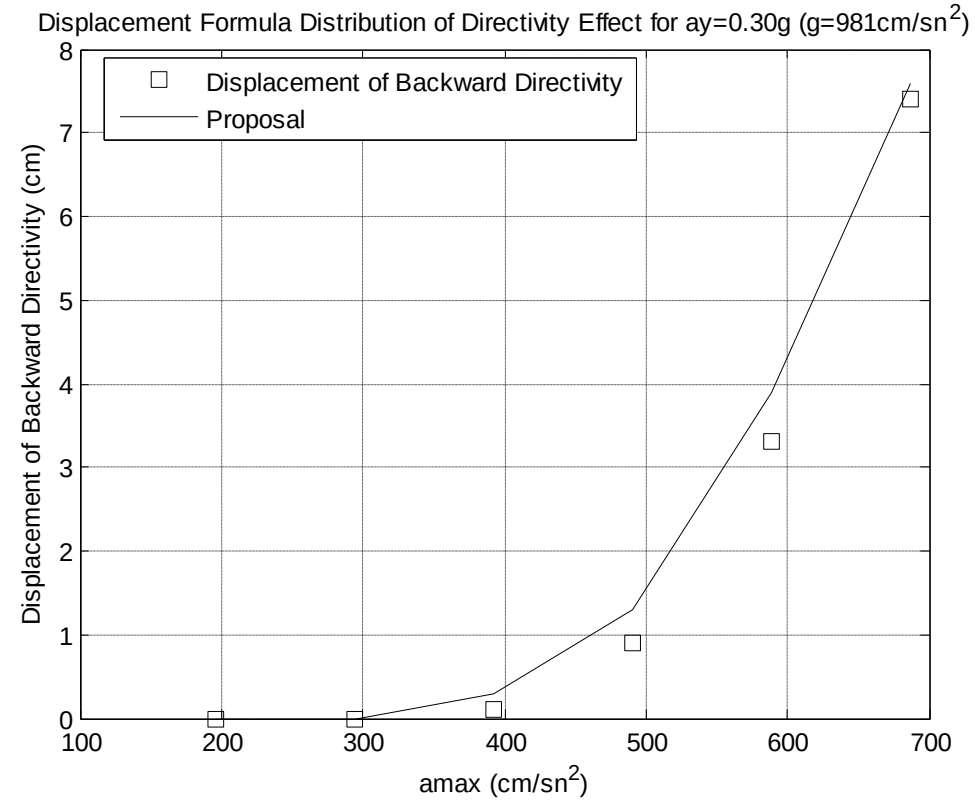

Figure B. 5 : Proposed displacement formula of backward displacement for a_y=0.30g, under same soil and fault normal component condition

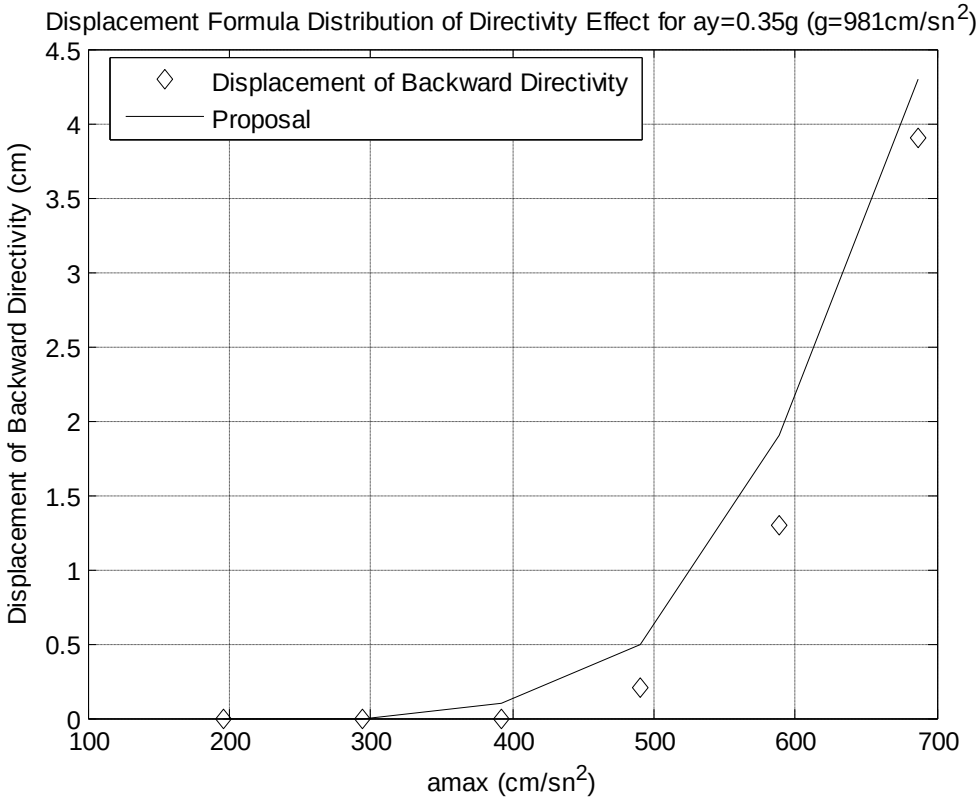

Figure B. 6 : Proposed displacement formula of backward displacement for a_y=0.35g, under same soil and fault normal component condition

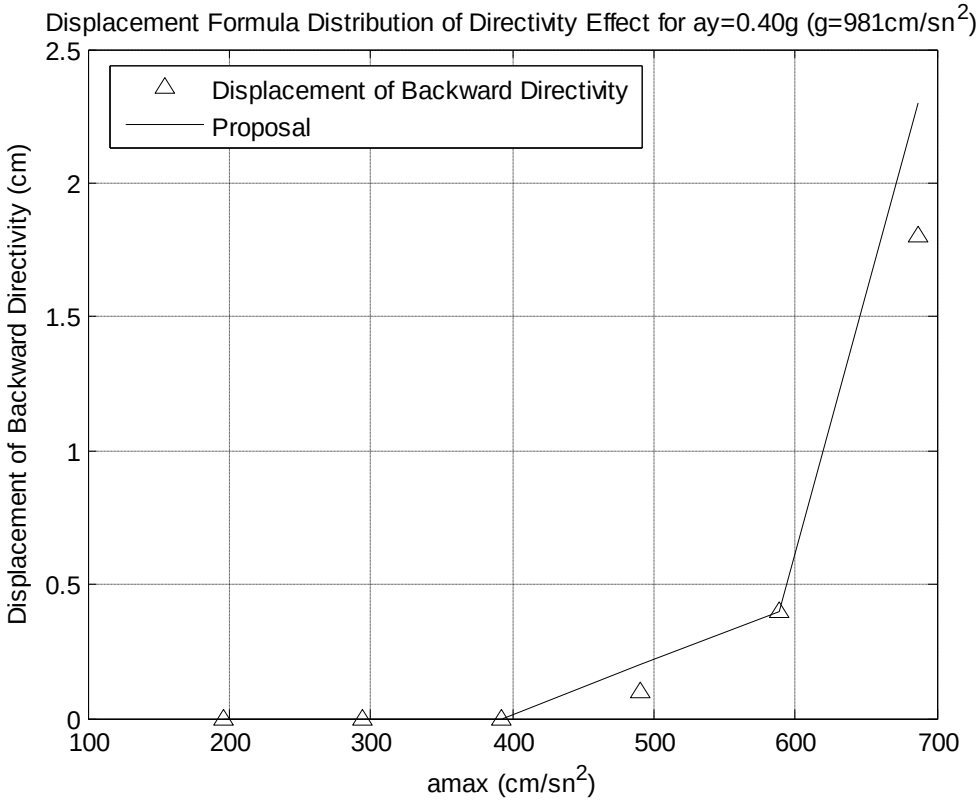

Figure B. 7 : Proposed displacement formula of backward displacement for a_y=0.40g, under same soil and fault normal component condition

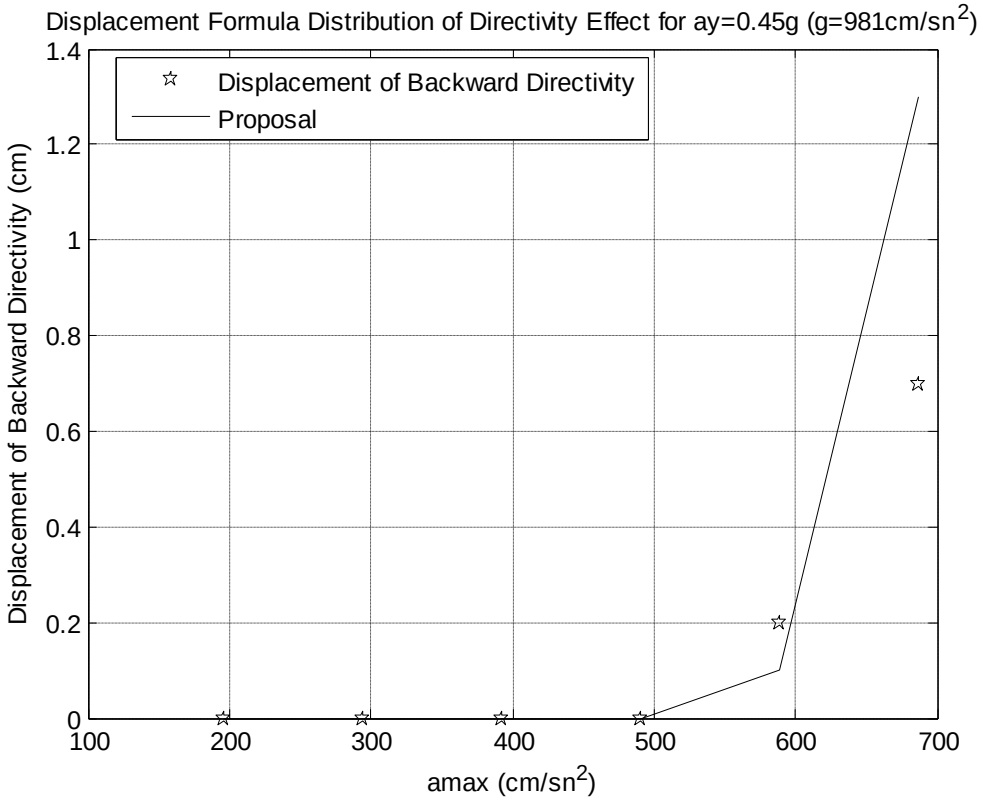

Figure B. 8 : Proposed displacement formula of backward displacement for a_y=0.45g, under same soil and fault normal component condition

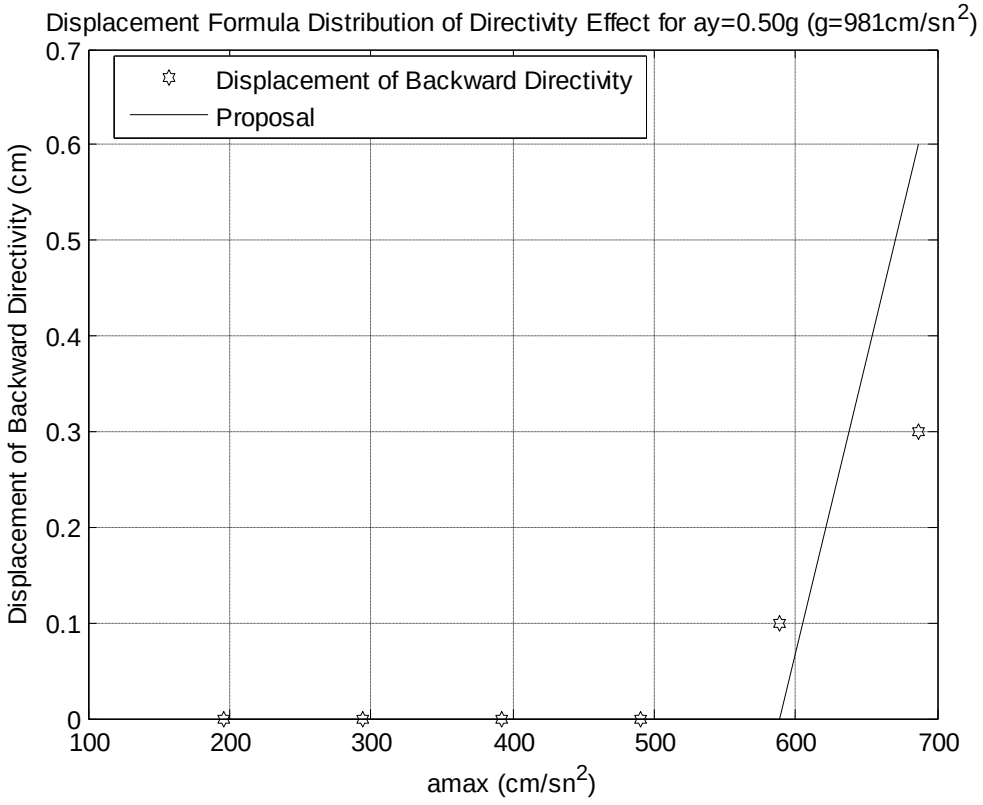

Figure B. 9 : Proposed displacement formula of backward displacement for a_y=0.50g, under same soil and fault normal component condition

APPENDIX C

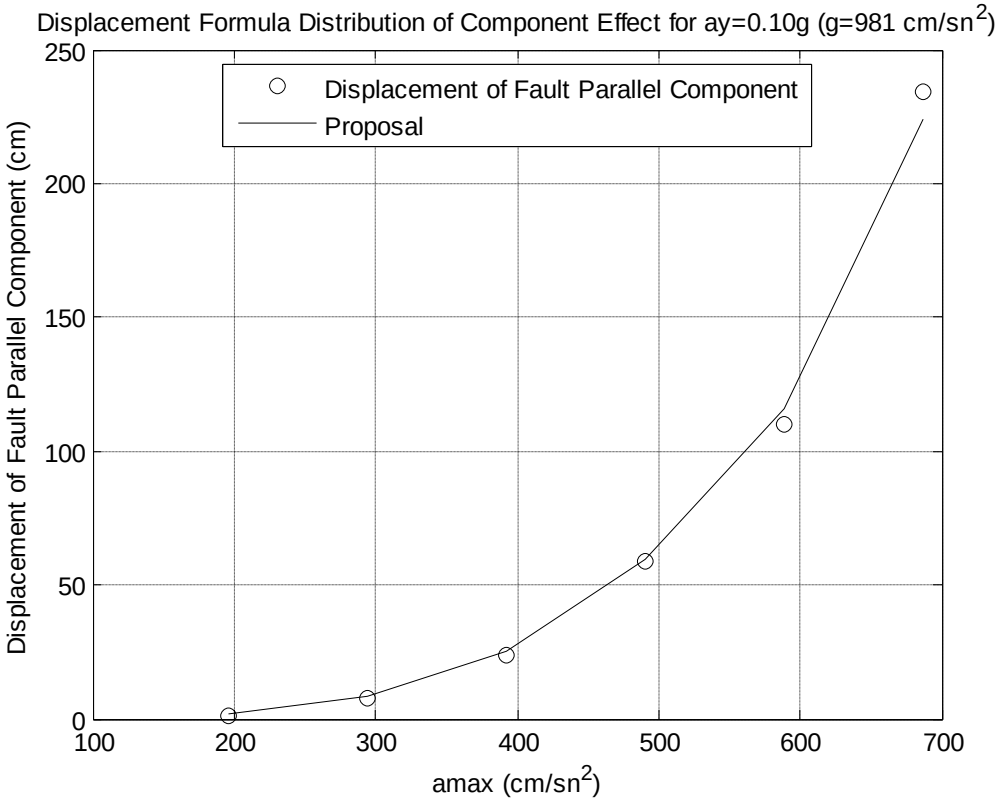

Figure C. 1 : Proposed displacement formula of component effect for a_y=0.10g, under same soil and forward directivity condition

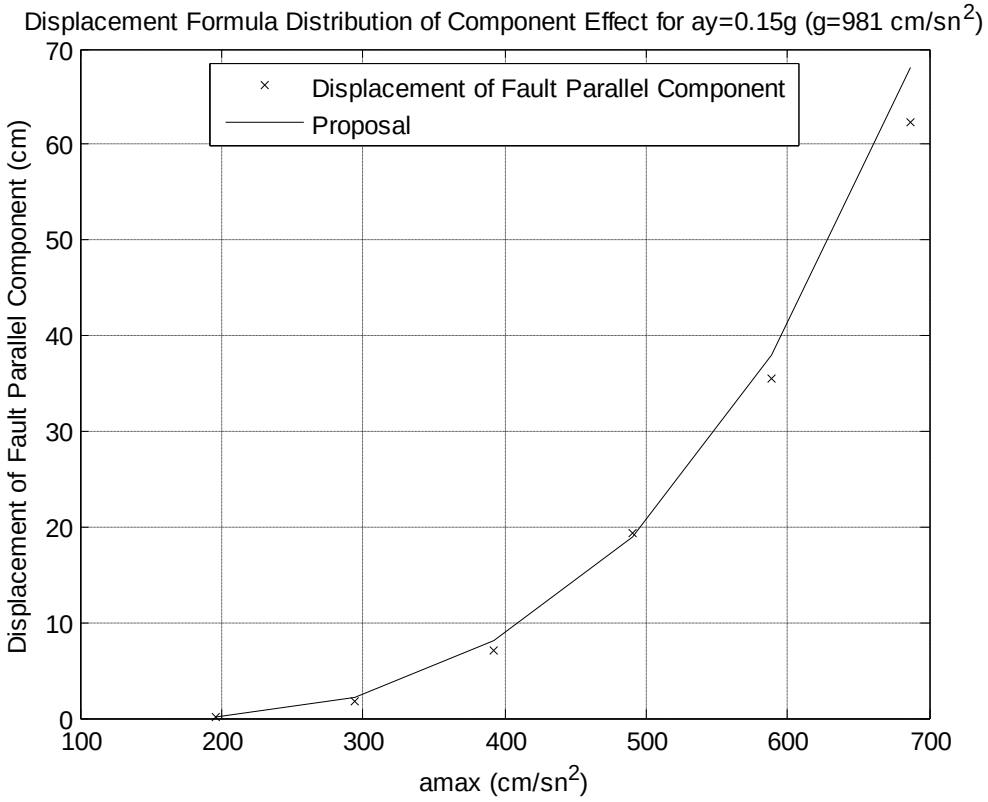

Figure C. 2 : Proposed displacement formula of component effect for a_y=0.15g, under same soil and forward directivity condition

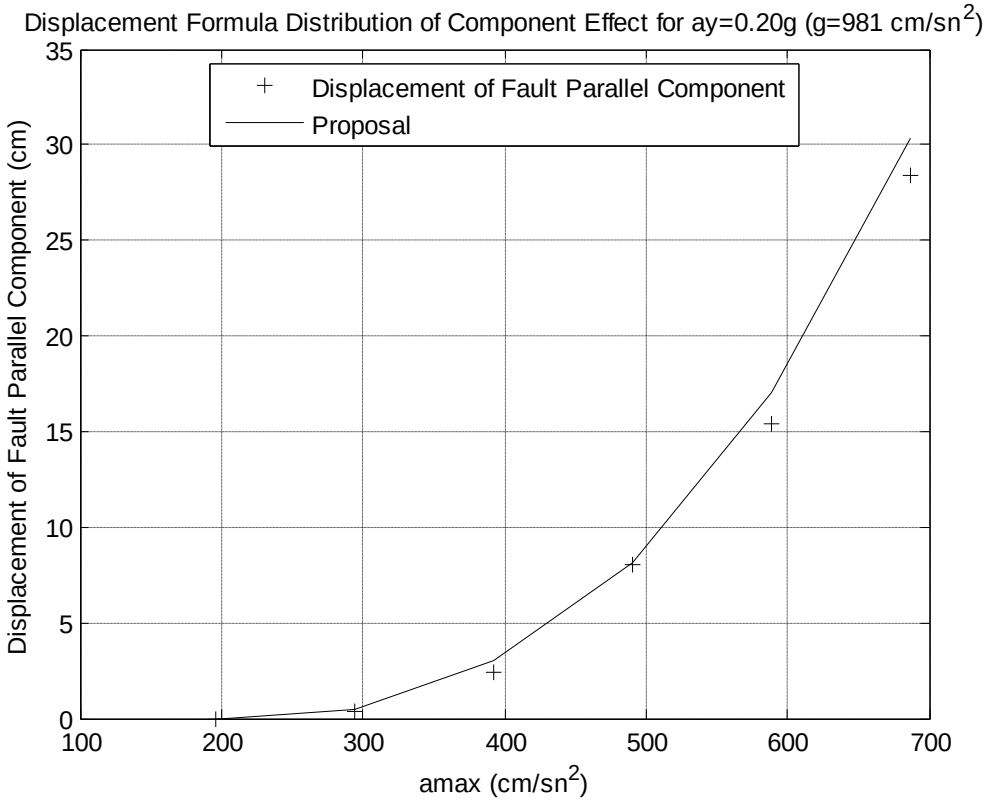

Figure C. 3 : Proposed displacement formula of component effect for a_y=0.20g, under same soil and forward directivity condition

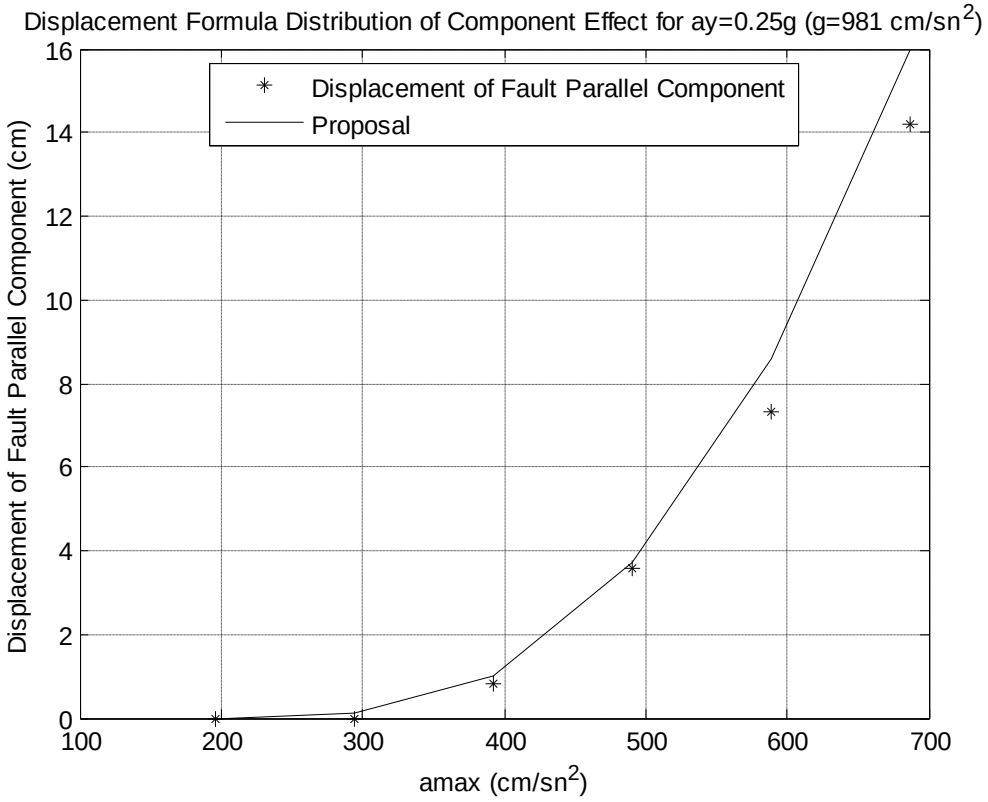

Figure C. 4 : Proposed displacement formula of component effect for a_y=0.25g, under same soil and forward directivity condition

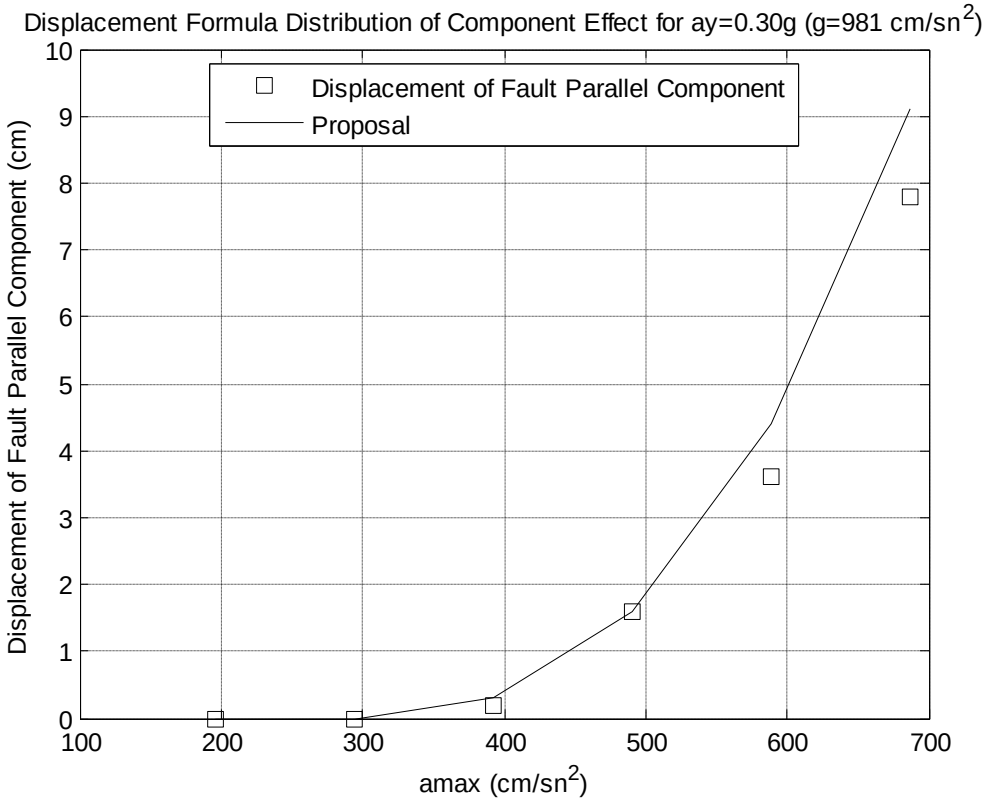

Figure C. 5 : Proposed displacement formula of component effect for a_y=0.30g, under same soil and forward directivity condition

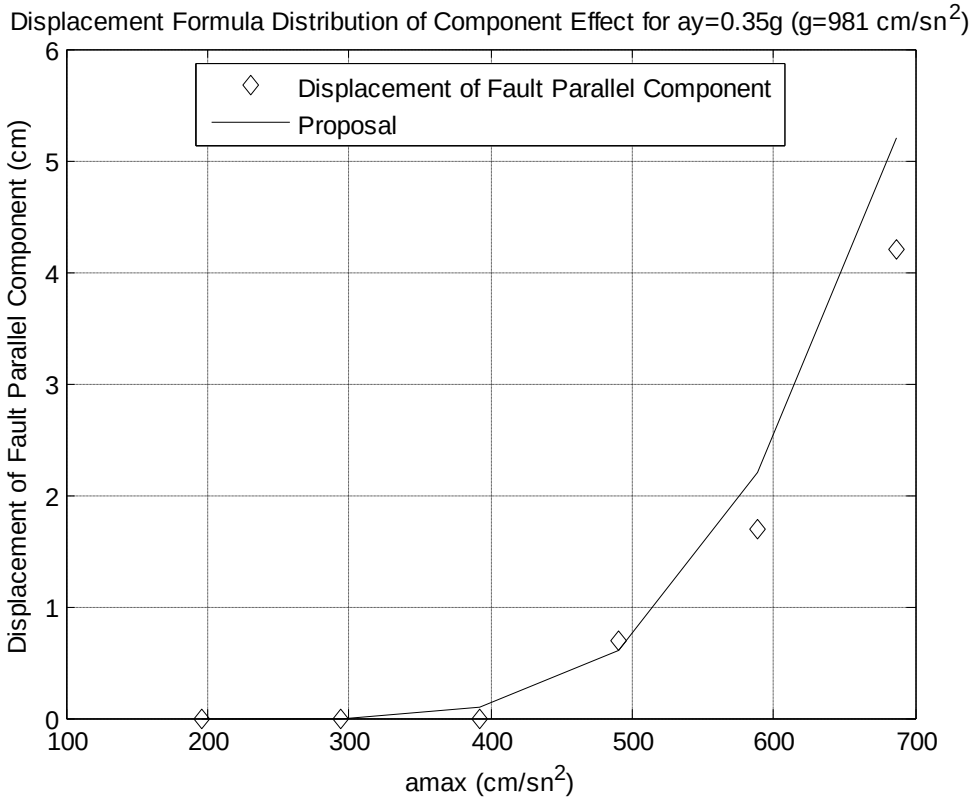

Figure C. 6 : Proposed displacement formula of component effect for a_y=0.35g, under same soil and forward directivity condition

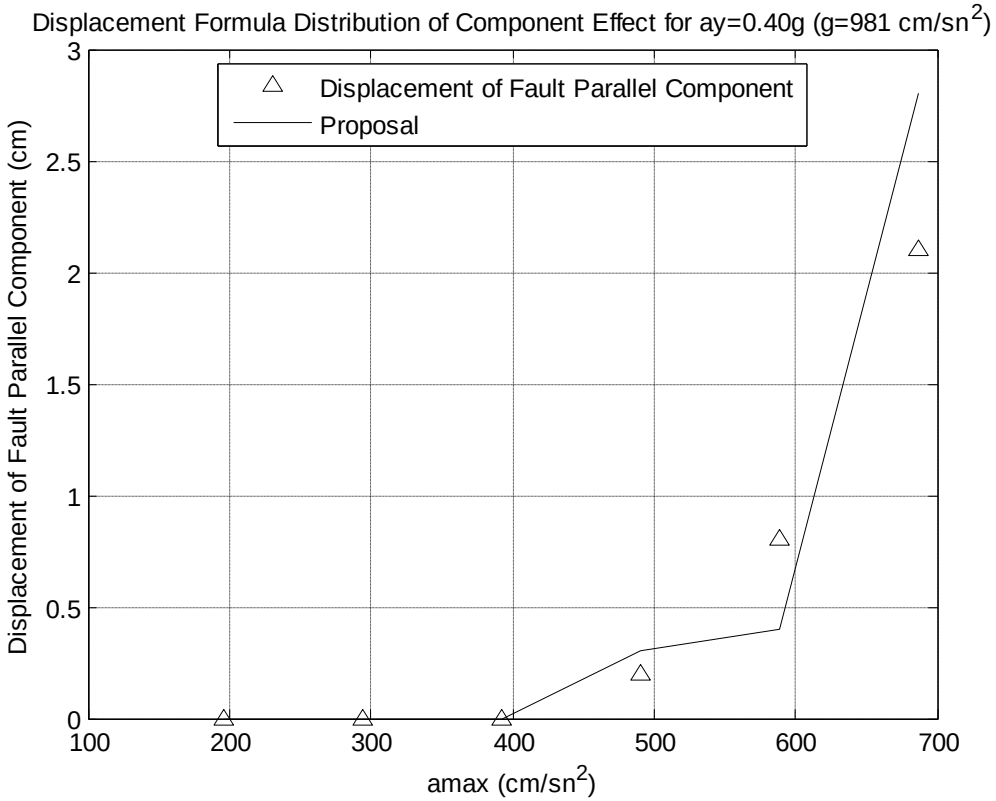

Figure C. 7 : Proposed displacement formula of component effect for a_y=0.40g, under same soil and forward directivity condition

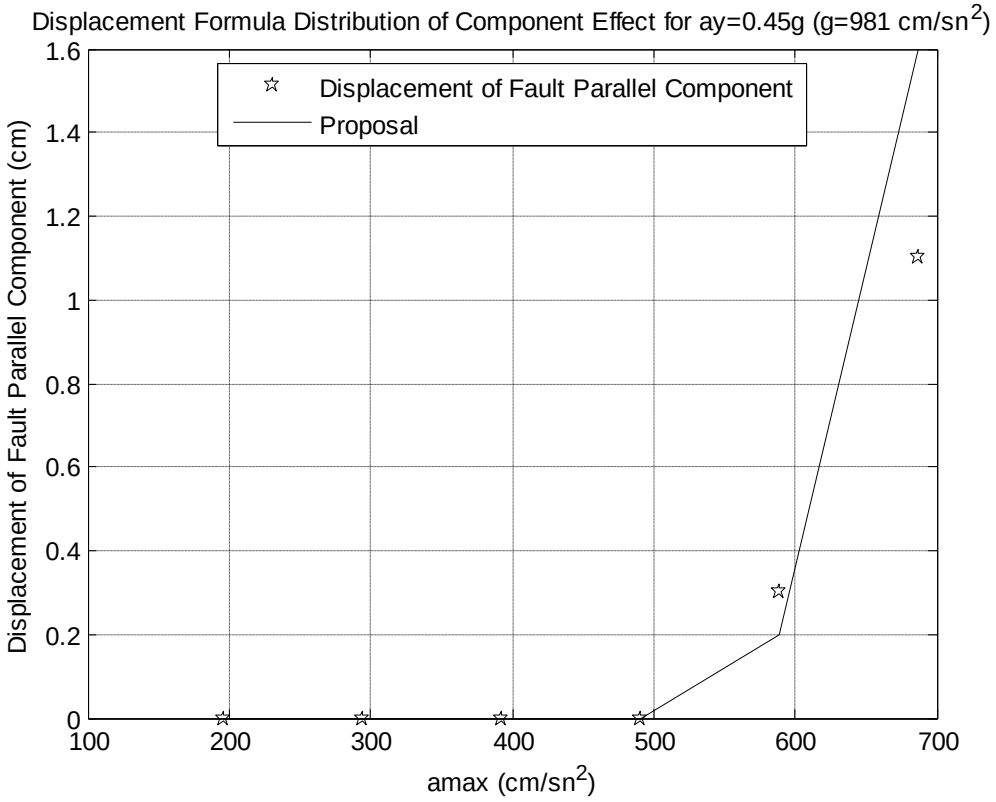

Figure C. 8 : Proposed displacement formula of component effect for a_y=0.45g, under same soil and forward directivity condition

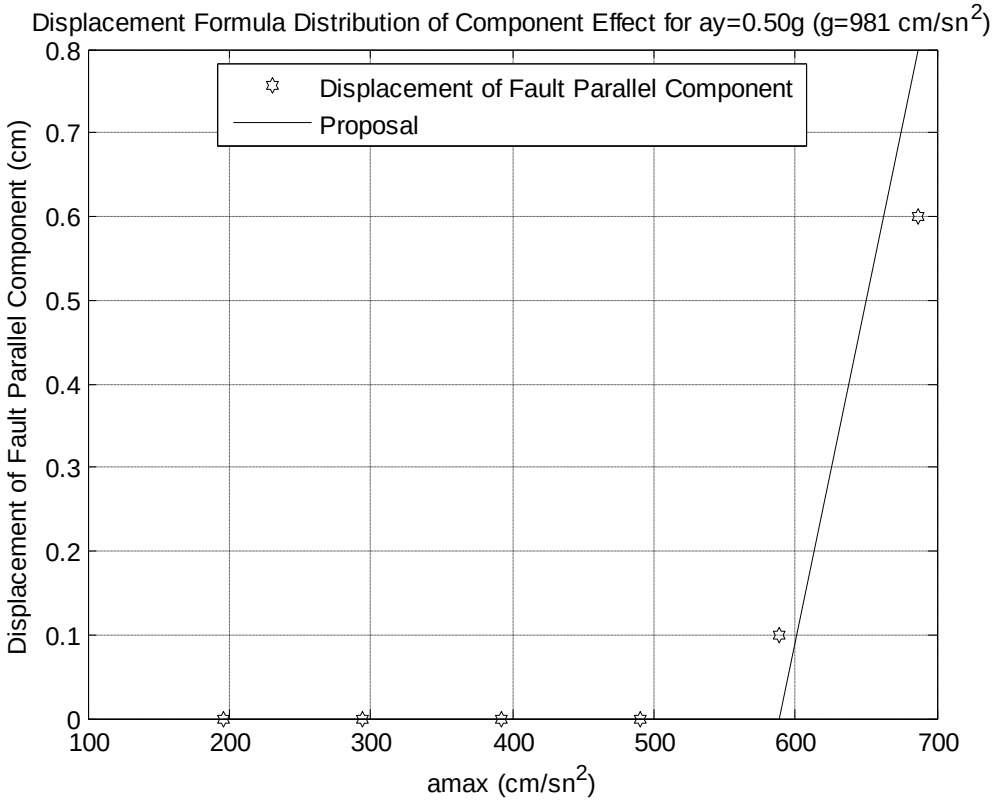

Figure C. 9 : Proposed displacement formula of component effect for a_y=0.50g, under same soil and forward directivity condition

APPENDIX D

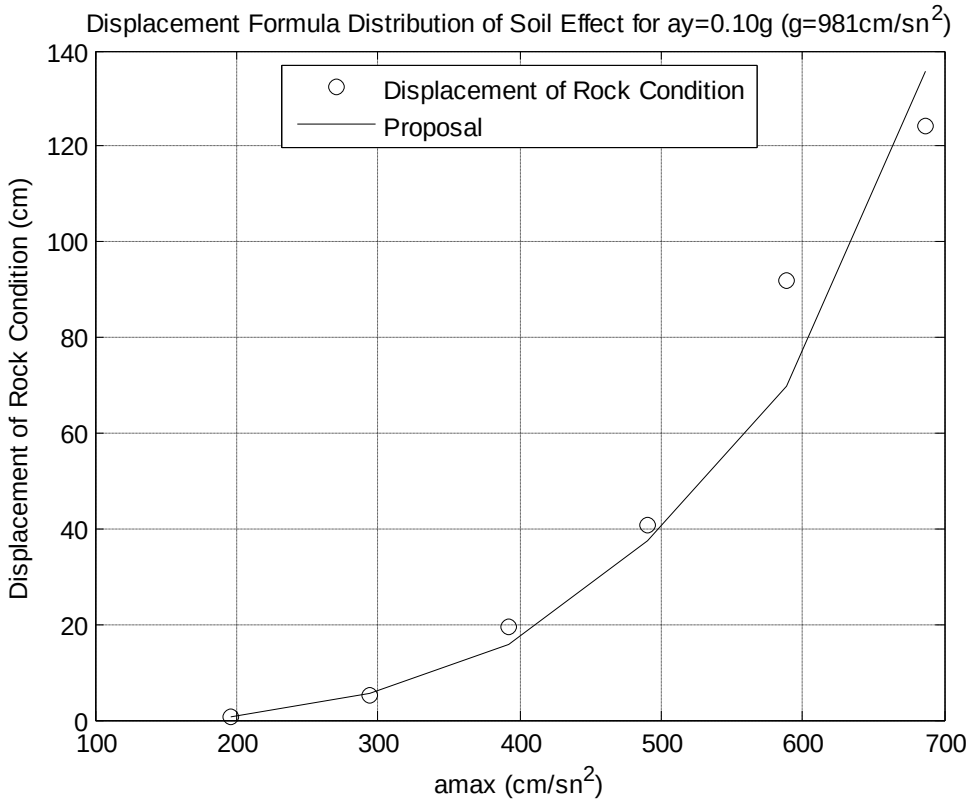

Figure D. 1 : Proposed displacement formula of soil effect for a_y=0.10g, under same fault normal component and forward directivity condition

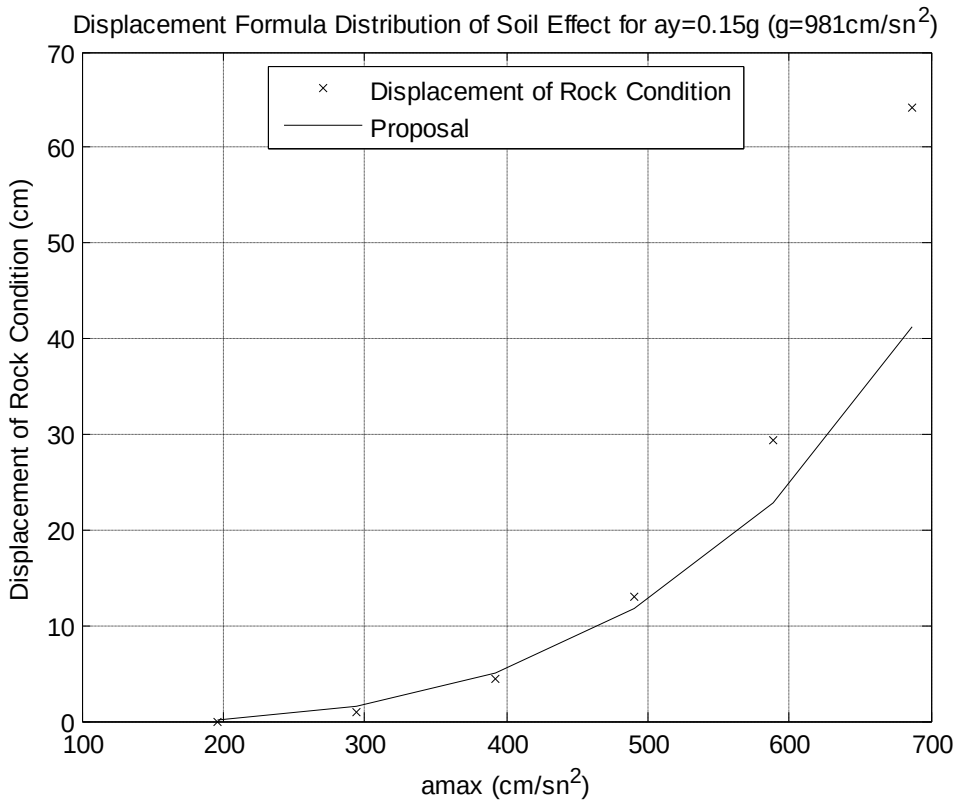

Figure D. 2 : Proposed displacement formula of soil effect for a_y=0.15g, under same fault normal component and forward directivity condition

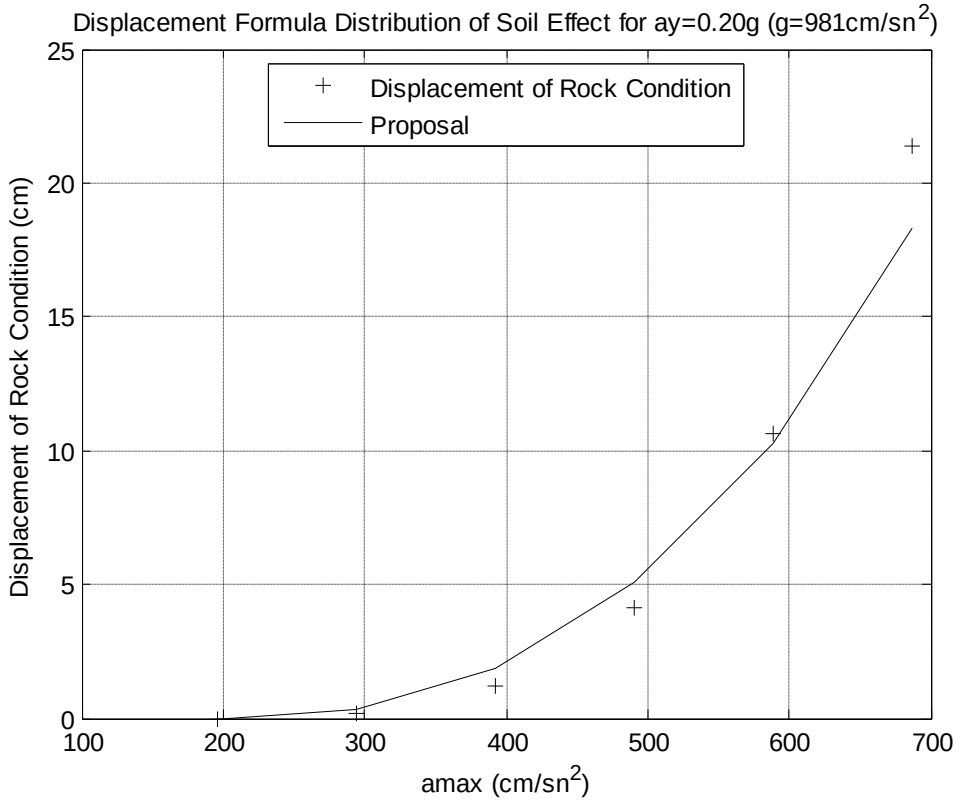

Figure D. 3 : Proposed displacement formula of soil effect for a_y=0.20g, under same fault normal component and forward directivity condition

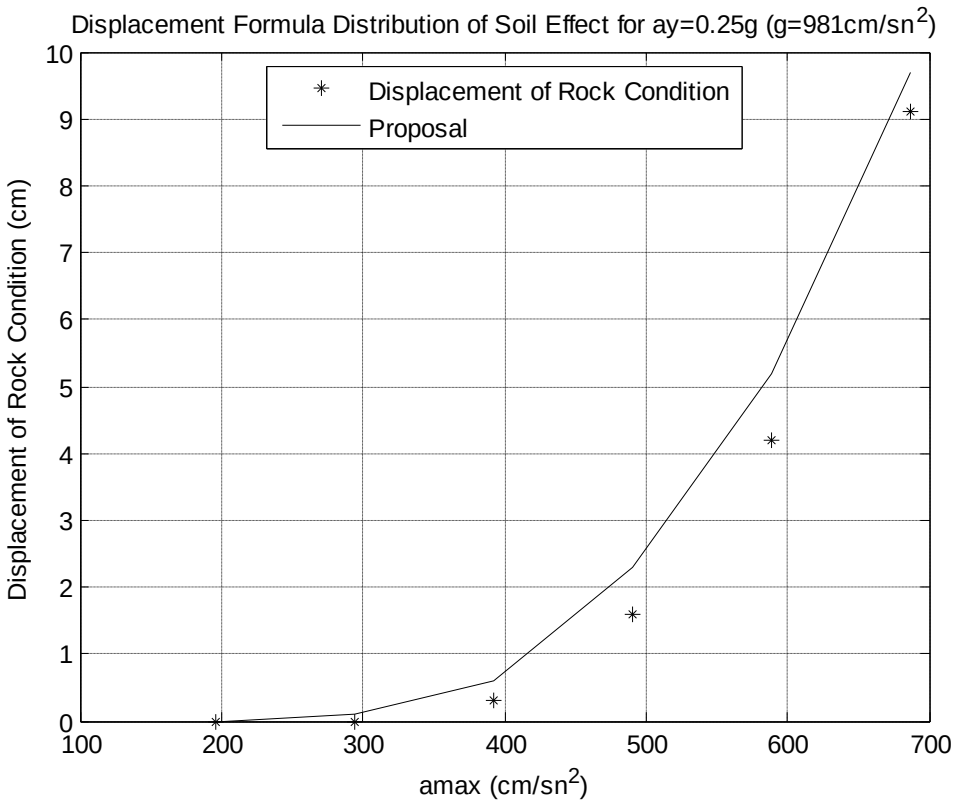

Figure D. 4 : Proposed displacement formula of soil effect for a_y=0.25g, under same fault normal component and forward directivity condition

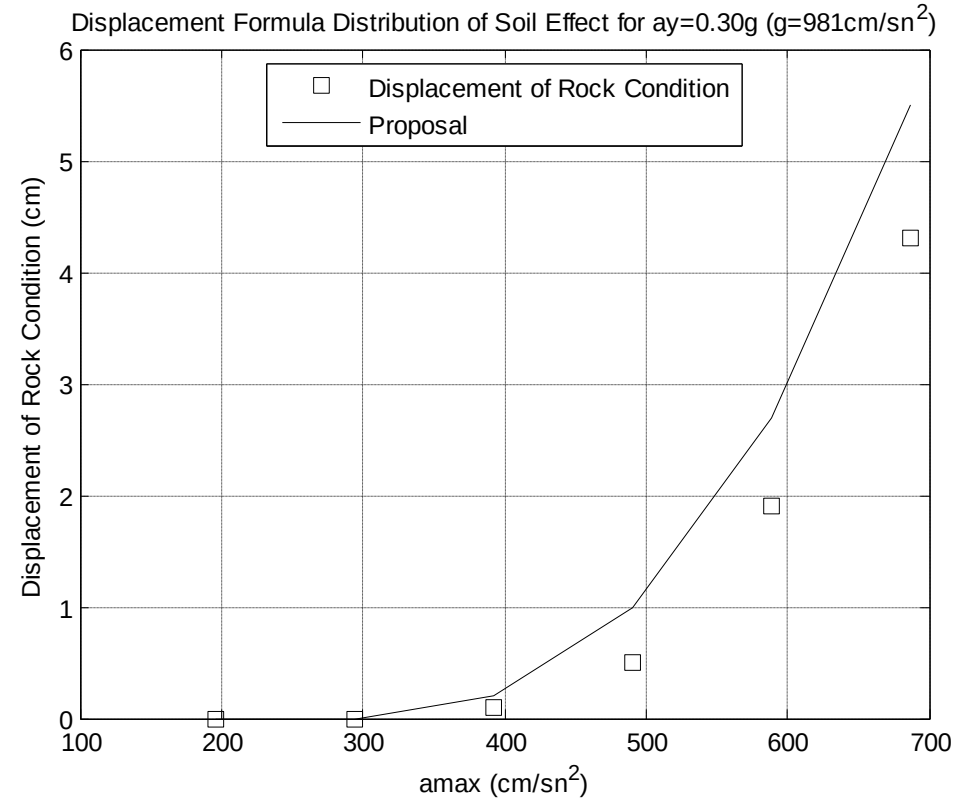

Figure D. 5 : Proposed displacement formula of soil effect for a_y=0.30g, under same fault normal component and forward directivity condition

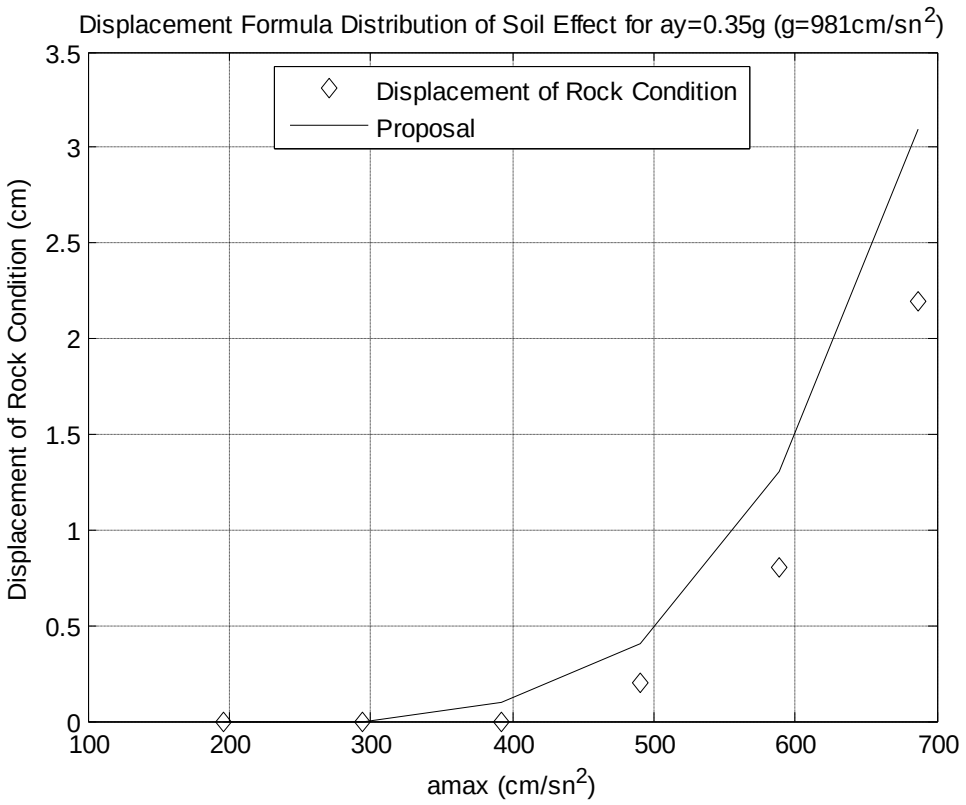

Figure D. 6 : Proposed displacement formula of soil effect for a_y=0.35g, under same fault normal component and forward directivity condition

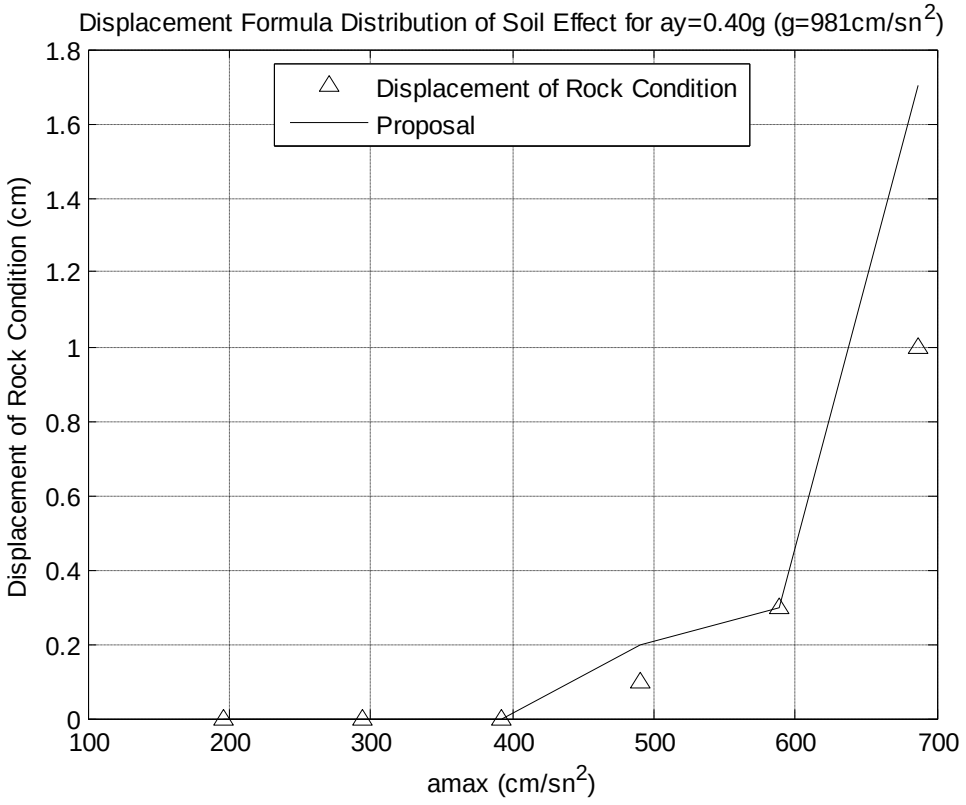

Figure D. 7 : Proposed displacement formula of soil effect for a_y=0.40g, under same fault normal component and forward directivity condition

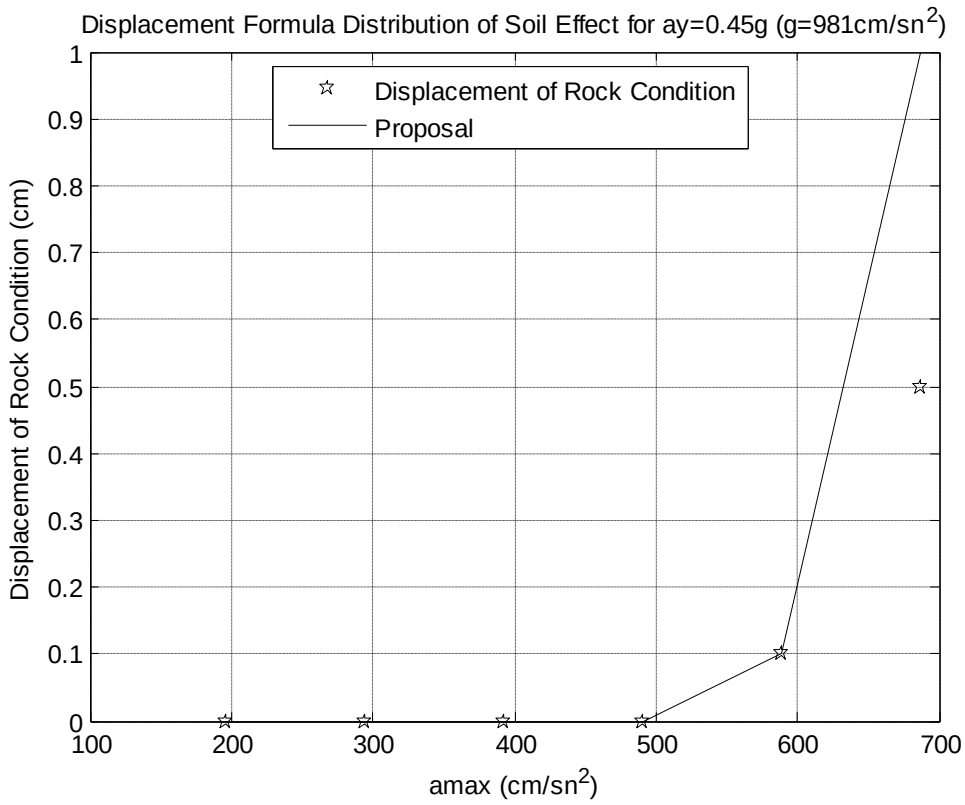

Figure D. 8 : Proposed displacement formula of soil effect for a_y=0.45g, under same fault normal component and forward directivity condition

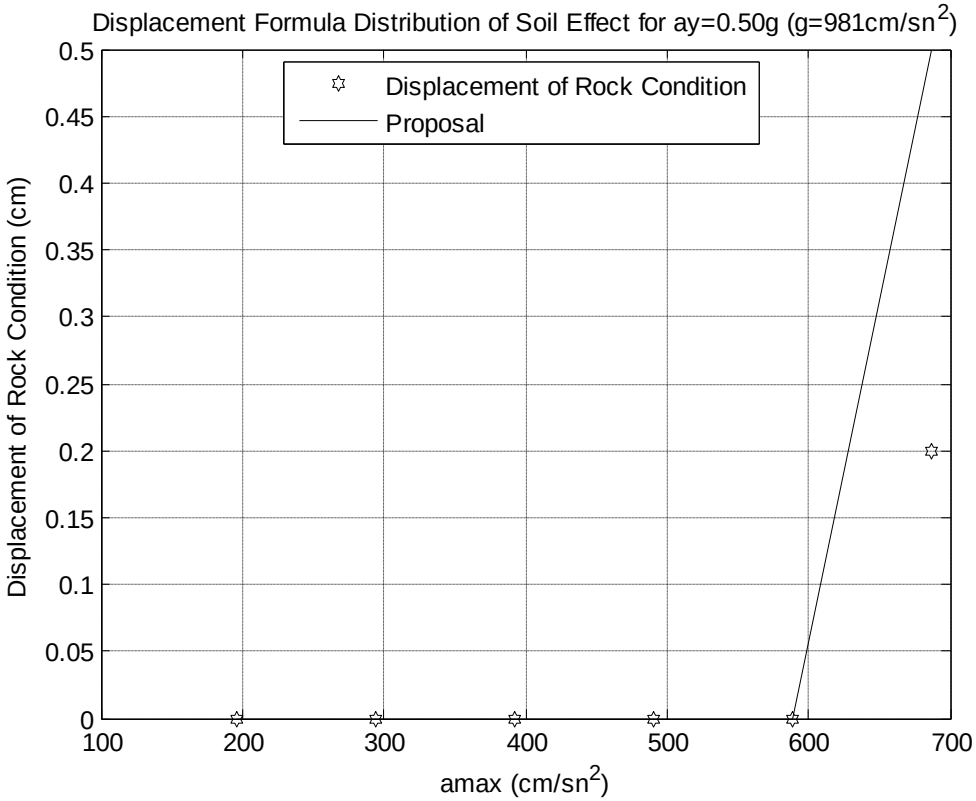

Figure D. 9 : Proposed displacement formula of soil effect for a_y=0.50g, under same fault normal component and forward directivity condition

APPENDIX E

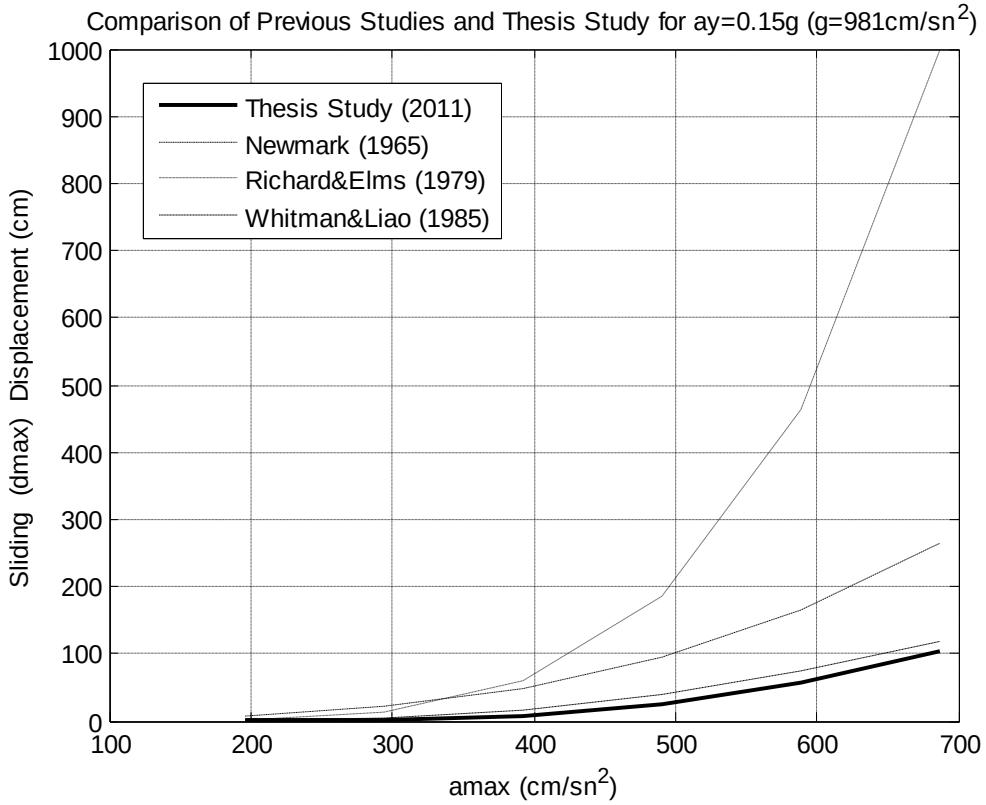

Figure E. 1 : Proposed simplified results for evaluating sliding displacement of Thesis Study (2011) for constant yield acceleration $a_y=0.15g$

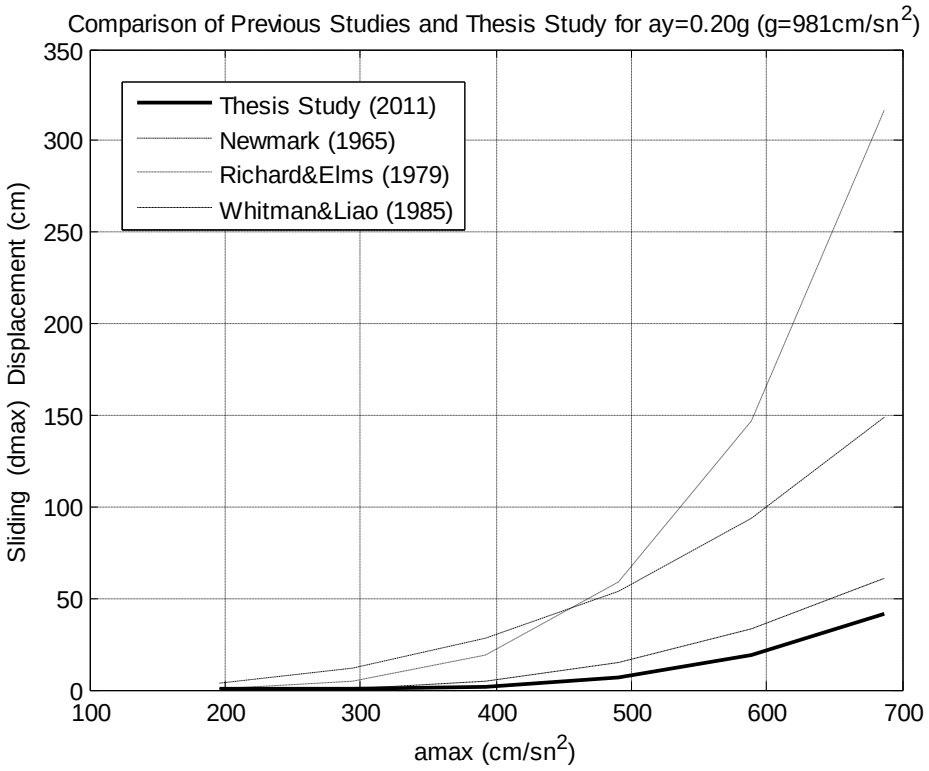

Figure E. 2 : Proposed simplified results for evaluating sliding displacement of Thesis Study (2011) for constant yield acceleration a_y=*0.20g*

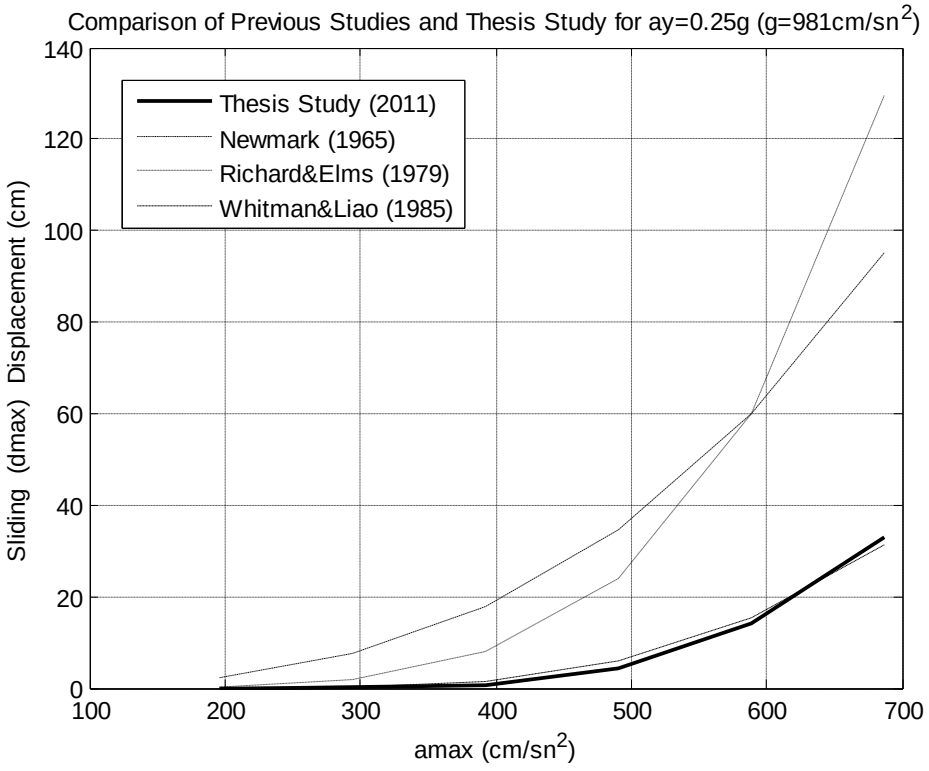

Figure E. 3 : Proposed simplified results for evaluating sliding displacement of Thesis Study (2011) for constant yield acceleration a_y=*0.25g*

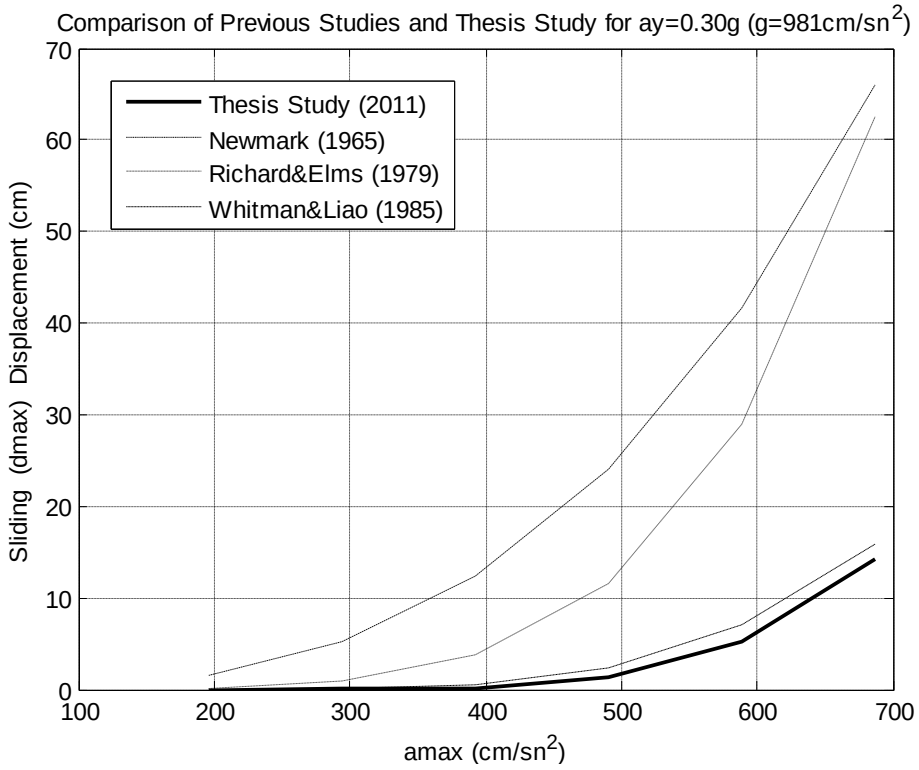

Figure E. 4 : Proposed simplified results for evaluating sliding displacement of Thesis Study (2011) for constant yield acceleration $a_y=0.30g$

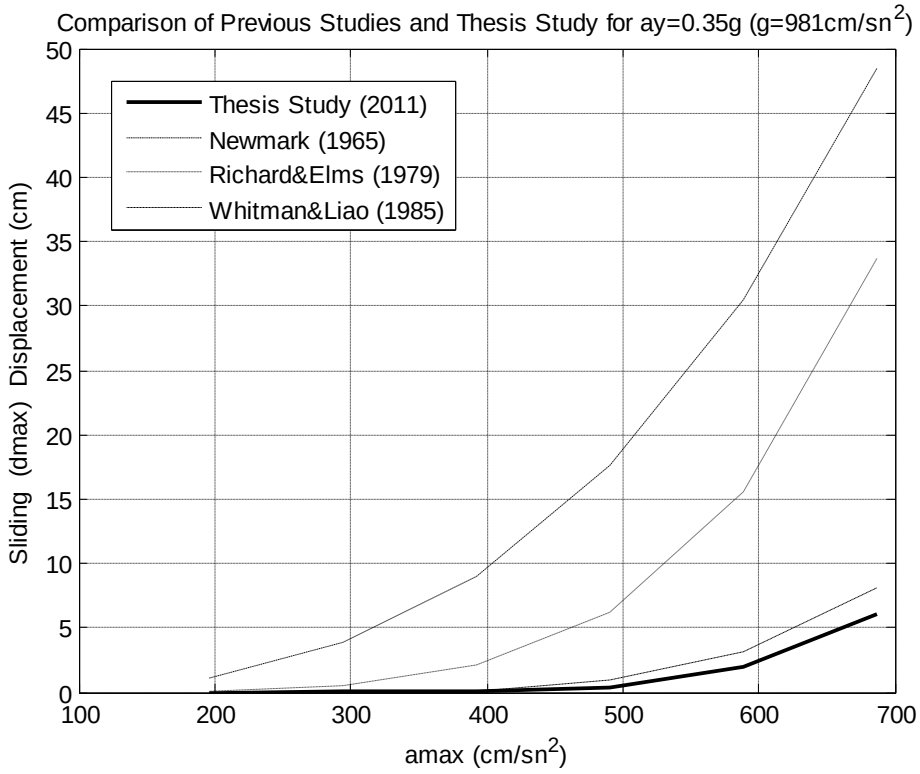

Figure E. 5 : Proposed simplified results for evaluating sliding displacement of Thesis Study (2011) for constant yield acceleration $a_y=0.35g$

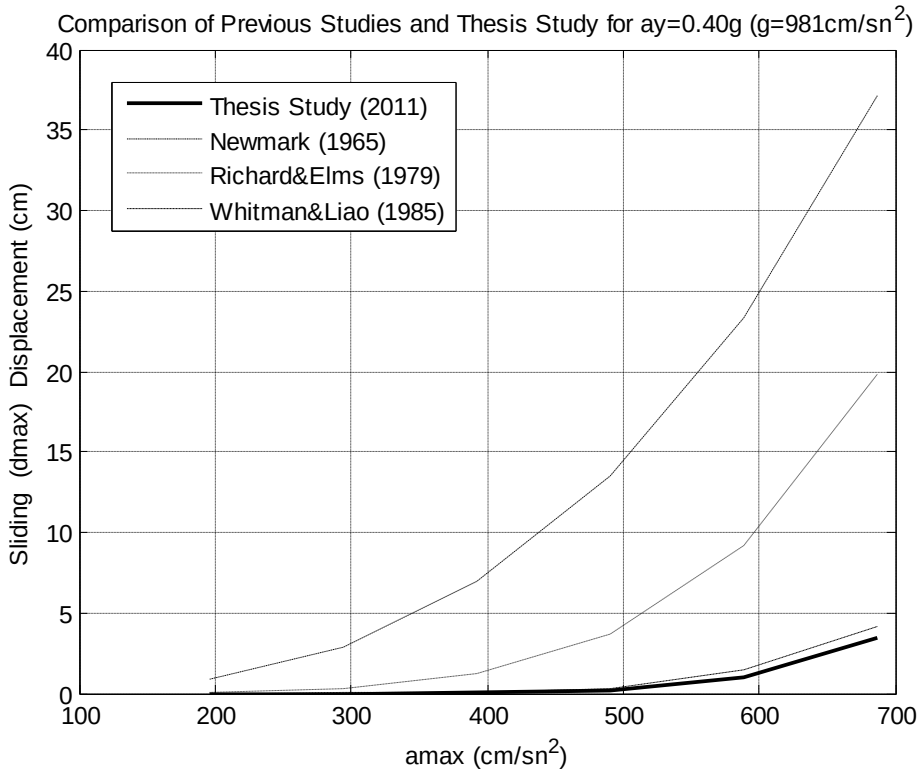

Figure E. 6 : Proposed simplified results for evaluating sliding displacement of Thesis Study (2011) for constant yield acceleration $a_y=0.40g$

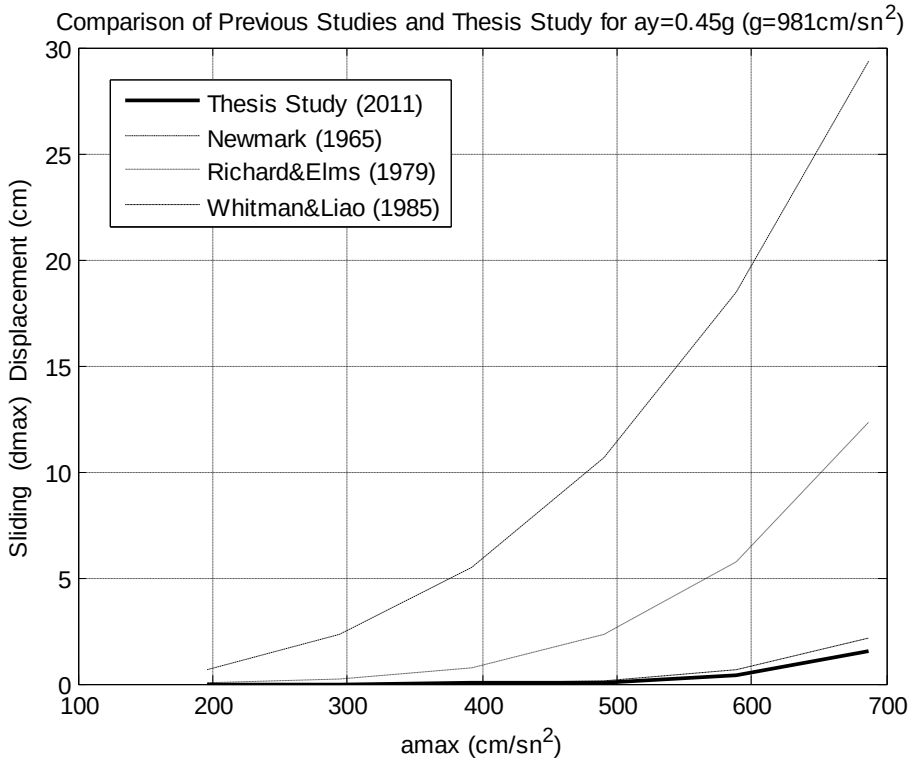

Figure E. 7 : Proposed simplified results for evaluating sliding displacement of Thesis Study (2011) for constant yield acceleration $a_y=0.45g$

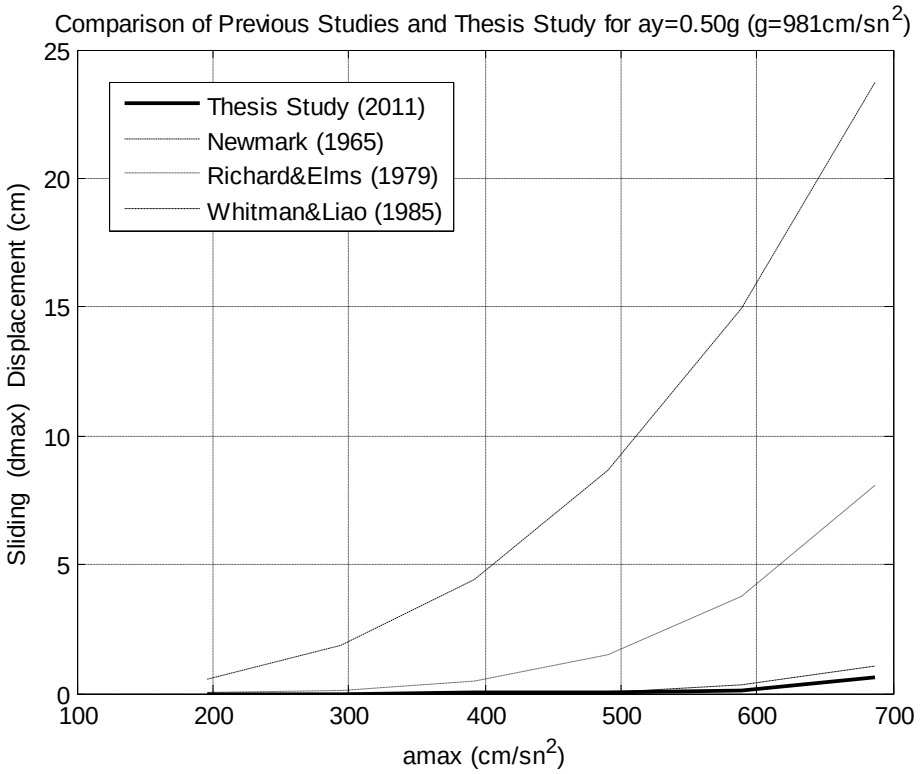

Figure E. 8 : Proposed simplified results for evaluating sliding displacement of Thesis Study (2011) for constant yield acceleration $a_y=0.50g$

APPENDIX F

Fit informations, input datas and results of regression analyis are presented for mentioned earlier in the title of main formula, directivity effect, component effect and soil effect respectively.

A. MAIN INITIAL FORMULA

Main initial formula contains Equation 5.8, Equation 5.9 and Equation 5.10 based on Equation 5.7.

A.1 Fit Information

DataFit version 9.0.59
Equation ID: Main-Initial Formula
Model Definition:
Y = (a*X3^2/X2)*exp(-b*X1/X2)

Number of observations = 36
Number of missing observations = 0
Solver type: Nonlinear
Nonlinear iteration limit = 250
Diverging nonlinear iteration limit =10
Number of nonlinear iterations performed = 12
Residual tolerance = 0.0000000001
Sum of Residuals = 74.9107395944994
Average Residual = 2.08085387762498
Residual Sum of Squares (Absolute) = 919.784017724237
Residual Sum of Squares (Relative) = 919.784017724237
Standard Error of the Estimate = 5.20119900691527
Coefficient of Multiple Determination (R^2) = 0.9897213669
Proportion of Variance Explained = 98.97213669%
Adjusted coefficient of multiple determination (Ra^2) = 0.9894190542
Durbin-Watson statistic = 1.45050448526656

Regression Variable Results

Variable				
a	**Value**	**Standard Error**	**t-ratio**	**Prob(t)**
b	91.5565655589236	7.55320615997933	12.12154992	0.0
	15.1041521738839	0.501644941082871	30.10924847	0.0

68% Confidence Intervals

Variable				
a	**Value**	**68% (+/-)**	**Lower Limit**	**Upper Limit**
b	91.5565655589236	7.62269565665114	83.9338699022725	99.1792612155747
	15.1041521738839	0.506260074540834	14.5978920993431	15.6104122484247

90% Confidence Intervals

Variable				
a	**Value**	**90% (+/-)**	**Lower Limit**	**Upper Limit**
b	91.5565655589236	12.771716295909	78.7848492630146	104.328281854833

	15.1041521738839	0.848231430877027	14.2559207430069	15.9523836047609

95% Confidence Intervals

Variable				
a	**Value**	**95% (+/-)**	**Lower Limit**	**Upper Limit**
b	91.5565655589236	15.34962555831	76.2069400006136	106.906191117234
	15.1041521738839	1.01944284926861	14.0847093246153	16.1235950231525

99% Confidence Intervals

Variable				
a	**Value**	**99% (+/-)**	**Lower Limit**	**Upper Limit**
b	91.5565655589236	20.6081676868876	70.948397872036	112.164733245811
	15.1041521738839	1.36868805725051	13.7354641166334	16.4728402311344

Variance Analysis

Source				
Regression	**DF**	**Sum of Squares**	**Mean Square**	**F Ratio**
Error	1	88565.268204498	88565.268204498	3273.832836
Total	34	919.784017724237	27.0524711095364	
	35	89485.0522222222		

A.2 Data Table

Min Residual	**Max Residual**
-15.299	10.646

X1:ay	X2:amax	X3:vmax	Y:dmax0	Calc Y	Residual	% Error	Abs Residual
98.1	196.2	36.9	1.8	0.334	1.466	81.467	1.466
98.1	294.3	55.3	10.1	6.192	3.908	38.698	3.908
98.1	392.4	73.7	29.5	29.039	0.461	1.562	0.461
98.1	490.5	92.1	70.2	77.204	-7.004	-9.977	7.004
98.1	588.6	110.6	138.2	153.499	-15.299	-11.070	15.299
98.1	686.7	129	267.1	256.454	10.646	3.986	10.646
147.15	196.2	36.9	0.2	0.008	0.192	96.178	0.192
147.15	294.3	55.3	2.7	0.499	2.201	81.500	2.201
147.15	392.4	73.7	9.4	4.396	5.004	53.237	5.004
147.15	490.5	92.1	22.3	17.048	5.252	23.551	5.252
147.15	588.6	110.6	45.2	43.598	1.602	3.544	1.602
147.15	686.7	129	81.1	87.189	-6.089	-7.508	6.089
196.2	294.3	55.3	0.6	0.040	0.560	93.284	0.560
196.2	392.4	73.7	3.6	0.665	2.935	81.517	2.935
196.2	490.5	92.1	9.6	3.765	5.835	60.786	5.835
196.2	588.6	110.6	20.3	12.383	7.917	38.999	7.917
196.2	686.7	129	36.1	29.643	6.457	17.888	6.457
245.25	294.3	55.3	0.1	0.003	0.097	96.749	0.097
245.25	392.4	73.7	1.2	0.101	1.099	91.607	1.099
245.25	490.5	92.1	4.4	0.831	3.569	81.107	3.569
245.25	588.6	110.6	10.2	3.517	6.683	65.518	6.683
245.25	686.7	129	19.1	10.078	9.022	47.236	9.022
294.3	392.4	73.7	0.4	0.015	0.385	96.188	0.385
294.3	490.5	92.1	1.9	0.184	1.716	90.339	1.716
294.3	588.6	110.6	5.3	0.999	4.301	81.151	4.301
294.3	686.7	129	10.9	3.426	7.474	68.566	7.474
343.35	392.4	73.7	0.1	0.002	0.098	97.692	0.098

X1:ay	X2:amax	X3:vmax	Y:dmax0	Calc Y	Residual	% Error	Abs Residual
343.35	490.5	92.1	0.7	0.041	0.659	94.209	0.659
343.35	588.6	110.6	2.6	0.284	2.316	89.087	2.316
343.35	686.7	129	6.2	1.165	5.035	81.212	5.035
392.4	490.5	92.1	0.3	0.009	0.291	97.016	0.291
392.4	588.6	110.6	0.5	0.081	0.419	83.882	0.419
392.4	686.7	129	3.3	0.396	2.904	87.999	2.904
441.45	588.6	110.6	0.2	0.023	0.177	88.555	0.177
441.45	686.7	129	1.9	0.135	1.765	92.914	1.765
490.5	686.7	129	0.9	0.046	0.854	94.914	0.854

B. DIRECTIVITY EFFECT FORMULA

Directivity effect formula covers Equation 5.12.

B.1 Fit Information

DataFit version 9.0.59
Equation ID: Directivity-Effect
Model Definition:
Y = X1/(a+X2/X3*b)

Number of observations = 35
Number of missing observations = 0
Solver type: Nonlinear
Nonlinear iteration limit = 250
Diverging nonlinear iteration limit =10
Number of nonlinear iterations performed = 16
Residual tolerance = 0.0000000001
Sum of Residuals = -4.2444454884029
Average Residual = -0.121269871097226
Residual Sum of Squares (Absolute) = 13.416193500519
Residual Sum of Squares (Relative) = 13.416193500519
Standard Error of the Estimate = 0.637613768826823
Coefficient of Multiple Determination (R^2) = 0.9996953707
Proportion of Variance Explained = 99.96953707%
Adjusted coefficient of multiple determination (Ra^2) = 0.9996861395
Durbin-Watson statistic = 2.10065986980499

Regression Variable Results

Variable				
a	**Value**	**Standard Error**	**t-ratio**	**Prob(t)**
b	133.322464097714	17.7308200866246	7.519249727	0.0
	-82.9151695353331	11.1457120513477	-7.439198963	0.0

68% Confidence Intervals

Variable				
a	**Value**	**68% (+/-)**	**Lower Limit**	**Upper Limit**
b	133.322464097714	17.9028090414649	115.419655056249	151.225273139179
	-82.9151695353331	11.2538254582457	-94.1689949935788	-71.6613440770874

90% Confidence Intervals

Variable				
a	**Value**	**90% (+/-)**	**Lower Limit**	**Upper Limit**

b	133.322464097714	30.0076399146035	103.314824183111	163.330104012317
	-82.9151695353331	18.8630030757008	-101.778172611034	-64.0521664596323

95% Confidence Intervals

Variable				
a	**Value**	**95% (+/-)**	**Lower Limit**	**Upper Limit**
b	133.322464097714	36.0733534662378	97.2491106314762	169.395817563952
	-82.9151695353331	22.6759511684668	-105.5911207038	-60.2392183668663

99% Confidence Intervals

Variable				
a	**Value**	**99% (+/-)**	**Lower Limit**	**Upper Limit**
b	133.322464097714	48.463650542771	84.858813554943	181.786114640485
	-82.9151695353331	30.4645747499486	-113.379744285282	-52.4505947853845

Variance Analysis

Source				
Regression	**DF**	**Sum of Squares**	**Mean Square**	**F Ratio**
Error	1	44027.6266636423	44027.6266636423	108295.373
Total	33	13.416193500519	0.406551318197545	
	34	44041.0428571428		

B.2 Data Table

Min Residual	**Max Residual**
-1.231	1.747

X1:dmax0	**X2:vmax_FD**	**X3:vmax_BD**	**Y:dmax_BD**	**Calc Y**	**Residual**	**% Error**	**Abs Residual**
1.8	36.9	23.2	1.1	1.246	-0.146	-13.286	0.146
10.1	55.3	34.7	7.3	8.531	-1.231	-16.867	1.231
29.5	73.7	46.3	21.8	22.036	-0.236	-1.084	0.236
70.2	92.1	57.9	49.7	49.040	0.660	1.329	0.660
138.2	110.6	69.5	101.4	100.582	0.818	0.807	0.818
267.1	129	81.1	185	186.106	-1.106	-0.598	1.106
0.2	36.9	23.2	0.1	0.138	-0.038	-38.460	0.038
2.7	55.3	34.7	1.7	2.281	-0.581	-34.155	0.581
9.4	73.7	46.3	6.6	7.022	-0.422	-6.389	0.422
22.3	92.1	57.9	16.9	15.578	1.322	7.822	1.322
45.2	110.6	69.5	32.8	32.896	-0.096	-0.294	0.096
81.1	129	81.1	57.7	56.508	1.192	2.066	1.192
0.6	55.3	34.7	0.2	0.507	-0.307	-153.404	0.307
3.6	73.7	46.3	2.2	2.689	-0.489	-22.235	0.489
9.6	92.1	57.9	6.6	6.706	-0.106	-1.610	0.106
20.3	110.6	69.5	14.6	14.774	-0.174	-1.194	0.174
36.1	129	81.1	26.9	25.153	1.747	6.494	1.747
1.2	73.7	46.3	0.5	0.896	-0.396	-79.278	0.396
4.4	92.1	57.9	2.8	3.074	-0.274	-9.775	0.274
10.2	110.6	69.5	7	7.424	-0.424	-6.051	0.424
19.1	129	81.1	13.4	13.308	0.092	0.685	0.092
0.4	73.7	46.3	0.1	0.299	-0.199	-198.796	0.199
1.9	92.1	57.9	0.9	1.327	-0.427	-47.476	0.427
5.3	110.6	69.5	3.3	3.857	-0.557	-16.889	0.557
10.9	129	81.1	7.4	7.595	-0.195	-2.632	0.195
0.7	92.1	57.9	0.2	0.489	-0.289	-144.500	0.289
2.6	110.6	69.5	1.3	1.892	-0.592	-45.560	0.592

X1:dmax0	X2:vmax_FD	X3:vmax_BD	Y:dmax_BD	Calc Y	Residual	% Error	Abs Residual
6.2	129	81.1	3.9	4.320	-0.420	-10.768	0.420
0.3	92.1	57.9	0.1	0.210	-0.110	-109.571	0.110
0.5	110.6	69.5	0.4	0.364	0.036	9.025	0.036
3.3	129	81.1	1.8	2.299	-0.499	-27.740	0.499
0.2	110.6	69.5	0.2	0.146	0.054	27.220	0.054
1.9	129	81.1	0.7	1.324	-0.624	-89.122	0.624
0	110.6	69.5	0.1	0.000	0.100	100.000	0.100
0.9	129	81.1	0.3	0.627	-0.327	-109.030	0.327

C. COMPONENT EFFECT FORMULA

Component effect formula covers Equation 5.13.

C.1 Fit Information

DataFit version 9.0.59
Equation ID: Component-Effect
Model Definition:
Y = X1/(a+X2/X3*b)

Number of observations = 34
Number of missing observations = 0
Solver type: Nonlinear
Nonlinear iteration limit = 250
Diverging nonlinear iteration limit =10
Number of nonlinear iterations performed = 17
Residual tolerance = 0.0000000001
Sum of Residuals = -27.9612314105681
Average Residual = -0.822389159134357
Residual Sum of Squares (Absolute) = 192.098302988698
Residual Sum of Squares (Relative) = 192.098302988698
Standard Error of the Estimate = 2.45011672546367
Coefficient of Multiple Determination (R^2) = 0.9970473455
Proportion of Variance Explained = 99.70473455%
Adjusted coefficient of multiple determination (Ra^2) = 0.996955075
Durbin-Watson statistic = 2.20920214290584

Regression Variable Results

Variable	Value	Standard Error	t-ratio	Prob(t)
a	-8.79451713354258	45.0161827720616	-0.195363458	0.84634
b	7.25890677054534	32.7688612967065	0.221518432	0.8261

68% Confidence Intervals

Variable	Value	68% (+/-)	Lower Limit	Upper Limit
a	-8.79451713354258	45.4753478363367	-54.2698649698793	36.6808307027941
b	7.25890677054534	33.1031036819329	-25.8441969113875	40.3620104524782

90% Confidence Intervals

Variable	Value	90% (+/-)	Lower Limit	Upper Limit
a	-8.79451713354258	76.2529119975952	-85.0474291311378	67.4583948640526

	7.25890677054534	55.5071741504911	-48.2482673799457	62.7660809210364

95% Confidence Intervals

Variable				
a	**Value**	**95% (+/-)**	**Lower Limit**	**Upper Limit**
b	-8.79451713354258	91.6934626884124	-100.487979821955	82.8989455548698
	7.25890677054534	66.7468935752614	-59.4879868047161	74.0058003458067

99% Confidence Intervals

Variable				
a	**Value**	**99% (+/-)**	**Lower Limit**	**Upper Limit**
b	-8.79451713354258	123.276816521291	-132.071333654833	114.482299387748
	7.25890677054534	89.7375266610307	-82.4786198904853	96.996433431576

Variance Analysis

Source				
Regression	**DF**	**Sum of Squares**	**Mean Square**	**F Ratio**
Error	1	64867.4278734819	64867.4278734819	10805.70551
Total	32	192.098302988698	6.00307196839681	
	33	65059.5261764706		

C.2 Data Table

Min Residual	**Max Residual**
-7.559	7.618

X1:dmax0	X2:vmax_FN	X3:vmax_FP	Y:dmaxFP	Calc Y	Residual	% Error	Abs Residual
1.8	36.9	26.8	1.2	1.500	-0.300	-24.998	0.300
10.1	55.3	40.2	7.7	8.480	-0.780	-10.134	0.780
29.5	73.7	53.7	23.6	25.259	-1.659	-7.030	1.659
70.2	92.1	67.1	59.2	60.056	-0.856	-1.447	0.856
138.2	110.6	80.5	109.7	117.259	-7.559	-6.890	7.559
267.1	129	93.9	234.4	226.782	7.618	3.250	7.618
0.2	36.9	26.8	0.1	0.167	-0.067	-66.664	0.067
2.7	55.3	40.2	1.8	2.267	-0.467	-25.945	0.467
9.4	73.7	53.7	7	8.049	-1.049	-14.981	1.049
22.3	92.1	67.1	19.4	19.078	0.322	1.661	0.322
45.2	110.6	80.5	35.5	38.351	-2.851	-8.031	2.851
81.1	129	93.9	62.3	68.858	-6.558	-10.527	6.558
0.6	55.3	40.2	0.4	0.504	-0.104	-25.945	0.104
3.6	73.7	53.7	2.4	3.082	-0.682	-28.436	0.682
9.6	92.1	67.1	8	8.213	-0.213	-2.661	0.213
20.3	110.6	80.5	15.4	17.224	-1.824	-11.844	1.824
36.1	129	93.9	28.4	30.651	-2.251	-7.925	2.251
1.2	73.7	53.7	0.8	1.027	-0.227	-28.436	0.227
4.4	92.1	67.1	3.6	3.764	-0.164	-4.562	0.164
10.2	110.6	80.5	7.3	8.654	-1.354	-18.554	1.354
19.1	129	93.9	14.2	16.217	-2.017	-14.204	2.017
0.4	73.7	53.7	0.2	0.342	-0.142	-71.249	0.142
1.9	92.1	67.1	1.6	1.625	-0.025	-1.591	0.025
5.3	110.6	80.5	3.6	4.497	-0.897	-24.914	0.897
10.9	129	93.9	7.8	9.255	-1.455	-18.650	1.455
0.7	92.1	67.1	0.7	0.599	0.101	14.450	0.101
2.6	110.6	80.5	1.7	2.206	-0.506	-29.766	0.506
6.2	129	93.9	4.2	5.264	-1.064	-25.336	1.064

X1:dmax0	X2:vmax_FN	X3:vmax_FP	Y:dmaxFP	Calc Y	Residual	% Error	Abs Residual
0.3	92.1	67.1	0.2	0.257	-0.057	-28.326	0.057
0.5	110.6	80.5	0.8	0.424	0.376	46.971	0.376
3.3	129	93.9	2.1	2.802	-0.702	-33.423	0.702
0.2	110.6	80.5	0.3	0.170	0.130	43.435	0.130
1.9	129	93.9	1.1	1.613	-0.513	-46.655	0.513
0.9	129	93.9	0.6	0.764	-0.164	-27.358	0.164

D. SOIL EFFECT FORMULA

Soil effect formula covers Equation 5.14.

D.1 Fit Information

DataFit version 9.0.59
Equation ID: Soil-Effect
Model Definition:
Y = X1/(a+X2/X3*b)

Number of observations = 33
Number of missing observations = 0
Solver type: Nonlinear
Nonlinear iteration limit = 250
Diverging nonlinear iteration limit =10
Number of nonlinear iterations performed = 11
Residual tolerance = 0.0000000001
Sum of Residuals = 20.2922981855257
Average Residual = 0.614918126834113
Residual Sum of Squares (Absolute) = 1180.19855691691
Residual Sum of Squares (Relative) = 1180.19855691691
Standard Error of the Estimate = 6.17016378963055
Coefficient of Multiple Determination (R^2) = 0.9536442958
Proportion of Variance Explained = 95.36442958%
Adjusted coefficient of multiple determination (Ra^2) = 0.9521489505
Durbin-Watson statistic = 2.28904092984787

Regression Variable Results

Variable				
a	**Value**	**Standard Error**	**t-ratio**	**Prob(t)**
b	-91.7204226878627	260.220978093703	-0.352471286	0.72687
	63.054725903833	175.306116281037	0.359683548	0.72152

68% Confidence Intervals

Variable				
a	**Value**	**68% (+/-)**	**Lower Limit**	**Upper Limit**
b	-91.7204226878627	263.005342559306	-354.725765247169	171.284919871443
	63.054725903833	177.181891725244	-114.127165821411	240.236617629077

90% Confidence Intervals

Variable				
a	**Value**	**90% (+/-)**	**Lower Limit**	**Upper Limit**
b	-91.7204226878627	441.204668357874	-532.925091045737	349.484245670012
	63.054725903833	297.231520154498	-234.176794250665	360.286246058331

95% Confidence Intervals

Variable				
a	**Value**	**95% (+/-)**	**Lower Limit**	**Upper Limit**
b	-91.7204226878627	530.720684822108	-622.441107509971	439.000262134245
	63.054725903833	357.536824155175	-294.482098251342	420.591550059008

99% Confidence Intervals

Variable				
a	**Value**	**99% (+/-)**	**Lower Limit**	**Upper Limit**
b	-91.7204226878627	714.046363889122	-805.766786576985	622.32594120126
	63.054725903833	481.039983075166	-417.985257171333	544.094708978999

Variance Analysis

Source				
Regression	**DF**	**Sum of Squares**	**Mean Square**	**F Ratio**
Error	1	24279.4202309619	24279.4202309619	637.7418636
Total	31	1180.19855691691	38.0709211908681	
	32	25459.6187878788		

D.2 Data Table

Min Residual	Max Residual
-17.816	21.110

X1:dmax0	X2:vmax_S	X3:vmax_R	Y:dmaxR	Calc Y	Residual	% Error	Abs Residual
1.8	36.9	24.8	0.6	0.858	-0.258	-42.932	0.258
10.1	55.3	37.3	5.3	5.729	-0.429	-8.101	0.429
29.5	73.7	49.7	19.5	16.543	2.957	15.166	2.957
70.2	92.1	62.1	40.7	39.097	1.603	3.938	1.603
138.2	110.6	74.5	92.1	73.186	18.914	20.536	18.914
267.1	129	86.9	124.1	141.916	-17.816	-14.356	17.816
2.7	55.3	37.3	0.9	1.532	-0.632	-70.178	0.632
9.4	73.7	49.7	4.3	5.271	-0.971	-22.587	0.971
22.3	92.1	62.1	12.9	12.420	0.480	3.723	0.480
45.2	110.6	74.5	29.4	23.936	5.464	18.584	5.464
81.1	129	86.9	64.2	43.090	21.110	32.882	21.110
0.6	55.3	37.3	0.2	0.340	-0.140	-70.178	0.140
3.6	73.7	49.7	1.2	2.019	-0.819	-68.231	0.819
9.6	92.1	62.1	4.1	5.347	-1.247	-30.406	1.247
20.3	110.6	74.5	10.6	10.750	-0.150	-1.417	0.150
36.1	129	86.9	21.4	19.181	2.219	10.371	2.219
1.2	73.7	49.7	0.3	0.673	-0.373	-124.308	0.373
4.4	92.1	62.1	1.6	2.451	-0.851	-53.159	0.851
10.2	110.6	74.5	4.2	5.402	-1.202	-28.609	1.202
19.1	129	86.9	9.1	10.148	-1.048	-11.519	1.048
0.4	73.7	49.7	0.1	0.224	-0.124	-124.308	0.124
1.9	92.1	62.1	0.5	1.058	-0.558	-111.637	0.558
5.3	110.6	74.5	1.9	2.807	-0.907	-47.721	0.907
10.9	129	86.9	4.3	5.791	-1.491	-34.683	1.491
0.7	92.1	62.1	0.2	0.390	-0.190	-94.929	0.190
2.6	110.6	74.5	0.8	1.377	-0.577	-72.109	0.577
6.2	129	86.9	2.2	3.294	-1.094	-49.736	1.094
0.3	92.1	62.1	0.1	0.167	-0.067	-67.082	0.067
0.5	110.6	74.5	0.3	0.265	0.035	11.739	0.035
3.3	129	86.9	1	1.753	-0.753	-75.336	0.753

X1:dmax0	X2:vmax_S	X3:vmax_R	Y:dmaxR	Calc Y	Residual	% Error	Abs Residual
0.2	110.6	74.5	0.1	0.106	-0.006	-5.913	0.006
1.9	129	86.9	0.5	1.010	-0.510	-101.902	0.510
0.9	129	86.9	0.2	0.478	-0.278	-139.094	0.278

APPENDIX G

EVALUATION of CASE HISTORY of KUSHIRO PORT (JAPAN)
CONSIDERING SEISMIC DESIGN OF GRAVITY QUAY WALLS

Here, the existing Kushiro Port quay wall is evaluated with its simplified dimensions. For backfill, several backfill properties are assumed and considered. Peak ground acceleration and peak ground velocities are used with respect to Kushiro Earthquake that damaged quay wall structure in 1993. The other assumptions and considerations are presented in next stages. Evaluation procedures are done according to DLH-DTY (2008).

A. CAISSON PROPERTIES

A.1 Caisson Geometry

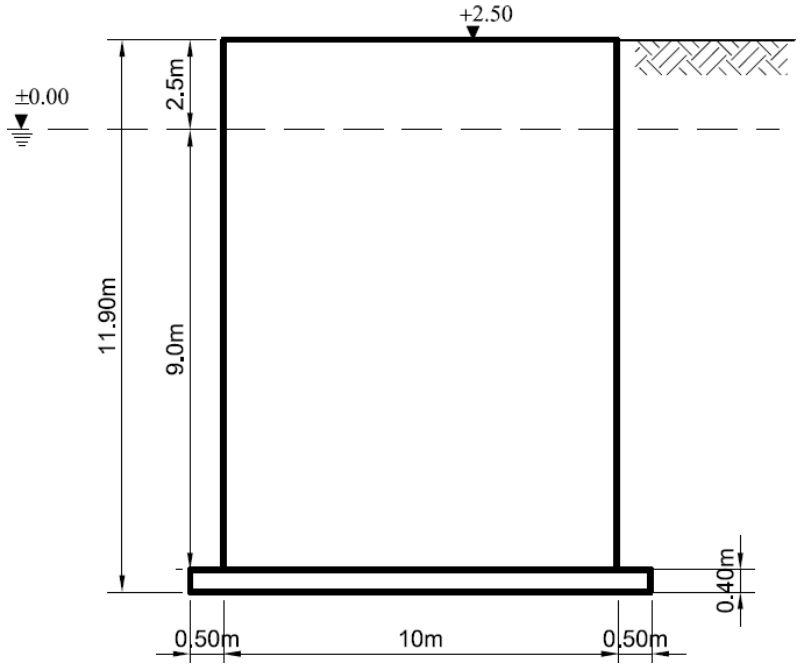

A.2 Caisson Weight

$\gamma_{concrete}$= 24 kN/m^3

γ_{water}= 10 kN/m^3

$W_{caisson\text{-}dry}$= 2865.6 kN/m (Equivalent dry weight of the caisson)

$W_{caisson\text{-}seis}$= 2865.6 kN/m

V_{sub}= 94.4 m^3/m

$W_{caisson\text{-}buo.}$= 1921.6 kN/m (G)

B. BACKFILL PROPERTIES

ϕ= 40 degrees
δ= 26.66 degrees
α= 0 degree
β= 0 degree
$\gamma_{backfill(dry)}$= 18 kN/m^3
$\gamma_{backfill(sat)}$= 21 kN/m^3
$\gamma_{backfill(sub)}$= 11 kN/m^3
$V_{backfill-act}$= 5.75 m^3/m
$W_{backfill-bou.}$= 72.00 kN/m
$W_{backfill-seis}$= 117.00 kN/m

C. SEISMIC GROUND MOTION

C.1 Seismic Condition

$a_{max} = 0.47g$
$v_{max} = 63cm/s$ (Refer to Table 2.6 of PIANC (2001))

C.2 Seismic Performance Levels

For Level 2 (L2), the quay structure is assumed Normal Structure considering performance grade. CD (Controlled Damage) is assumed damage level.

C.3 Equivalent Seismic Coefficient

Above Water;

$k_h = (1/3)0.47^{(1/3)} = 0.259$

(Horizontal seismic coefficient refer to Section 1.2.3.2 of DLH-DTY (2008))

$\lambda = \tan^{-1}(k_h) \Rightarrow \lambda = \tan^{-1}(0.259) = 14.520$

(λ angle represents seismic loading coefficient refer to Section 1.3.2.1.3 of DLH-DTY (2008))

Under Water;

$$k_h' = \frac{\sum_{j=1}^{ND}(\gamma_j h_j) + \sum_{j=ND+1}^{N}(\gamma_{sj} h_j) + q_o}{\sum_{j=1}^{ND}(\gamma_j h_j) + \sum_{j=ND+1}^{N}(\gamma_{bj} h_j) + q_o} k_h$$

(Horizontal eismic coefficient refer to Section 1.3.2.2.3 of DLH-DTY (2008))

$$k_h' = \frac{18\times 2.5 + 21\times 9.4 + 0}{18\times 2.5 + 11\times 9.4 + 0} \times 0.259 = 0.423$$

$\lambda = \tan^{-1}(k_h') \Rightarrow \lambda = \tan^{-1}(0.423) = 22.928^o$

(λ angle represents seismic loading coefficient refer to Section 1.3.2.1.3 of DLH-DTY (2008))

D. TOTAL ACTIVE EARTH PRESSURE COEFFICIENT

Above Water;

$$K_{ai,t} = \frac{\cos^2\ \varphi_i - \lambda - \alpha}{\cos\lambda\cos^2\alpha\cos\ \delta + \alpha + \lambda}\left[1 + \sqrt{\frac{\sin(\varphi_i + \delta)\sin(\varphi_i - \lambda - \beta)}{\cos\ \delta + \alpha + \lambda\ \cos\ \alpha - \beta}}\right]^{-2}$$

(Total active pressure coefficient refer to Section 1.3.2.3.1 of DLH-DTY (2008))

$$K_{ai,t} = \frac{\cos^2\ 40 - 14.520 - 0}{\cos(14.520)c\,os^2(0)\cos\ 26.66 + 0 + 14.520}\left[1 + \sqrt{\frac{\sin(40 + 26.66)\sin(40 - 14.520 - 0)}{\cos\ 26.66 + 0 + 14.520\ \cos\ 0 - 0}}\right]^{-2} = 0.376$$

$K_{ai,d}$=$K_{ai,t}$-$K_{ai,s}$

(Dynamic active pressure coefficient refer to Section 1.3.2.3.3 of DLH-DTY (2008))

$$K_{ai,s} = \frac{\cos^2\ 40 - 0 - 0}{\cos(0)c\,os^2(0)\cos\ 26.66 + 0 + 0}\left[1 + \sqrt{\frac{\sin(40 + 26.66)\sin(40 - 0 - 0)}{\cos\ 26.66 + 0 + 0\ \cos\ 0 - 0}}\right]^{-2} = 0.200$$

(Static active pressure coefficient refer to Section 1.3.2.3.3 of DLH-DTY (2008))

$K_{ai,d}$=0.376-0.200=0.176

Under Water;

$$K_{ai,t} = \frac{\cos^2\ \varphi_i - \lambda - \alpha}{\cos\lambda\cos^2\alpha\cos\ \delta/2 + \alpha + \lambda}\left[1 + \sqrt{\frac{\sin(\varphi_i + \delta/2)\sin(\varphi_i - \lambda - \beta)}{\cos\ \delta/2 + \alpha + \lambda\ \cos\ \alpha - \beta}}\right]^{-2}$$

(Total active pressure coefficient refer to Section 1.3.2.3.1 and 1.3.2.3.2 of DLH-DTY (2008))

$$K_{ai,t} = \frac{\cos^2\ 40 - 22.928 - 0}{\cos(22.928)c\,os^2(0)\cos\ 13.33 + 0 + 22.928}\left[1 + \sqrt{\frac{\sin(40 + 13.33)\sin(40 - 22.928 - 0)}{\cos\ 13.33 + 0 + 22.928\ \cos\ 0 - 0}}\right]^{-2} = 0.519$$

$K_{ai,d}$=$K_{ai,t}$-$K_{ai,s}$

(Dynamic active pressure coefficient refer to Section 1.3.2.3.3 of DLH-DTY (2008))

$$K_{ai,s} = \frac{\cos^2\ 40 - 0 - 0}{\cos(0)c\,os^2(0)\cos\ 13.33 + 0 + 0}\left[1 + \sqrt{\frac{\sin(40 + 13.33)\sin(40 - 0 - 0)}{\cos\ 13.33 + 0 + 0\ \cos\ 0 - 0}}\right]^{-2} = 0.202$$

(Static active pressure coefficient refer to Section 1.3.2.3.3 of DLH-DTY (2008))

$K_{ai,d}$=0.519-0.202=0.317

E. HORIZONTAL FORCES

E.1 Horizontal Component of Static Earth Pressure and Force

$$p_{ai,s} = K_{ai,s}\left[\sum_{j=1}^{ND}(\gamma_j h_j) + \sum_{j=ND+1}^{i}(\gamma_{bj} h_j) + \frac{q_o \cos\alpha}{\cos\ \alpha - \beta}\right]\cos\alpha$$

(Static active pressure refer to Section 1.3.2.2. of DLH-DTY (2008))

Above Water;

$$p_{ai,s} = 0.200\ 18 \times 2.5\ \times \cos(0) = 9.0 kN/m^2$$

$$P_{ASh} = 9.0 \times \frac{2.5}{2} \times \cos(26.66) = 10.05 kN/m$$

$$M_{ASh} = 10.05 \times \left(\frac{1}{3} \times 2.5 + 9.4\right) = 102.85 kNm/m$$

Under Water;

$$p_{ai,s} = 0.202\ 11 \times 9.4\ \times \cos(0) = 20.88 kN/m^2$$

$$P_{ASh} = 20.88 \times 9.4 \times \cos(13.33) + 20.88 \times \frac{9.4}{2} \times \cos(13.33) = 190.98 + 95.49 = 286.47 kN/m$$

$$M_{ASh} = 190.98 \times \frac{1}{2} \times 9.4 + 95.49 \times \frac{1}{3} \times 9.4 = 1196.81 kNm/m$$

$$\sum P_{ASh} = 10.05 + 286.47 = 296.52 kN/m$$

$$\sum M_{ASh} = 102.85 + 1196.81 = 1299.66 kNm/m$$

E.2 Horizontal Component of Dynamic Earth Pressure and Force

$$p_{ai,d} = K_{ai,d}\left[\sum_{j=1}^{ND}(\gamma_j h_j) + \sum_{j=ND+1}^{i}(\gamma_{bj} h_j) + \frac{q_o \cos\alpha}{\cos\ \alpha - \beta}\right]\cos\alpha$$

(Dynamic active pressure refer to Section 1.3.2.2. of DLH-DTY (2008))

Above Water;

$$p_{ai,d} = 0.176\ 18 \times 2.5\ \times \cos(0) = 7.92 kN/m^2$$

$$P_{ADh} = 7.92 \times \frac{2.5}{2} \times \cos(26.66) = 8.85 kN/m$$

$$M_{ADh} = 8.85 \times \left(\frac{1}{3} \times 2.5 + 9.4\right) \times 1.5 = 135.84 kNm/m$$

(Refer to Section 2.2.2.2.5 of DLH-DTY (2008))

Under Water;

$$p_{ai,d} = 0.317\ 11 \times 9.4\ \times \cos(0) = 32.77 kN/m^2$$

$$P_{ADh} = 32.77 \times 9.4 \times \cos(13.33) + 32.77 \times \frac{9.4}{2} \times \cos(13.33) = 299.74 + 149.87 = 449.61 kN/m$$

$$M_{ADh} = 1.5 \times \left[299.74 \times \frac{1}{2} \times 9.4 + 149.87 \times \frac{1}{3} \times 9.4 \right] = 2817.56 kNm/m$$

(Refer to Section 2.2.2.2.5 of DLH-DTY (2008))

$$\sum P_{ADh} = 8.85 + 449.61 = 458.46 kN/m$$

$$\sum M_{ADh} = 135.84 + 2817.56 = 2953.40 kNm/m$$

E.3 Equivalent Hydrodynamic Water Force

$$P_{w,d} = \frac{7}{12} k_h \gamma_w H^2$$

$$P_{w,d} = \frac{7}{12} \times 0.259 \times 10 \times 9.4^2 = 133.50 kN/m$$

$$M_{w,d} = 133.50 \times \frac{2}{5} \times 9.4 = 501.96 kNm/m$$

E.4 Equivalent Seismic Inertia Force

$$F_{i-caisson} = 2865.6 \times 0.259 = 742.19 kN/m$$

$$M_{i-caisson} = 742.19 \times 5.931 = 4401.93 kNm/m$$

$$F_{i-backfill} = \ 22.5 + 94.5 \ \times 0.259 = 5.83 + 24.47 = 30.30 kN$$

$$M_{i-caisson} = 5.83 \times (\frac{2.5}{2} + 9.4) + 24.47 \times (\frac{9}{2} + 0.4) = 182.00 kNm$$

F. VERTICAL FORCES

F.1 Caisson and Backfill Weight (incl. Bouyancy)

$$W_{caisson} \cong 1921.6 kN/m$$

$$M_{v-caisson} = 1921.6 \times \frac{11.0}{2} = 10568.80 kNm/m$$

$$W_{backfill} \cong 72.00 kN/m$$

$$M_{v-backfill} = 72.00 \times \left(11.0 - \frac{0.50}{2} \right) = 774.00 kNm/m$$

F.2 Vertical Component of Static Earth Pressure

Above Water;

$$P_{ASv} = 9 \times \frac{2.5}{2} \times \sin(26.66) = 5.05 kN/m$$

$$M_{ASv} = 5.05 \times (10.00 + 0.50) = 53.03 kNm/m$$

Under Water;

$$P_{ASv} = 20.88 \times 9.4 \times \sin(13.33) + 20.88 \times \frac{9.4}{2} \times \sin(13.33) = 45.26 + 22.63 = 67.89 kN/m$$

$$M_{ASv} = 67.89 \times (10.00 + 0.50) = 712.84 kNm/m$$

$$\sum P_{ASv} = 5.05 + 67.89 = 72.94 kN/m$$

$$\sum M_{ASv} = 53.03 + 712.84 = 765.87 kN/m$$

F.3 Vertical Component of Dynamic Earth Pressure

Above Water;

$$P_{ADv} = 7.92 \times \frac{2.5}{2} \times \sin(26.66) = 4.44 kN/m$$

$$M_{ADv} = 4.44 \times (10.00 + 0.50) = 46.20 kNm/m$$

Under Water;

$$P_{ADv} = 32.77 \times 9.4 \times \sin(13.33) + 32.77 \times \frac{9.4}{2} \times \sin(13.33) = 69.35 + 35.51 = 104.86 kN/m$$

$$M_{ASv} = 104.86 \times (10.00 + 0.50) = 1101.03 kNm/m$$

$$\sum P_{ASv} = 4.44 + 104.86 = 109.3 kN/m$$

$$\sum M_{ASv} = 46.20 + 1101.3 = 1147.23 kN/m$$

G. RESISTANCE BASED DESIGN CHECK

Resistance based design check is evaluated refer to Section 2.2.2 of DLH-DTY (2008)

Load combinations are considered as;

Horizontal Forces= $(D_M) + (Z_S) + (Z_D) + 0.5(Z_{SQ}) + 0.5(Z_{DQ}) + (S_D) + 0.5(B)$

Vertical Forces= $(G) + (S_K)$

Uniformly distributed (surcharge) live loads on backfill and any bollard (mooring) load did not considered.

G.1 Sliding Stability

$$H = 772.49 + 296.52 + 458.46 + 133.5 = 1657.97 kNm/m$$

$$V = 1921.6 + 72 + 72.94 + 109.3 = 2175.84 kN$$

$$F_{sk} = \frac{\mu W}{P} \Rightarrow F_{sk} = \frac{0.6 \times \ 2175.84}{1657.97} = 0.787 < 1.0$$

Factor of safety against sliding is not satisfied according to the given limits in DLH-DTY (2008).

G.2 Overturning Stability

Overturning Moments=

$$M_{ot} = 1299.66 + 2953.40 + 501.96 + 4401.93 + 182.00 = 9338.95 kNm/m$$

Resisting Moments= $M_{rt} = 10568.80 + 774.00 + 765.87 + 1147.23 = 13255.90 kNm/m$

$$F_{ot} = \frac{13255.90}{9338.95} = 1.42 > 1.1$$

Factor of safety against overturning is satisfied according to the given limits in DLH-DTY (2008).

H. DEFORMATION BASED DESIGN CHECK

As it can be seen from sliding stability check, resistance based design is not satisfied for the existing damaged gravity type caisson quay structure of Kushiro Port. Considering this study's proposal approach based on sliding block analysis, the measured horizontal displacement after Kushiro-Oki earthquake will be evaluated with respect to deformation based design. As mentioned earlier, k_y corresponds the yield acceleration, that yield acceleration $a_y=k_yg$. Yield acceleration makes the factor of safety coefficient against sliding 1.0. First of all, k_y yield (threshold) seismic coefficient from pseudo static analysis is obtained by iteration. That yield (threshold) coefficient is obtained as k_y=0.196. From this point of view, yield acceleration calculated as $a_y=0.196g$. Equation 5.8 of this study is used to compute sliding displacement considering peak ground acceleration (a_{max}), peak ground velocity (v_{max}), and obtained yield acceleration (a_y), as follows. g is considered as $981cm/sn^2$.

$$d_{\max} = \frac{70 \times 63^2}{0.47 \times 981} \exp\left(\frac{-13 \times 0.196 \times 981}{0.47 \times 981} \right) = 2.664 cm$$

The other studies mentioned in Literature Review ara also compared with the measured displacement. The comparison is presented in the following diagram chart. As seen from the chart there is quite difference between the measured displacement values and each displacement estimation methods.

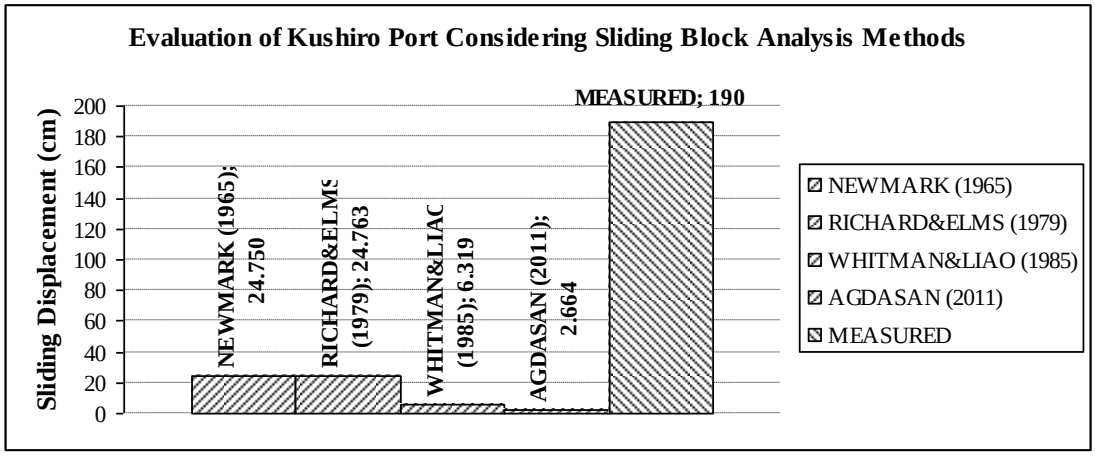

However, measured sliding displacement is 190cm. As stated in PIANC (2001), seaward displacement of caisson type quay wall constructed on firm foundation is caused because of liquefaction of backfill. If soil structure interaction could be considered, approximately sliding displacement might be obtained. Here, it is thought that liquefaction has a negative effect on displacement. It can be concluded that, sliding block analyis methods are just an estimation procedure and methods of sliding displacement values under earthquake conditions. The obtained and computed values may not reflect and predict the real damage that can occur after an earthquake.

CURRICULUM VITAE

Candidate's full name:	**Alper AĞDAŞAN**
Place and date of birth:	**Kars-03.03.1986**
Permanent Address:	**Mahmut Yesari Cad. No:17 Koşuyolu/İstanbul**
e-mail:	**alperagdasan@gmail.com**
Universities and Colleges attended:	**Istanbul Technical University (Graduated at 2009)**
	Faculty of Civil Engineering,
	Civil Engineering Deparment.

Publications: